



Since January 2020 Elsevier has created a COVID-19 resource centre with free information in English and Mandarin on the novel coronavirus COVID-19. The COVID-19 resource centre is hosted on Elsevier Connect, the company's public news and information website.

Elsevier hereby grants permission to make all its COVID-19-related research that is available on the COVID-19 resource centre - including this research content - immediately available in PubMed Central and other publicly funded repositories, such as the WHO COVID database with rights for unrestricted research re-use and analyses in any form or by any means with acknowledgement of the original source. These permissions are granted for free by Elsevier for as long as the COVID-19 resource centre remains active.



Synthetic and computational efforts towards the development of peptidomimetics and small-molecule SARS-CoV 3CLpro inhibitors

Abhik Paul, Arnab Sarkar, Sanjukta Saha, Avik Maji, Pritha Janah, Tapan Kumar Maity*

Department of Pharmaceutical Technology, Jadavpur University, West Bengal, Kolkata 700032, India

ARTICLE INFO

Keywords:

SARS-CoV
Coronavirus
3CLpro
Peptidomimetic inhibitors (PIs)
Small-molecule inhibitors (SMIs)
Organic synthesis
Medicinal chemistry

ABSTRACT

Severe Acute Respiratory Syndrome (SARS) is a severe febrile respiratory disease caused by the beta genus of human coronavirus, known as SARS-CoV. Last year, 2019-*n*-CoV (COVID-19) was a global threat for everyone caused by the outbreak of SARS-CoV-2. 3CLpro, chymotrypsin-like protease, is a major cysteine protease that substantially contributes throughout the viral life cycle of SARS-CoV and SARS-CoV-2. It is a prospective target for the development of SARS-CoV inhibitors by applying a repurposing strategy. This review focuses on a detailed overview of the chemical synthesis and computational chemistry perspectives of peptidomimetic inhibitors (PIs) and small-molecule inhibitors (SMIs) targeting viral proteinase discovered from 2004 to 2020. The PIs and SMIs are one of the primary therapeutic inventions for SARS-CoV. The journey of different analogues towards the evolution of SARS-CoV 3CLpro inhibitors and complete synthetic preparation of nineteen derivatives of PIs and ten derivatives of SMIs and their computational chemistry perspectives were reviewed. From each class of derivatives, we have identified and highlighted the most compelling PIs and SMIs for SARS-CoV 3CLpro. The protein–ligand interaction of 29 inhibitors were also studied that involved with the 3CLpro inhibition, and the frequent amino acid residues of the protease were also analyzed that are responsible for the interactions with the inhibitors. This work will provide an initiative to encourage further research for the development of effective and drug-like 3CLpro inhibitors against coronaviruses in the near future.

1. Introduction

In November 2002, Severe Acute Respiratory Syndrome (SARS) was first identified in Guangdong Province of Southern China and immediately within a few months was considered to be a global threat because of its highly contagious and deadly nature. From November 2002 to 2003, it spread rapidly over 29 countries. Total 8439 cases were reported globally till 3rd July 2003, and among which 812 patients died^{1,2}. The etiological agent solely responsible for this SARS was found to be a novel human coronavirus called SARS-CoV. Some changes in the phylogenetic characters and gene sequence of SARS-CoV distinguish it from other previously discovered^{3,4} SARS is characterized by fever, and after a few days, it is followed by shortness of breath and dry nonproductive cough, headache, dyspnea, lower respiratory tract infection, lymphopenia, and diarrhoea⁵.

Coronaviruses are enveloped, positive-stranded RNA virus and belong to order *Nidovirales*, family *Coronaviridae*, sub-family *Coronavirinae* genus *Coronavirus*. Genus is of four types alpha, beta, gamma, and delta Coronavirus. The beta coronavirus with “b” lineage is mainly responsible for SARS-CoV disease^{3,6}. The schematic representation of the taxonomy is described in Figure 1. Coronaviruses are zoonotic viruses, primarily originated from non-humans (animal reservoirs, especially bats and avian species) and then transmitted to humans⁷. The seven coronaviruses known to infect humans include HCoV-229E, HCoV-OC43, HCoV-NL63, HCoV-HKU1, SARS-CoV, MERS-CoV, and recently SARS-CoV-2. Amongst these seven SARS-CoV, Middle East Respiratory Syndrome Coronavirus (MERS-CoV) and SARS-CoV-2 are the most infectious and fatal⁸. MERS-CoV was first reported in June 2012 in Saudi Arabia and caused severe respiratory problems. By the end of August 2015, 1511 cases were reported with 574 deaths (fatality

Abbreviations: SARS-CoV, Severe Acute Respiratory Syndrome-coronavirus; 3CLpro, Chymotrypsin-like protease; PIs, Peptidomimetic inhibitors; SMIs, Small-molecule inhibitors; K_i , Inhibition constant; IC_{50} , half maximal inhibitory concentration; FRET, Fluorescence Resonance Energy Transfer; SAR, Structure-Activity Relationship; $\mu\text{M}/\mu\text{M}$, Micromolar; SKAE, Sharpless–Katsuki asymmetric epoxidation; SAD, Sharpless asymmetric dihydroxylation.

* Corresponding author at: Department of Pharmaceutical Technology, Synthetic and Natural Product Research Laboratory, Jadavpur University, 188, Raja S.C. Mallick Rd, Kolkata 700032, West Bengal, India.

E-mail address: jutkmaity@yahoo.com (T. Kumar Maity).

<https://doi.org/10.1016/j.bmc.2021.116301>

Received 26 February 2021; Received in revised form 25 June 2021; Accepted 27 June 2021

Available online 3 July 2021

0968-0896/© 2021 Elsevier Ltd. All rights reserved.

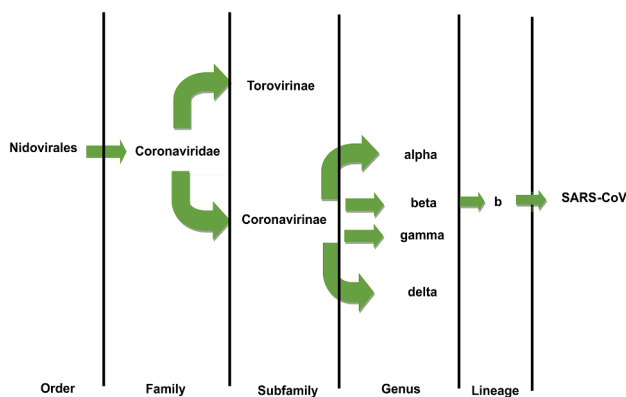


Figure 1. Taxonomic classification of SARS-CoV.

rate – 38%)^{8,9}. The disease caused by SARS-CoV-2, also known as coronavirus disease 19 (COVID-19), as the first case was reported in Wuhan, China, in December 2019. COVID-19 has been declared a worldwide pandemic by World Health Organization (WHO) on March 11, 2020. Till the mid of August 2020, 21.2 million cases were reported, including 76,100 deaths^{10,11}. Even though the death rate is lower than SARS-CoV, the infection rate is quite high, so SARS-CoV-2 is considered a severe medical emergency. In recent times, several pharmaceutical companies successfully developed vaccines to treat COVID-19, but no specific anti-viral drugs have been discovered. Chymotrypsin-like cysteine protease (3CLpro) is the major protease involved in viral replication of SARS-CoV, and it has also been found that the sequence similarity between SARS-CoV and SARS-CoV-2 is 96%^{5,8}. By targeting this protease enzyme, many researchers have designed and developed potential inhibitors against coronaviruses. The potential SARS-CoV 3CLpro inhibitors have a particular parent moiety that can be modified structurally to develop a new effective drug. The most advanced pre-clinical therapeutic drugs for SARS-CoV-2 3CLpro are PF-00835231, PF-07304814, GC-376, and PF-07321332 (Figure 2)^{12,13}. Based on the identical sequence similarity between SARS-CoV and SARS-CoV-2, the inventors of PF-00835231 have recently developed a new covalent inhibitor for treating COVID-19¹⁴. Another potent and selective SMI against SARS-CoV-2 3CLpro is ALG-097111 which was evaluated in the COVID-19 infected Syrian Hamster Model for antiviral activity¹⁵.

To combat the current outbreak of COVID-19, the scientific community is trying to develop effective treatment within a feasible time. Many well-established strategies are taken by the research organizations to eradicate the COVID-19 pandemic^{16,17}. In the field of drug discovery and development, repurposing of existing drugs is one of the organized and economic strategies to fight against novel diseases, like novel coronavirus¹⁸. The bioinformatics and pharmacoinformatic approaches have played a massive role in repurposing the existing drugs. By this strategy, many scientific workers have generated and identified

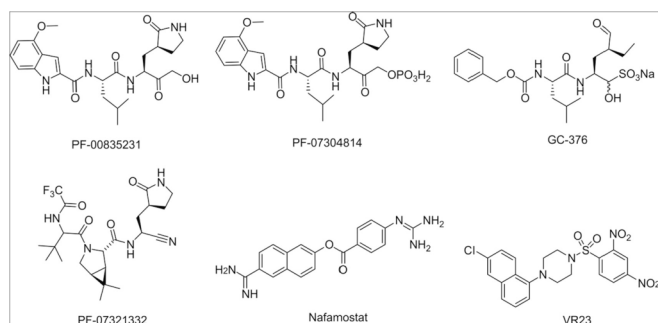


Figure 2. Structure of PF-00835231, PF-07304814, GC-376, PF-07321332, Nafamostat, and VR23.

numerous newer inhibitors against target diseases¹⁹. In the battle of COVID-19, the anti-SARS-CoV compounds are mostly explored and repurposed for screening the best-fit inhibitors⁶. With the help of computational chemistry, recently, Bhowmik and their collaborators identified Nafamostat and VR23 as promising candidates for treating COVID-19 by targeting SARS-CoV-2 3CLpro (Figure 2). The pharmacodynamic study revealed that the Nafamostat and VR23 are promising for drug-likeness but further pre-clinical/clinical investigation studies are needed to be procured for understanding the efficacy and potency of the compounds²⁰.

Apart from the pharmacoinformatic approaches, chemical synthesis is an integral part of drug discovery and development; to synthesize the novel molecules for the target diseases²¹. Since now, many organic chemists have explored and discovered the different types of novel inhibitors targeting the SARS-CoV 3CLpro, such as peptidomimetic inhibitors (PIs), small-molecule inhibitors (SMIs), and metal conjugate inhibitors. Researchers can't evaluate the in vitro or in vivo efficacy and potency of inhibitors without the chemical synthesis of designed inhibitors. So, wet lab chemical synthesis has always a great interest for researchers in the pharmaceutical industry and scientific field to develop novel chemical entities as a drug²².

Considering the global pandemic of COVID-19, this review focuses on the chemical synthesis and computational chemistry perspectives of SARS-CoV 3CLpro inhibitors, specially PIs and SMIs, which has been discovered by applying chemical synthesis, in vitro biological assay, and computational chemistry from 2004 to 2020.

The journey of different analogues towards development of SARS-CoV 3CLpro inhibitors is provided in Figure 3. Here, we have classified the SARS-CoV 3CLpro inhibitors into two categories: 1) Peptidomimetic inhibitors (PIs), and 2) Small-molecule inhibitors (SMIs). The PIs consist of different analogues, including: Keto-Glutamine analogues²³, Anilide analogues²⁴, Peptidomimetic α,β -unsaturated esters²⁵, Glutamic acid and glutamine peptides²⁶, Peptidomimetic (TG-0205221)²⁷, Phthalhydrazide peptide analogues²⁸, Cinanserin analogues²⁹, Trifluoromethyl ketone containing peptides³⁰, Trifluoromethyl, benzothiazolyl or thiazolyl ketone containing peptidomimetics³¹, Michael type of peptidomimetics³², Cysteine protease inhibitors³³, Potent dipeptide type of peptidomimetics³⁴, Novel dipeptide type of peptidomimetics³⁵, Nitrile based peptidomimetics³⁶, Tripeptide type of peptidomimetics³⁷, Peptidomimetics containing cinamoyl warhead³⁸, Peptidomimetics containing decahydroisoquinolin moiety³⁹, Ketone-based covalent inhibitors¹⁴, and α -Ketoamide derivatives⁴⁰. The SMIs are classified into: isatin derivatives⁴¹, Chloropyridyl ester derivatives⁴², pyrazolone derivatives⁴³, pyrimidine derivatives⁴⁴, macrocyclic inhibitors⁴⁵, 5-sulphonyl isatin derivatives⁴⁶, pyrazolone derivatives⁴⁷, serine derivatives⁴⁸, phenylisoserine derivatives⁴⁹, and Octahydroisochromene derivatives⁵⁰.

We have also identified the most promising anti-SARS compounds from each class of derivatives and highlighted their structural features and binding information. This work, chemical synthesis, and computational chemistry aspect of SARS-CoV 3CLpro inhibitors will provide an initiative to encourage further research to the organic chemist and medicinal chemists for the design and synthesis of new 3CLpro inhibitors effective against coronaviruses in coming years.

2. SARS-CoV 3CLpro and its structural features:

Coronaviruses are positive polarity family of polyadenylated single-stranded RNA. In several animal species, even human beings, this virus can cause acute and chronic pulmonary and nervous system diseases⁵¹. Coronavirus virions feature the largest viral genomes ranging from 27 to 31 kb long found to date. The genome is helically encapsidated by nucleocapsid (N) proteins⁵². Virus cores are formed by the matrix proteins that surround the filamentous nucleocapsid. The virus membrane includes various spike-like protuberances called spike (S) proteins, a type of glycoprotein I along with membrane protein (M) that covers the

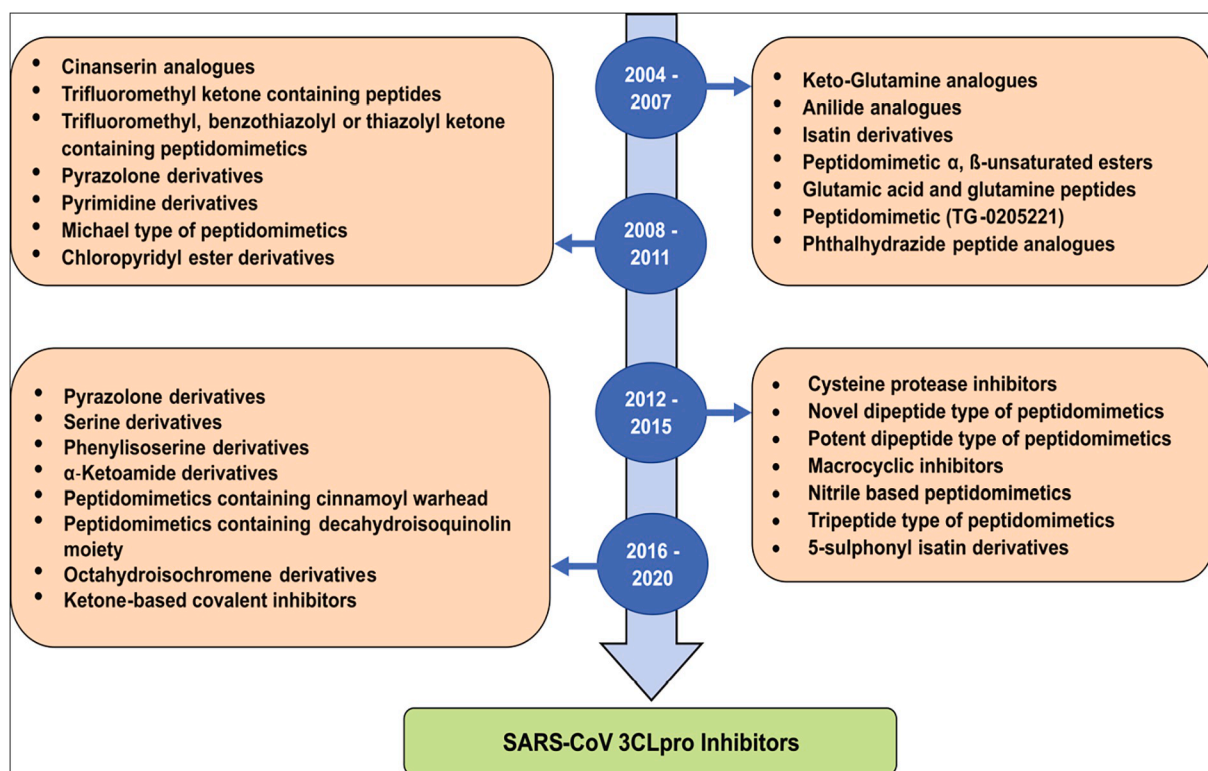


Figure 3. Journey of different analogues in the discovery of SARS-CoV 3CLpro inhibitors.

membrane, and a hydrophobic protein called envelope protein (E) that surrounds the entire virus structure⁵³. These proteins make a crown-like appearance, hence the justification of the name Corona, which is derived from a Latin word, while seen in an electron microscope. S proteins act as a protein that binds with the receptor of the host and is a fusion of the viral and cellular membranes^{54,55}. The schematic figure is given in Figure 4.

The SARS-CoV genome consists of two open reading frames bound by a ribosomal frameshift that encodes two overlapping polyproteins, pp1a (approximately 450 kDa) and pp1ab (approximately 750 kDa), that helps to moderate the mechanism of viral replication and transcription. Complex proteolytic processing is involved in the maturation of coronavirus that controls viral gene expression and replication⁵⁶. Some viruses from the same family make use of three proteases in the proteolytic

process. In comparison, it is known to encode only two proteases in the case of SARS-CoV. Other than 3CLpro, it also has papain-like cysteine protease (PLpro). 3CLpro, also known as the Main Protease (Mpro), plays a crucial role in the mechanism of viral replication and infection, allowing this macromolecule a prime candidate for antiviral therapy (PDB ID: 1UJ1)^{6,57}.

Yang et al solved the X-ray crystallographic structure of hexapeptidylchloromethyl ketone (CMK) inhibitor, which is bound to Mpro at various pH values. It was stated that with the two promoters referred to as "A" and "B" are focused almost perpendicular to each other, SARS-CoV 3CLpro acts as a dimer. As shown in the schematic diagram (Figure 5), the SARS-CoV Mpro crystal structure, analogous to other 3CLpro crystals, contains three domains. Domain I have 8–101 residues, and Domain II has 102–184 residues. Domain I and II contain β -sheets

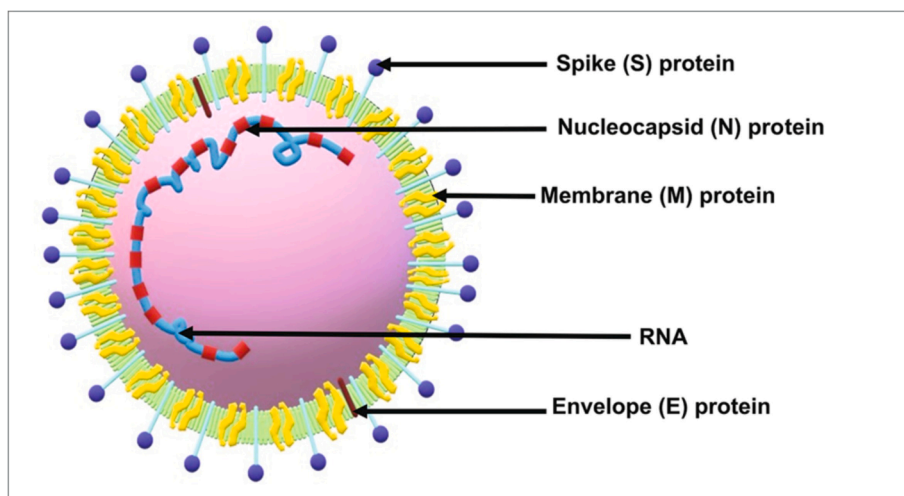


Figure 4. Structure of SARS-CoV and its proteins (S, M, E, and N).

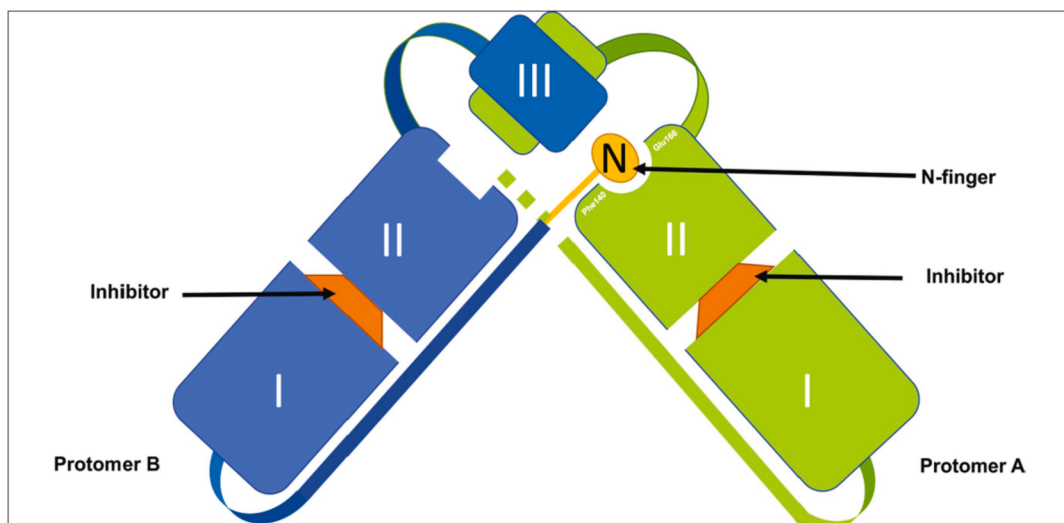


Figure 5. Schematic diagram demonstrating the essential role of the *N*-finger in both dimerization and preservation of the enzyme's active form⁵⁸.

that form the framework of chymotrypsin, while domain III, having 201–306 residues, consists mainly of alpha-helices. The Cysteine-Histidine (Cys-His) catalytic dyad is present in SARS-CoV Mpro, and between domain I and domain II in a cleft, the binding site for the inhibitor is present. The inhibitor showing in Figure 6, having binding subsite S1 specificity of a coronavirus protease in protomer A bestows complete specificity for the enzyme residue of the P1-Gln substrate. Squeezed between domain II and domain III of the parent monomer and domain II of the other monomer, each *N*-terminus residue (*N*-finger) plays an essential part in the dimerization process and development of the Mpro active site. The Mpro SARS-CoV dimer is intensely active, while the monomer is somewhat inactive. The study revealed that the pH-dependent triggering switch is a unique feature of SARS-CoV 3CLpro, resulting in significant, cooperative activities of the Glu-166, Phe-140, Leu-141, and Tyr-118 side chains and the dimer N terminus of the other protomer. A physiological reason for the lower P2 specificity of the SARS enzyme than those of other coronaviruses is due to the unusual binding mode of the substrate-analogue inhibitor. To facilitate the design and screening of inhibitors with anti-SARS action, these structures provide important structural details on dimerization and substrate binding sites^{6,58,59}.

3. Chemical synthesis of SARS-CoV 3CLpro inhibitors:

3.1. Peptidomimetic inhibitors (PIs):

Therapeutic interactions between two proteins or protein–protein interactions (PPIs) have been essential in drug design in recent times against various diseases, including metabolic disorders, cancer, neurodegenerative disorders, and several other illnesses. It also has a significant role in various biological processes, including cell proliferation,

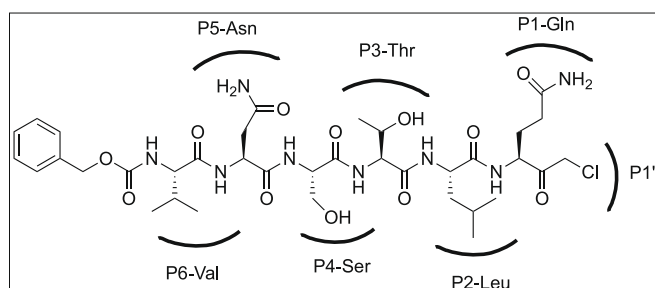


Figure 6. Structure of SARS-CoV 3CLpro inhibitor.

signal transduction, and apoptosis⁶⁰. Peptidomimetics are molecules whose basic elements in 3D space resemble a standard peptide or protein, which maintain the capability to interact and create the same therapeutic effect with the biological target. Peptidomimetics are intended to overcome some of the complications associated with a native peptide, including proteolysis that affects the duration or half-life of the protein and low bioavailability. Other such properties may also be significantly improved, which includes receptor specificity and efficacy. Thus, in drug development, peptidomimetics have enormous potential. The peptidomimetic design method begins with developing the relationships between structure and activity, also known as SAR that can describe the biological effect^{61,62}.

There are various instances of PPI-targeting peptides and peptidomimetics that's been in clinical trials. For example, the first potent and specific p53 re-activator, an important tumor suppressor protein that binds and acts as an inhibitor of two p53 suppressor proteins, namely MDM2 and MDMX, is Aileron (ALRN-6924). p53 is one of the most favoured targets of antineoplastic drugs activated by its vital role in stopping multiple cancers from initiating and advancing⁶³. KAI Pharmaceuticals developed a small peptide named KAI-9803, which directly acts as dPKC inhibitor with its intracellular receptor, RACK. During reperfusion, dPKC activation initiates molecular pathways for cell death, which gradually leads to inflammation and injury during a stroke in the heart or brain. In phase II clinical trial to determine safety and effectiveness, KAI-9803 was evaluated for its efficacy in acute myocardial infarction patients⁶⁴.

The chemical synthesis of PIs under Keto-Glutamine analogues²³, Anilide analogues²⁴, Peptidomimetic α,β -unsaturated esters²⁵, Glutamic acid and glutamine peptides²⁶, Peptidomimetic (TG-0205221)²⁷, Phthalhydrazide peptide analogues²⁸, Cinanserin analogues²⁹, Trifluoromethyl ketone containing peptides³⁰, Trifluoromethyl, benzothiazolyl or thiazolyl ketone containing peptidomimetics³¹, Michael type of peptidomimetics³², Cysteine protease inhibitors³³, Potent dipeptide type of peptidomimetics³⁴, Novel dipeptide type of peptidomimetics³⁵, Nitrile based peptidomimetics³⁶, Tripeptide type of peptidomimetics³⁷, Peptidomimetics containing cinnamoyl warhead³⁸, Peptidomimetics containing decahydroisoquinolin moiety³⁹, Ketone-based covalent inhibitors¹⁴, and α -Ketoamide derivatives⁴⁰; are discussed below:

3.1.1. Keto-Glutamine analogues:

In 2004, Jain and co-researchers synthesized a series of keto-glutamine analogues targeting the SARS-CoV 3CLpro²³. The synthesized compounds have been evaluated against SARS-CoV 3CLpro by

using fluorometric assays and found the most potent inhibitors with IC_{50} values ranging from 0.60 to 70 μM . The compounds have been designed based on their previously synthesized molecule previously evaluated against human rhinovirus-14 (HRV-14) and hepatitis A virus (HAV) targeting on picornaviral 3C protease enzyme. The reported keto-glutamine analogues **1** and **2** of HAV 3C proteinase inhibitors with IC_{50} values are shown in Figure 7. Jain et al designed the three synthesis scheme (Scheme 1: **1A**, **1B**, and **1C**) by modification at P2, P3, and P4 position with amino acids of previously reported compound⁶⁵.

The synthetic route of a tetrapeptide, Scheme 1A initiated according to the previously reported literature⁶⁵⁻⁶⁷ to produced **4a-c**. After that, it reacts with trifluoroacetic acid for removal of the Boc group. Simultaneously, tripeptide Ac-Val-Thr(OBn)-Leu-OH was added in the reaction medium of DMF to generate tetrapeptide **5a-b**. In Scheme 1A, the **5a** and **5b** compounds were reacted with respective reagents under specific reaction conditions to generate compounds **5c** and **5d** as shown in Scheme 1B, the **9a** and **9b** compounds were reacted with appropriate reagents under specific reaction conditions to get another **9c** and **9d** compounds^{67,68}. Another compound **11** was synthesized without the keto-phthalhydrazide group to analyze the effect of tetrapeptide moiety in the compound **9a-d**, as shown in Scheme 1C. In-silico studies of the inhibitor **9b** revealed that the pyrrolidine-2-one of S1 site interacted with His163 and nitro group of 5-nitro-2,3-dihydrophthalazine-1,4-dione of S2 site interacted with Asn142 residue of the protease (Figure 8). From all synthesized molecules, **9b** has been found the most potent reversible inhibitors against SARS-CoV 3CLpro with IC_{50} value 0.6 μM (Figure 8)²³.

3.1.2. Anilide analogues:

A multiple series of peptide anilides were developed by Shie and co-workers in 2005 based on antihelmintic drug (Niclosamide)⁶⁹ and evaluated the anti-SARS activity targeting the 3CLpro enzyme²⁴. The anilide analogues were derived from 2-chloro-4-nitroaniline, L-phenylalanine, and 4-(dimethylamino)benzoic acid. Based on 2-chloro-4-nitroanilide containing dipeptide (Scheme 2, 2A), Shie et al synthesized various anilide analogues, such as tripeptide anilide, tetrapeptide anilide, dimeric anilide, and ketomethylene anilide (Scheme 2, 2B and 2C).

The di-peptide anilides analogues **14a-e** were synthesized by

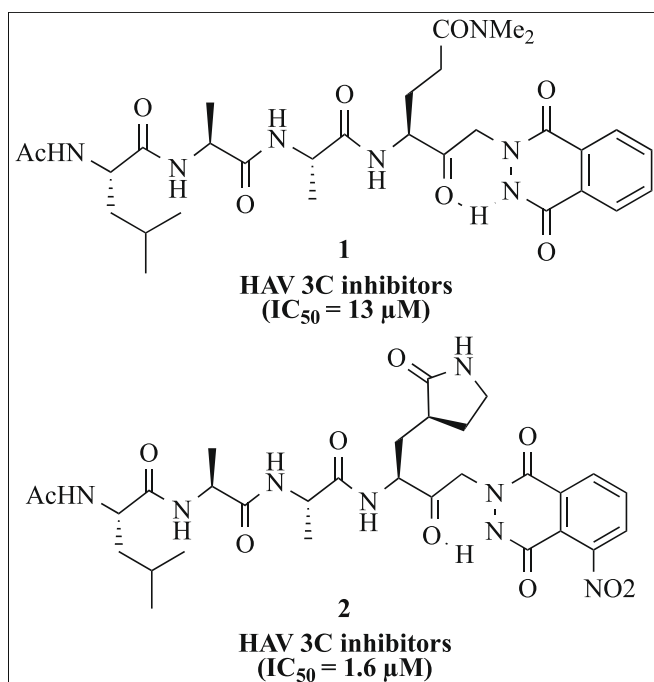


Figure 7. Keto-glutamine peptides as a potent inhibitor of HAV 3C-pro.

following previously reported synthetic strategy⁷⁰. First, **12** was reacted with Boc-L-phenylalanine to produced **13** and then, **13** was again treated with substituted carboxylic acid to produce the di-peptides **14a-e** via coupling reaction (Scheme 2, 2A). The intermediate compound **13** was taken further to synthesize the tripeptide **15a-x** and tetrapeptide anilides **16a-x** analogues via coupling with appropriate peptide (Scheme 2, 2B). The synthesis of tripeptide ketomethylene anilide analogues **22a-p** was synthesized via multistep organic reaction. First, intermediate **19** was prepared by adding two starting compounds, **17**, **18**, and then **19** was again reacted with HCl to remove Boc protection and substituted with respective R_1COCl to form compound **20**. The compound **20** further on coupling with another 2-chloro-4-nitroaniline derivative **21** in the presence of Palladium-tetrakis(triphenylphosphine) form tripeptide anilide analogues **22a-p**.

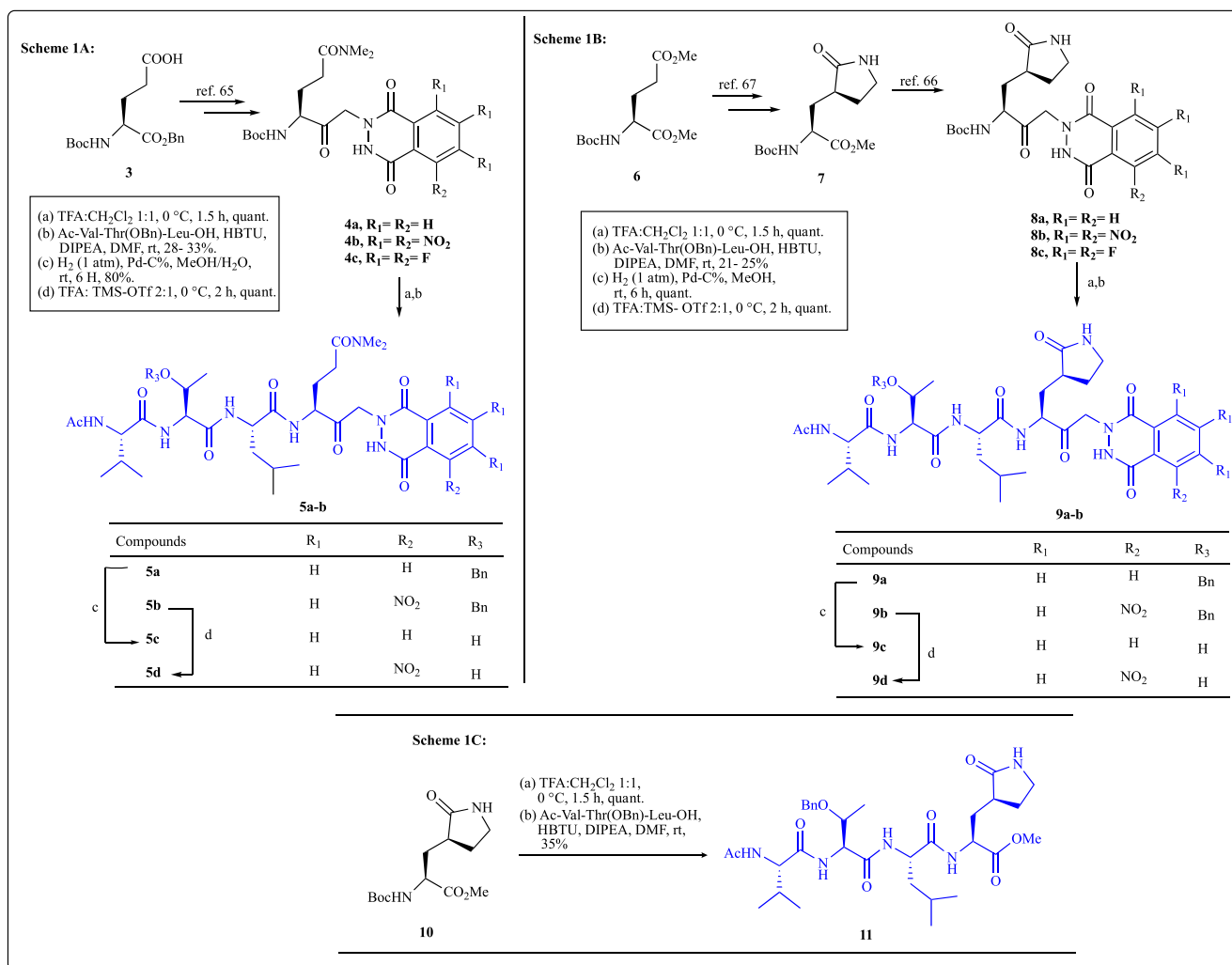
All the synthesized molecules were screened via biological assay with fluorogenic tetrapeptide substrate⁷¹, and the molecular docking study with PDB ID (1UK4) showed the binding affinity towards SARS-CoV 3CLpro enzyme. Under anilide peptide analogues, the most potent structure is **14a** (shown in Figure 7), which acts as a competitive inhibitor of SARS-CoV 3CLpro with IC_{50} value 0.06 μM and K_i value 0.03 μM . Computer-modelling of the inhibitor **14a** binding with SARS-CoV 3CLpro found that the benzyl group of S1 site was occupying Cys145, Ser144, His163, and Phe140 or the pocket formed by Thr25, His41, Cys44, Thr45, and Ala46. The 2-chloro-4 nitro benzyl group comprising the S2 site was found to interact with Ala46, while the chlorine atom is within 3 Å of Cys145 and His41. The dimethylamino benzyl of S3 site was found to be fitted into the pockets formed by Gln189-Gln192 and Met165-Pro68 residues (Figure 8)²⁴.

3.1.3. Peptidomimetic α,β -unsaturated esters:

In 2005, Shie and co-researchers synthesized a series of peptidomimetics containing α,β -unsaturated esters targeting the 3CLpro for SARS-CoV²⁵. Researchers have synthesized a compound AG7088 and its related tripeptide α,β unsaturated ester, and ketomethylene isosteres (Scheme 3) and evaluated their inhibitory properties against SARS-CoV 3CLpro enzyme. These unsaturated peptidomimetic esters and ketomethylene isosteres showed moderate inhibition against the same enzyme. AG7088, previously reported as a potent PI active against HRV-3CLpro that contain an α,β -unsaturated ester side chain⁷². Based on this evidence, it has been thought that AG7088 could be a potent inhibitor of SARS-CoV 3CLpro but, it turned out to have no inhibition even in the concentration of 100 μM in an enzymatic assay. Although the related α,β unsaturated ester and ketomethylene isosteres were showed moderate inhibitory activity against SARS-CoV 3CLpro enzyme with IC_{50} value ranging from 11 to 39 μM ²⁵.

The synthesis of PIs (AG7088) containing α,β -unsaturated ester warhead and related compounds were synthesized based on previously developed literature^{25,73}. The synthesis strategy was divided into three parts: Scheme 3, 3A, for the synthesis of intermediate **27**; Scheme 3, 3B, for the synthesis of intermediate **30**; and Scheme 3, 3C, for the synthesis of PIs (AG7088) via coupling of **27** and **30** intermediates.

Based on molecular modelling study, four different series (**1**, **2**, **3**, and **4**) of AG7088 were designed and established. The series **1**, **2**, **3**, and **4** were synthesized by changing in the three locations of the AG7088 (Scheme 3, 3C). From that above series, it was found that the series **4** compounds were most promising for SARS-CoV 3CLpro inhibition. The set of Phe-Phe dipeptides containing conjugated amido moieties at the N-terminals were designed with the help of software. The series **4** compounds **38a-e** were synthesized by using previously reported methods⁷⁴. The main starting material for the synthesis of **38a-e** is Phe-Phe dipeptidyl α,β -unsaturated ester (Scheme 3, 3C). Amidation of N-Boc-phenylalanine by 4-amino-5-phenyl-2-pentanoate and subsequent removal of Boc group with the help of 1,4-dioxane and HCl produces compound Phe-Phe dipeptides α,β -unsaturated ester. Then, with compound Phe-Phe dipeptides α,β -unsaturated ester, several α,β -unsaturated carboxylic acid were reacted to produce a series of analogues (Scheme



Scheme 1. Synthesis of Keto-Glutamine analogues. **Scheme 1, 1A:** Synthesis of N,N-dimethylglutamine analogues; **Scheme 1, 1B:** Synthesis of cyclic glutamine analogues with keto-phthalhydrazide moiety; **Scheme 1, 1C:** Synthesis of cyclic glutamine analogues without keto-phthalhydrazide moiety.

3, 3C). Before isolating the compounds, they have done an enzymatic assay and found that the compound **38c** was the most potent inhibitor against SARS-CoV 3CLpro enzyme (Figure 8). Molecular modelling study reveals that, out of four series of compounds, the compounds of series 3 and 4 showed better inhibitory results than the compounds of 1 and 2 series against SARS-CoV 3CLpro enzyme. The in-silico study of compound **38c** indicates that the (dimethylamino)cinnamyl group of S1 site was occupied by Glu166, Gln189, and Gln192 residues via hydrogen bonding (Figure 8) ²⁵.

3.1.4. Glutamic acid and glutamine peptides:

It has been established that glutamic acid and glutamine peptides with trifluoromethyl ketone groups show good inhibitory activity against the 3CLpro of SARS-CoV. Sydnes and co-workers synthesized a new series of tri- and tetra-glutamic acid and glutamine peptide and evaluated against 3CLpro inhibitory activity using a fluorescence-based peptide cleavage assay ²⁶. Many research groups suggested that the trifluoromethyl ketone (CF₃-ketone) moiety containing molecules play an important role in protease enzyme inhibition and an important group for fluorescence. Due to this background information, they thought that the trifluoromethyl ketone (CF₃-ketone) could play a key role in SARS-CoV 3CLpro inhibition. Based on substrate binding recognition, the synthetic strategy of CF₃-ketone containing glutamic acid and glutamine peptides has been designed. Four peptides were synthesized and biologically evaluated (enzyme inhibition assay) against SARS-CoV 3CLpro using

fluorogenic substrate (**Scheme 4: Series 4A, 4B, and 4C**). Although the related four peptides showed moderate inhibitory activity against the SARS-CoV 3CLpro enzyme, the most potential CF₃-ketone containing glutamic acid and glutamine peptide was **53** with K_i value 116.1 ± 13.6 μM (Figure 8) ²⁶.

The Synthesis of CF₃-ketone containing glutamic acid and glutamine peptides can be accomplished by starting with compound **39**. The synthesis of target compounds were divided into three parts: **Scheme 4, 4A**, synthesis of intermediate **45** (trifluoromethyl-β-amino alcohol), **Scheme 4, 4B**, synthesis of intermediate **48** (glutamic acid and glutamine peptides with a CF₃-ketone unit), and **Scheme 4, 4C**, Synthesis of the target compound (glutamic acid and glutamine peptides with a CF₃-ketone unit) by coupling reaction. First, compound **39** was treated with paraformaldehyde and *para*-toluene sulfonic acid in a toluene mixture to produce oxazolidinone acid **40**. The formation of oxazolidinone acid **40** was developed by Luesch et al ⁷⁵. Then, compound **40** was transferred into **41**, and subsequently, compound **41** was also converted into **42** under specific reaction conditions (**Scheme 4, 4A**). The compound **42** was formed in two forms of stereoisomers, but the diastereomer form of **42** was further reacted with TBAF to produce **43**. Then, the compound **42** and **43** were also transferred into compound **44** by reacting with sodium borohydride and methanol. Finally, by hydrogenation using Pd/C, compound **44** was transferred into final product **45** (**Scheme 4, 4A**). The second part of synthesis is focused on peptide formation. The target compound **48** was synthesized based on published literature ^{76,77}. At

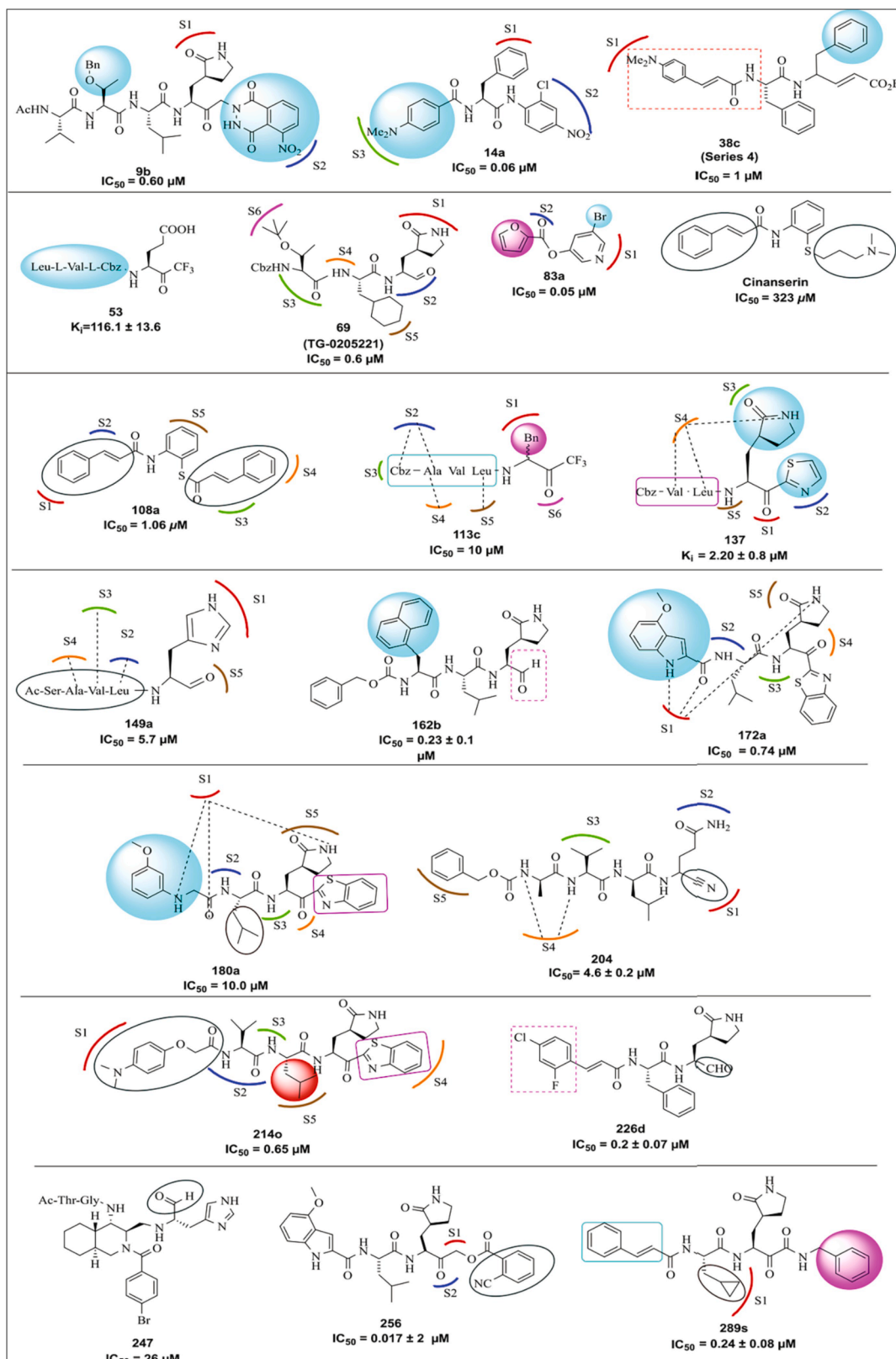
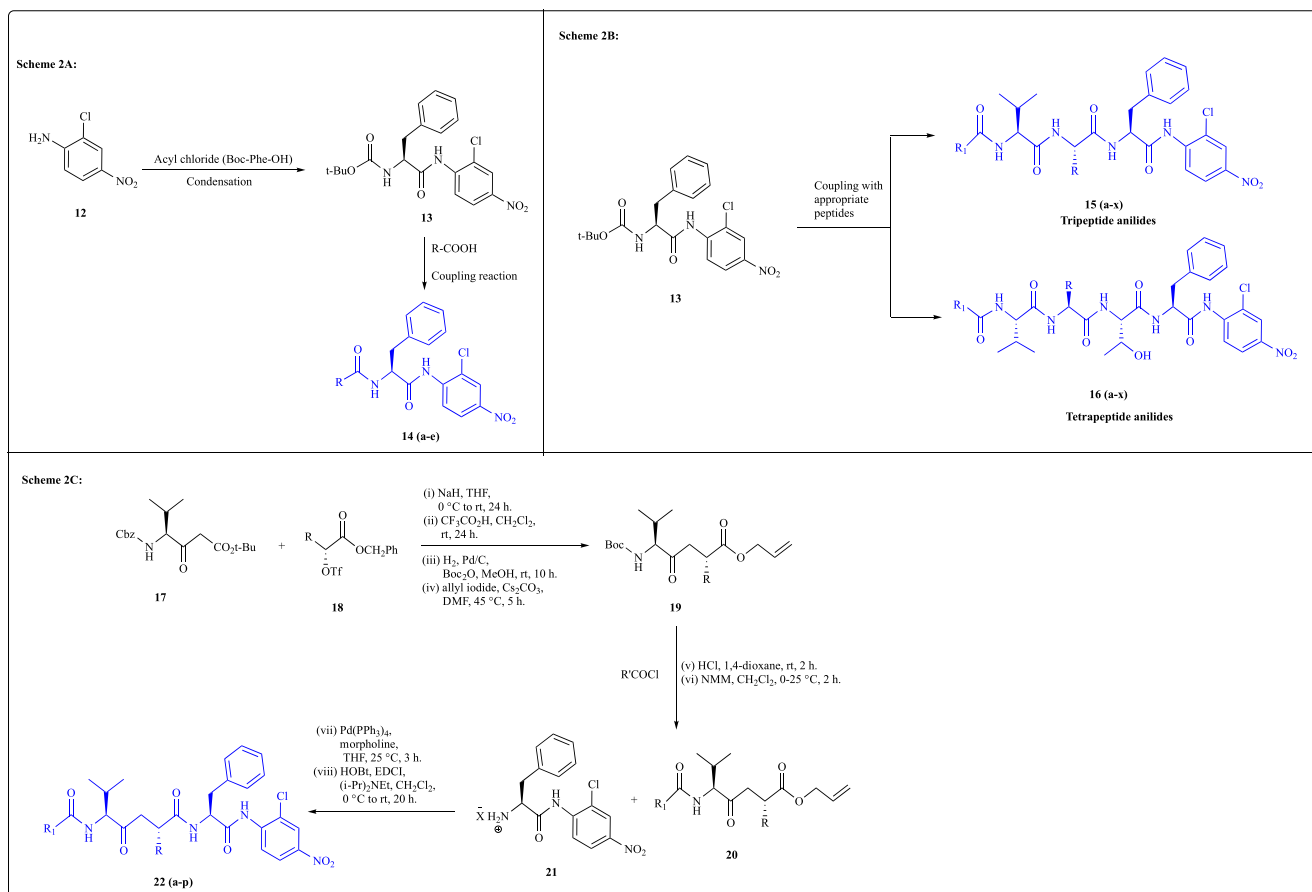


Figure 8. Structure of peptidomimetic SARS-CoV 3CLpro inhibitors (9b, 14a, 38c, 53, 69, 83a, cinanserin, 108a, 113c, 137, 149a, 162b, 172a, 180a, 204, 214o, 226d, 247, 256 and 289s).

first, compound **46** was treated with H_2 and Pd/C for the hydrogenation process that produced compound **47**. Further, it was coupled with Cbz-L-Ala-OSu under basic medium to produce target peptide **48** (Scheme 4, 4B). In the third part of the synthesis, the starting compound **45** was

synthesized as shown in Scheme 4, 4A. The compound **45** was reacted with different synthesized peptides such as: **46**, **48**, and **49** to get respective product **50**, **51**, and **52**. Then, compounds **50**, **51**, and **52** reacted with TFA for removal of *tert*-butyl group to form compound **53**,



Scheme 2. Synthesis of anilide analogues. **Scheme 2, 2A:** Synthesis of di-peptide anilides analogues; **Scheme 2, 2B:** Synthesis of tripeptide and tetrapeptide anilides analogues; **Scheme 2, 2C:** Synthesis of tripeptide ketomethylene anilide analogues.

54, and **55**. In the final step, the last forming compounds **53**, **54**, and **55** were converted into respective compounds **56**, **57**, and **58** under suitable reaction conditions (**Scheme 4, 4C**)²⁶.

3.1.5. Peptidomimetic (TG-0205221):

TG-0205221 is a synthetic compound designed and synthesized by the scientists Syaulan Yang and their research group in 2006²⁷. The compound was compared with one natural peptide substrate and it was found that the natural compound showed moderate inhibition against the 3Cpro enzyme but a lower inhibitory activity against 3CLpro of SARS-CoV. Also, from the crystal structure of the drug-receptor complex, it was established that TG-0205221 binds firmly with the 3CLpro enzyme with extensive hydrophobic contact and involves ten hydrophobic bonds and one covalent bond. The compound TG-0205221 (**69**) was synthesized by a multi-step organic reaction showed in **Scheme 5** and evaluated the inhibitory activity against SARS-CoV 3CLpro by using 229E and MRC-5 cells. The cytopathic effect was also performed with infected SARS-CoV Vero E6 cells. TG-0205221, **69** showed exceptional activity against SARS-CoV with K_i value 0.053 μM shown in **Figure 8**.

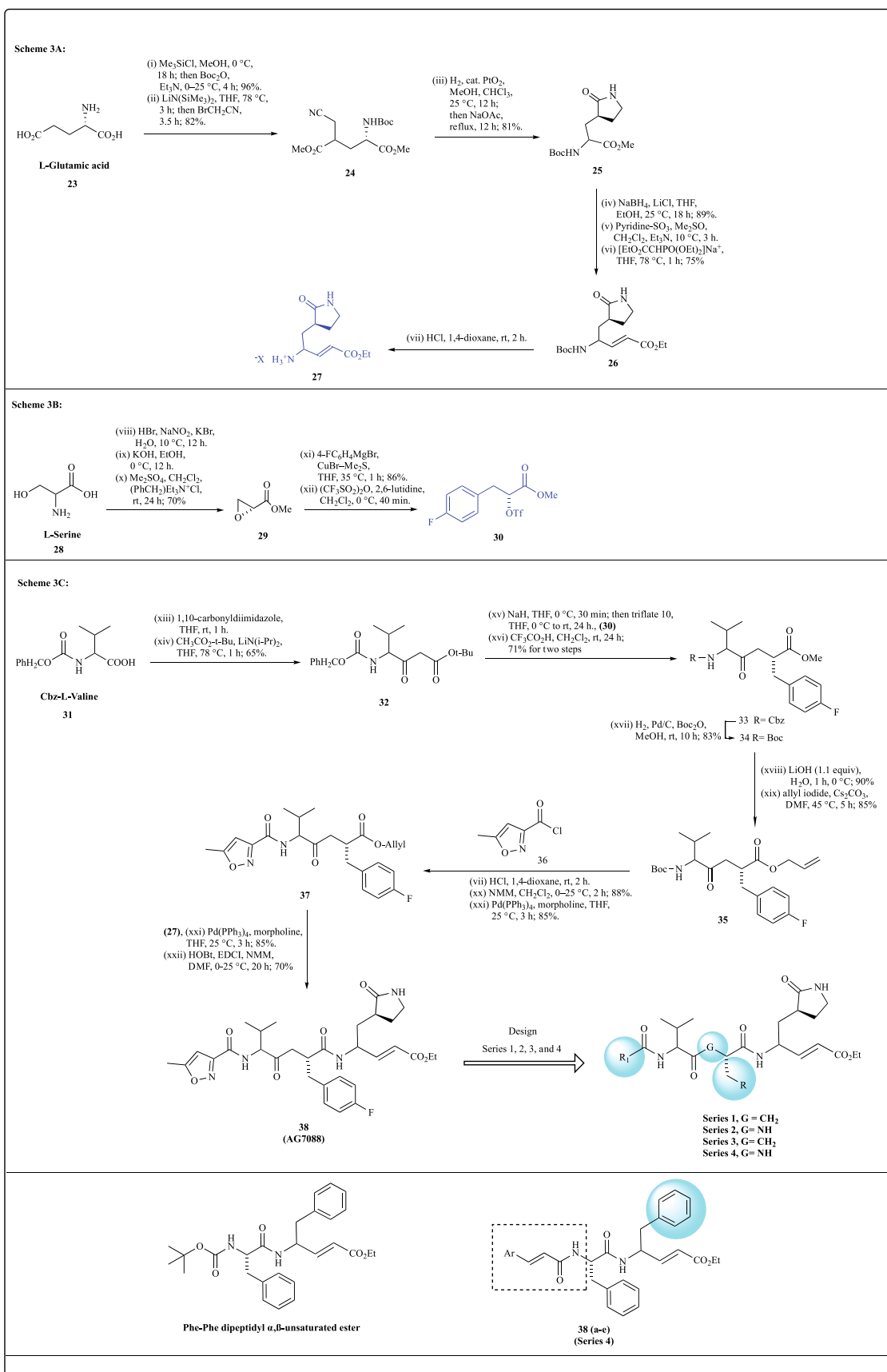
The synthesis of TG-0205221 (**69**) can be accomplished by a multi-step organic reaction. First, the L-Glutamic acid **59** was reacted with trimethylsilyl chloride and methanol as a solvent for 15 h and continued the reaction. After the desired time, the amine group was protected with Boc by adding Di-*tert*-butyl decarbonate and tri-ethylamine; and formed the compound **60**. The compound **60** was again treated with strong base Lithium bis(trimethylsilyl)amide and bromo acetonitrile to get the compound **61**. The intermediate compound **62** was formed by the hydrogenation of compound **61** and further reacted with base triethylamine to form cyclization product **63**. Next, Boc protection of compound **63** was removed by adding the HCl at room temperature. After that, the

addition of Boc-β-cyclohexyl-Ala-OH to the compound **64** produces the compound **65** and further deprotection of Boc produces the compound **66**. In the next step, the Cbz-Thr(*t*Bu)-OH was reacted with compound **66** to form compound **67**. In the final step, the ester group of compound **67** was transferred to the alcohol by reacting with lithium hydride and forming compound **68**. Further, reaction with triethylamine produced the final compound **69** (**Scheme 5**).

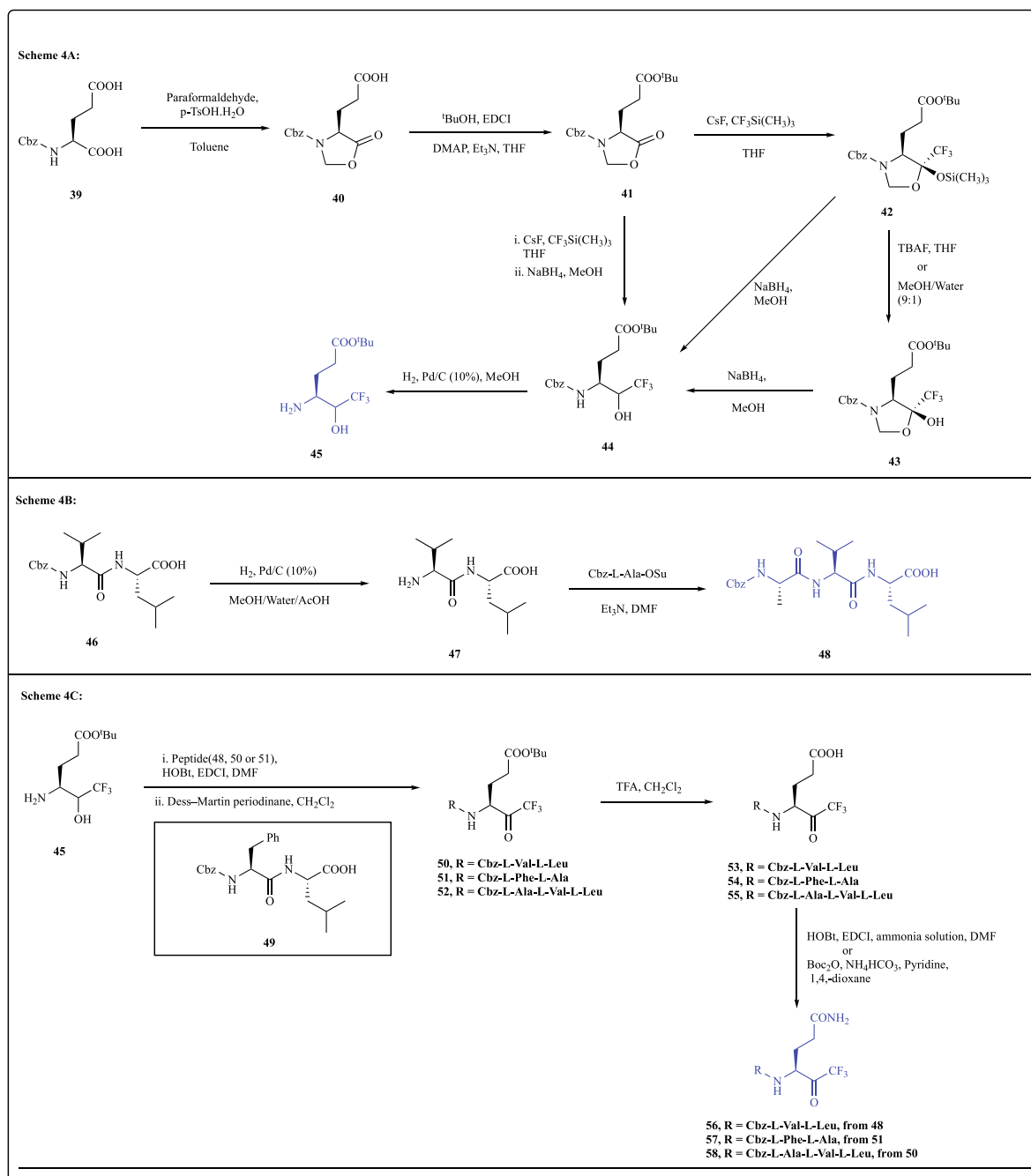
An in-silico study detected the binding interaction of compound **69** with 3CLpro. The result showed that the pyrrolidine-2-one of the S1 site was interacting with His163, Glu166, Phe140, and Asn142 residue. The amino acid residues, such as His164, Cys145, and Gly143, also interacted with the S2 site of aldehyde moiety. Similarly, in the N of -NHCbz and O of acetamide S3 site, the Glu166 amino acid residue interacted. The S4 site comprising amide residue was found to interact with Gln189 residue and cyclohexane moiety of S5 site interacted with His41. The trimethyl group of S6 site interacted with Met165, Leu167, Pro168, Asp187, Met49, Ala191, Arg188, and Thr190 residue (**Figure 8**)²⁷.

3.1.6. Phthalhydrazide peptide analogues:

Zhang et al designed and synthesized a series of tetrapeptide containing phthalhydrazide ketones, pyridinyl esters, and their different analogues²⁸. They have designed the molecules based on a previous literature report on potent SARS-CoV 3CLpro inhibitor and screened the three compounds, such as keto-glutamine analogues²³, AG7088⁷⁸, and aromatic ester⁷⁹; for the development of new potent SARS-CoV 3CLpro inhibitor molecule. They synthesized the designed peptides molecules via **Scheme 6: 6A, 6B, and 6C**. The pyridinyl esters and their different analogues were also synthesized by two methods (method A and method B), shown in **Scheme 6E, Scheme 6F, Scheme 6G, and Scheme 6H**. All synthesized molecules were evaluated as SARS-CoV 3CLpro inhibitors



Scheme 3. Synthesis of peptidomimetics (AG7088) containing α,β -unsaturated ester warhead. **Scheme 3, 3A:** Synthesis of intermediate 27; **Scheme 3, 3B:** Synthesis of intermediate 30; **Scheme 3, 3C:** Synthesis of peptidomimetic (AG7088) via coupling of 27 and 30 intermediates.

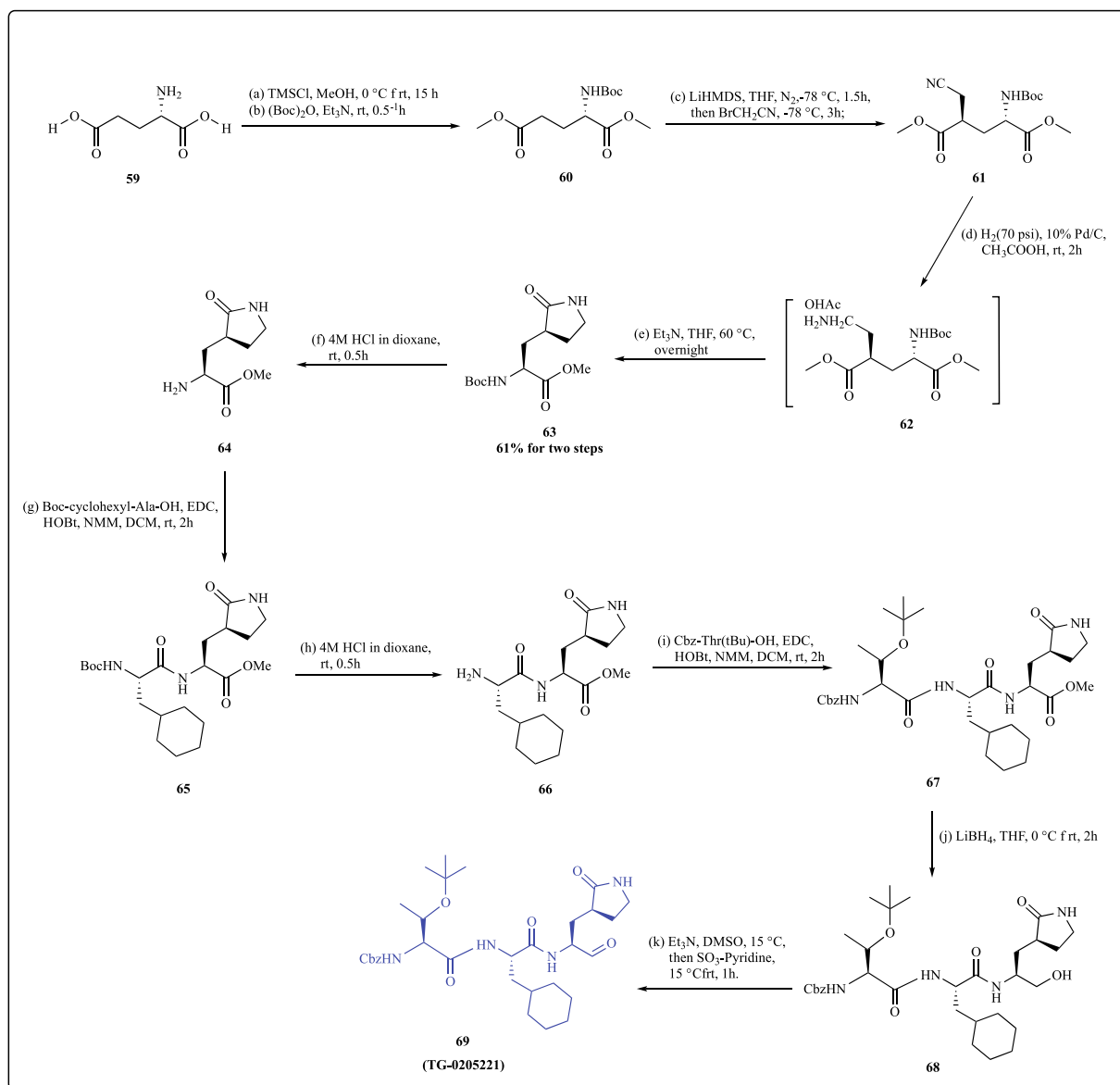


Scheme 4. Synthesis of CF₃-ketone containing glutamic acid and glutamine peptides. **Scheme 4, 4A:** Synthesis of intermediate **45** (trifluoromethyl-*b*-amino alcohol); **Scheme 4, 4B:** Synthesis of intermediate **4z** (glutamic acid and glutamine peptides with a CF₃-ketone unit); **Scheme 4, 4C:** Synthesis of target compound (glutamic acid and glutamine peptides with a CF₃-ketone unit) by coupling reaction.

by enzyme assay (FRET assay). The assay result revealed that some pyridinyl esters were a potent inhibitor against SARS-CoV 3CLpro with IC₅₀ value ranging from 50 to 65 nM. Among them, the most potent inhibitor is **83a** (IC₅₀ value- 0.05 μM) (Figure 8)²⁸.

The synthesis of tetrapeptide **73** started via bromination of Boc-L-phenylalanine **70** in the presence of Ethyl chloroformate and triethylamine. The brominated product **71**, then reacted with Phthalhydrazide using DMF as the solvent and formed a new substituent product **72**. In the last step of the reaction, compound **72** was treated with analogue of peptide molecule Ac-Val-Thr(OBn)-Leu-OH under suitable reaction conditions to produce the final tetrapeptide compound **73** (Scheme 6, 6A). The other two tetrapeptides, **77** and **78** were also synthesized by changing the carboxylic part of compound **74**. At first,

the Boc-protected cyclic glutamic acid **74** was reacted with *N*,*O*-Dimethylhydroxylamine hydrochloride and other reactants, formed compound **75**. Then, compound **75** was substituted with 2-Thienylmagnesium bromide under Isopropylmagnesium chloride solution to form compound **76**. From this substituted product **76**, the two tetrapeptides **77** and **78** were formed by reacting with different peptides (Scheme 6, 6B). Based on Scheme 6, 6B, they have synthesized another tetrapeptide **82**, where the starting compound is Boc-protected cyclic glutamic acid ester **79**. In the same fashion, the intermediates compounds were synthesized by reacting with peptide molecule, and treatment of lithium hydroxide leads to the compound **81**. In the last step, the 5-Chloro-3-pyridinol was treated with compound **81** to produce the tetrapeptide compound **82**. To explore the effect of Chloropyridinyl Esters in



Scheme 5. Synthesis of inhibitor TG-0205221 (69).

tetrapeptides, they have designed two methods (Method A and B) for synthesizing a series of tetrapeptides containing 3-Chloropyridinyl Esters group (Scheme 6, 6D). The 3-Chloro-5-furan-(2-ylmethoxy)pyridine **85** was formed by reacting compound **84**, 3-Chloro pyridinol and triphenylphosphine (Scheme 6, 6E). The Furan-2-yl Nicotinate **87** was synthesized by the reaction of compound **86**, thionyl chloride, and 2-Furanone (Scheme 6, 6F). Another N-(Pyridin-3-yl)thiophene-2-sulfonamide **89** was also synthesized by treating compound **88** with 3-Aminopyridine (Scheme 6, 6G). The synthesis of 2-(Pyridin-3-yl)-1-(thiophen-2-yl)ethanone **92** and 2-(5-Bromopyridin-3-yl)-1-(furan-2-yl)ethanone **95** are shown in Scheme 6H and 6I. To explore the effect of aldehyde group, they synthesized the thiazole-4-carbaldehyde **97** and 5-(4-Chlorophenyl)furan-2-carbaldehyde **99** (Scheme 6, 6J, and 6 K).

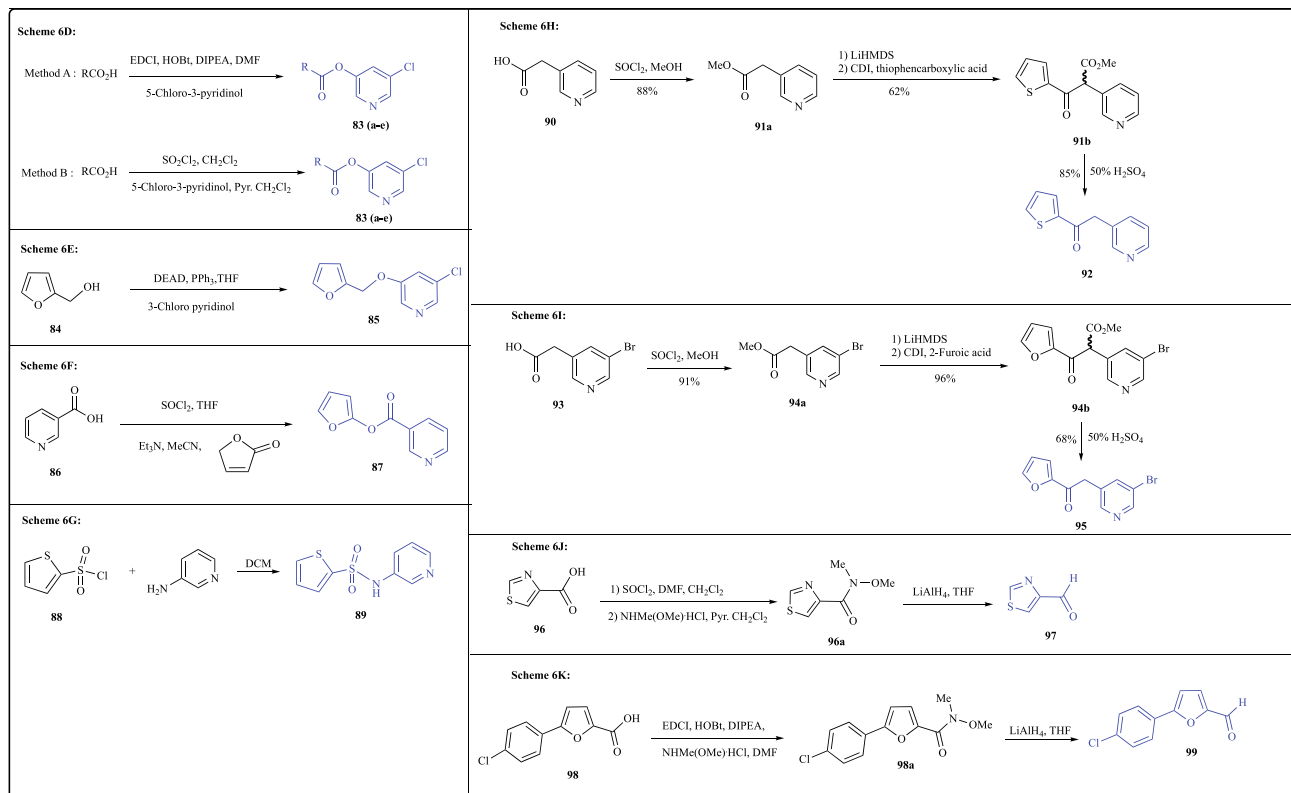
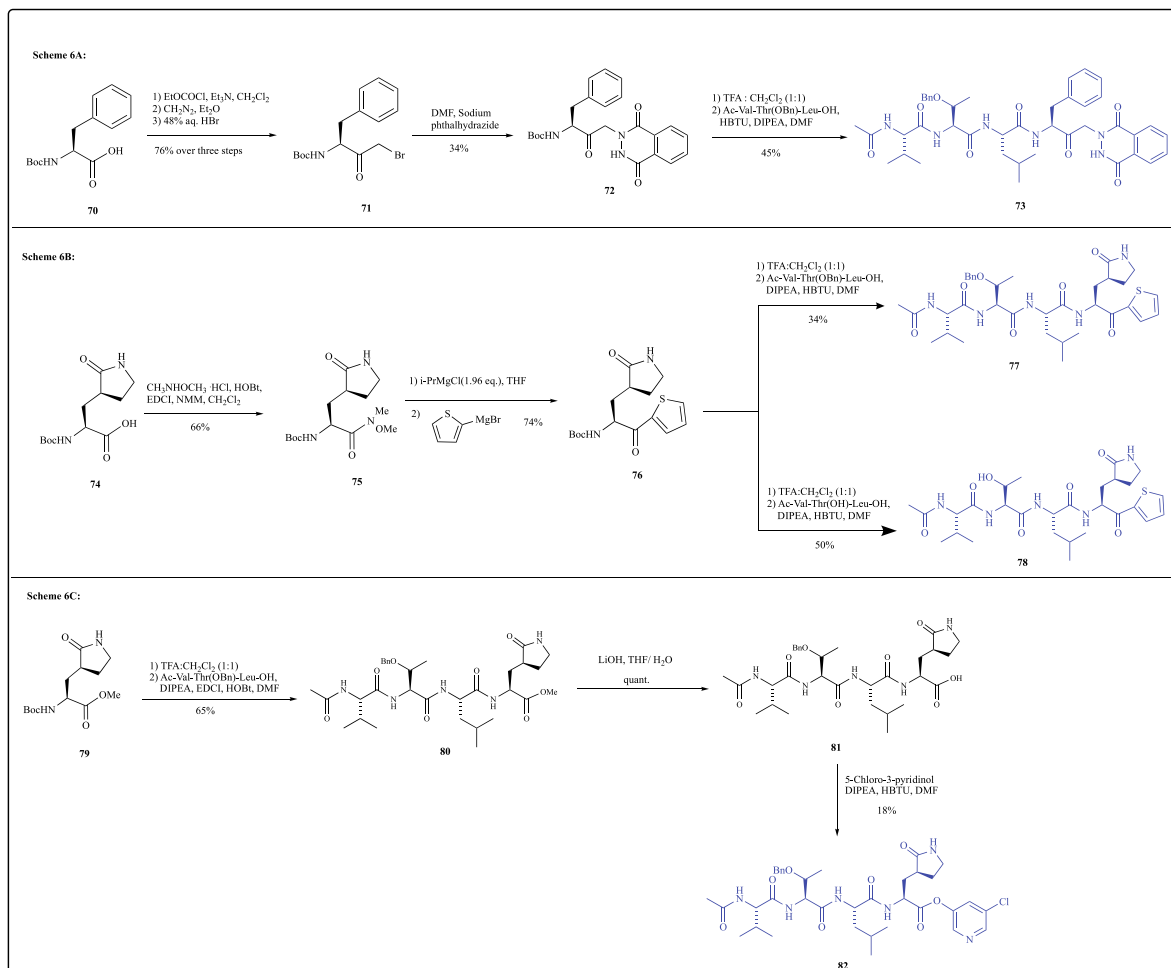
The result obtained from the in-silico study of compound **83a** showed that the pyridine ring in the S1 site of the compound interacted with the Phe140, Leu141, Asn142, Glu166, His172, His163 amino acid residue and that of the keto group of S2 site interacted with the Ser144, Gly143, Cys145 amino acid residue of the protease (Figure 8)²⁸.

3.1.7. Cinanserin analogues:

Cinanserin is a 5-HT receptor antagonist which was discovered in the

1960 s and clinically used in the treatment of neurological disorder in 1973 s. In 2005, Chen et al identified the cinanserin as an inhibitor of SARS-CoV 3CLpro, which was virtually screened from the structural database of existing drugs (more than 8000) and identified the best-fitted molecule to the target (SARS-CoV 3CLpro) through docking study. The virtual screening has identified the top 10 potential molecules that can act as anti-SARS agents and cinanserin is one of them. To confirmed the anti-SARS activity, the cinanserin was further evaluated in HCoV-229E tissue culture assays. It showed that the cinanserin has strong anti-SARS activity (IC₅₀ ranging from 19 to 34 μM) via inhibiting the 3CLpro⁸⁰.

Based on the above research findings, the same research group designed and synthesized a series of cinanserin analogues (Figure 8) for SARS-CoV 3CLpro inhibition by collaborating the work with another research group and published the potential cinanserin analogues in 2008. All synthesized compounds were evaluated against SARS-CoV 3CLpro by FRET assay and showed that some of the compounds are potent and selective inhibitors with IC₅₀ values ranging from 1.06 to 43.7 μM. The most potential cinanserin analogue is shown in Figure 8 (108a, IC₅₀ value- 1.06 μM) and molecular interaction data showed that, the compound **108a** binds tightly with 3CLpro enzyme subsite than



(caption on next page)

Scheme 6. Phthalhydrazide peptide analogues. **Scheme 6, 6A:** Synthesis of tetrapeptide **73**, **Scheme 6, 6B:** Synthesis of tetrapeptide **77** and **78**; **Scheme 6, 6C:** Synthesis of tetrapeptide **82**; **Scheme 6, 6D:** Synthesis of a series of 3-Chloropyridinyl Esters by Method A or B; **Scheme 6, 6E:** Synthesis of 3-Chloro-5-furan-(2-ylmethoxy)pyridine (**85**); **Scheme 6, 6F:** Synthesis of Furan-2-yl Nicotinate (**87**); **Scheme 6, 6G:** Synthesis of and N-(Pyridin-3-yl)thiophene-2-sulfonamide (**89**); **Scheme 6, 6H:** Synthesis of 2-(Pyridin-3-yl)-1-(thiophen-2-yl)ethanone (**92**); **Scheme 6, 6I:** Synthesis of 2-(5-Bromopyridin-3-yl)-1-(furan-2-yl)ethanone (**95**); **Scheme 6, 6J:** Synthesis of Thiazole-4-carbaldehyde (**97**), **Scheme 6, 6K:** Synthesis of 5-(4 Chlorophenyl)furan-2-carbaldehyde (**99**).

cinanserin²⁹.

The cinanserin analogues were designed and synthesized via three series; **series I**, **series II**, and **series III**. In **series I** (**Scheme 7**), the compound **100** was reacted with various alkyl halides in the presence of isopropyl alcohol to produce the respective substituted product **101a-n**. Again, these products are treated with substituted acyl chloride in the reaction medium and produce the final substituted product **102a-n** (**Scheme 7, Series I**). Similarly, using another substituted starting material **103a-b**, they synthesized **104a-b** and **105a-b** (**Scheme 7, Series II**). In **series III**, they reacted the substituted compounds **107a-b** with previous starting material **100** and by simple condensation process, the final compound was formed **108a-b** (**Scheme 7, Series III**).

The hydrophobic interaction atom pairs between the compound **108a** and the enzyme were detected by using the LIGPLOT and it was evident that the benzyl group of S1, S4, S5 positions interacts with Thr25, Leu27, Gly143 (S1); Gln189, Met165, Cys145, Glu166 (S2); and His163, Phe140 (S3) respectively. The unsaturated alkyl chain of S2 and S3 sites was found interacting with His41 and Met49 amino acid residues (**Figure 8**)²⁹.

3.1.8. Trifluoromethyl ketone containing peptides:

In 2008, Shao and co-workers designed and synthesized a series of trifluoromethyl ketones (TFMKs) targeting the 3CLpro for SARS-CoV³⁰. The P1-P4 sites of the TFMKs plays a vital role in covalent binding with the enzyme, like that of the substrate. They designed the compounds such that incorporation of benzyl group at P1 site and long-chain alkyl/ varying amino acid at P2-P4 site significantly increased the binding ability. The four steps involved in the synthesis of the compounds is shown in **Scheme 8**. All the compounds were subjected to in vitro assay, like enzyme and fluorescent substrate peptide assay against SARS-CoV

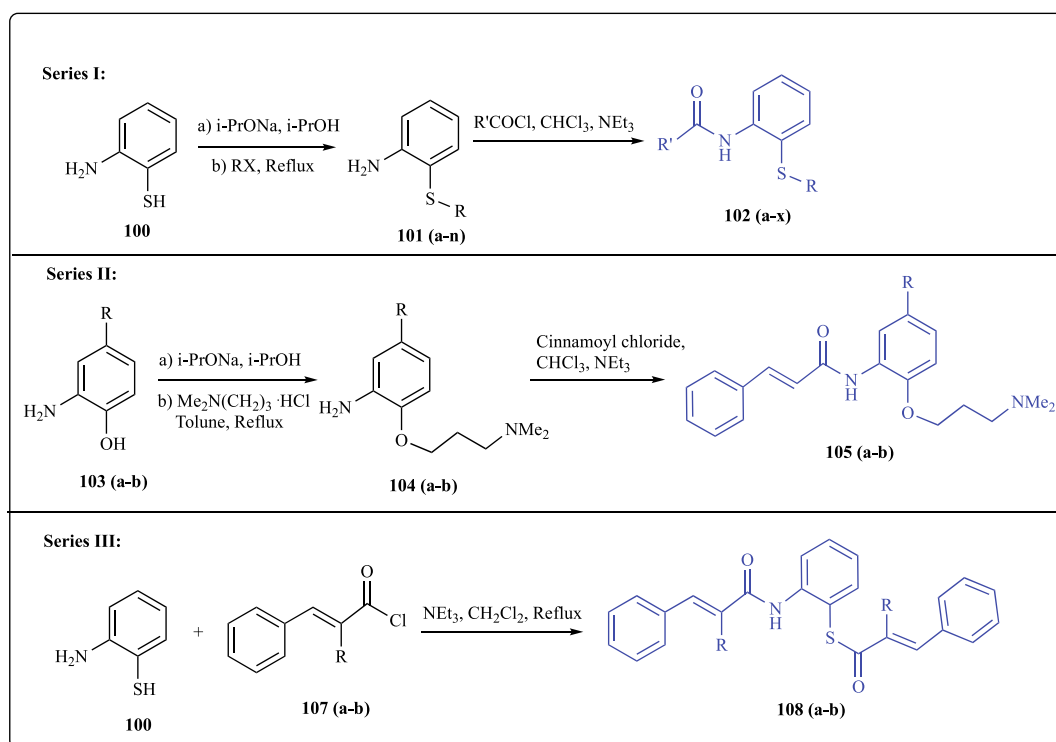
3CLpro. Amongst all the compounds, the most potent inhibitory activity was shown by compounds **113a**, **113b**, **113c** with IC₅₀ values 15 μM, 20 μM, and 10 μM, respectively. The compound **113c** also showed a time-dependent decrease in SARS-CoV 3CLpro enzyme activity with respect to inhibitor concentration when incubated with 3CLpro for 4hrs (**Figure 8**).

The synthesis of trifluoromethyl ketone containing peptides can be accomplished in four steps. In the first step, the substituted compound **109a** was reacted with sodium nitrate in the presence of DMF and formed the intermediate compound **110a-c**. Then, the compound **110a-c** reacted with Trifluoroacetaldehyde ethyl hemiacetal under reaction conditions to form compound **111a-e** and hydrogenation as well as reaction with N-protected amino acids transform the compound into **112a-g**. In the last step, reduction of compound **112a-g** leads to final compound **113a-h**, as trifluoromethyl ketone containing peptides (**Scheme 8**).

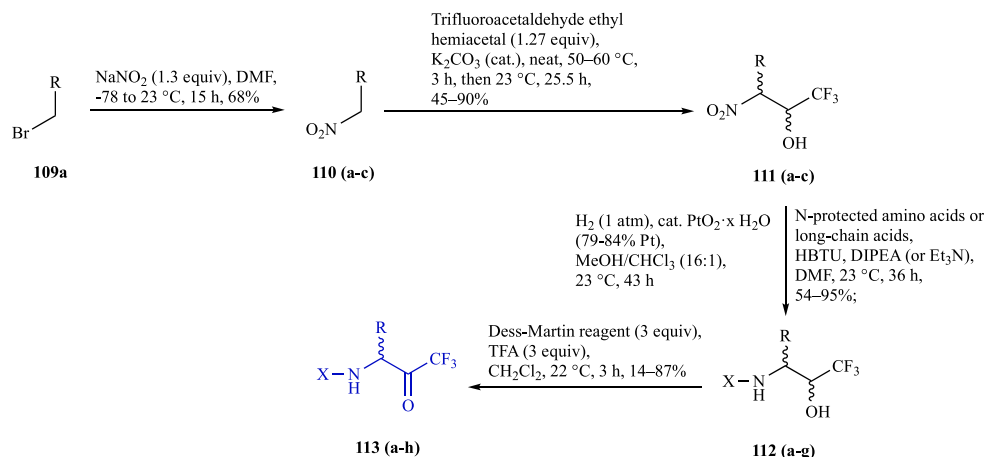
From the computational studies, the interaction between inhibitor **113c** and enzyme was studied. The interaction result showed that the benzyl group of S1 site interacting with Met165, Met49, His41, and Cbz-Ala of S2 site interacted with Gln189 amino acid residue. The cbz group of S3 site and alanine of S4 site interacting with amino acid residues, such as Pro168 (S3) and Glu166 (S4). Similarly, amino acid His163 and Phe140 were associated with leucine of S5 site; and keto group of S6 was also found to interact with amino acid residues Gly143 and Cys145 (**Figure 8**)³⁰.

3.1.9. Trifluoromethyl, benzothiazolyl or thiazolyl ketone containing peptidomimetic inhibitors:

In 2006, Cai and co-workers reported moderate activity of trifluoromethyl ketone containing peptides against SARS-CoV 3CLpro. It



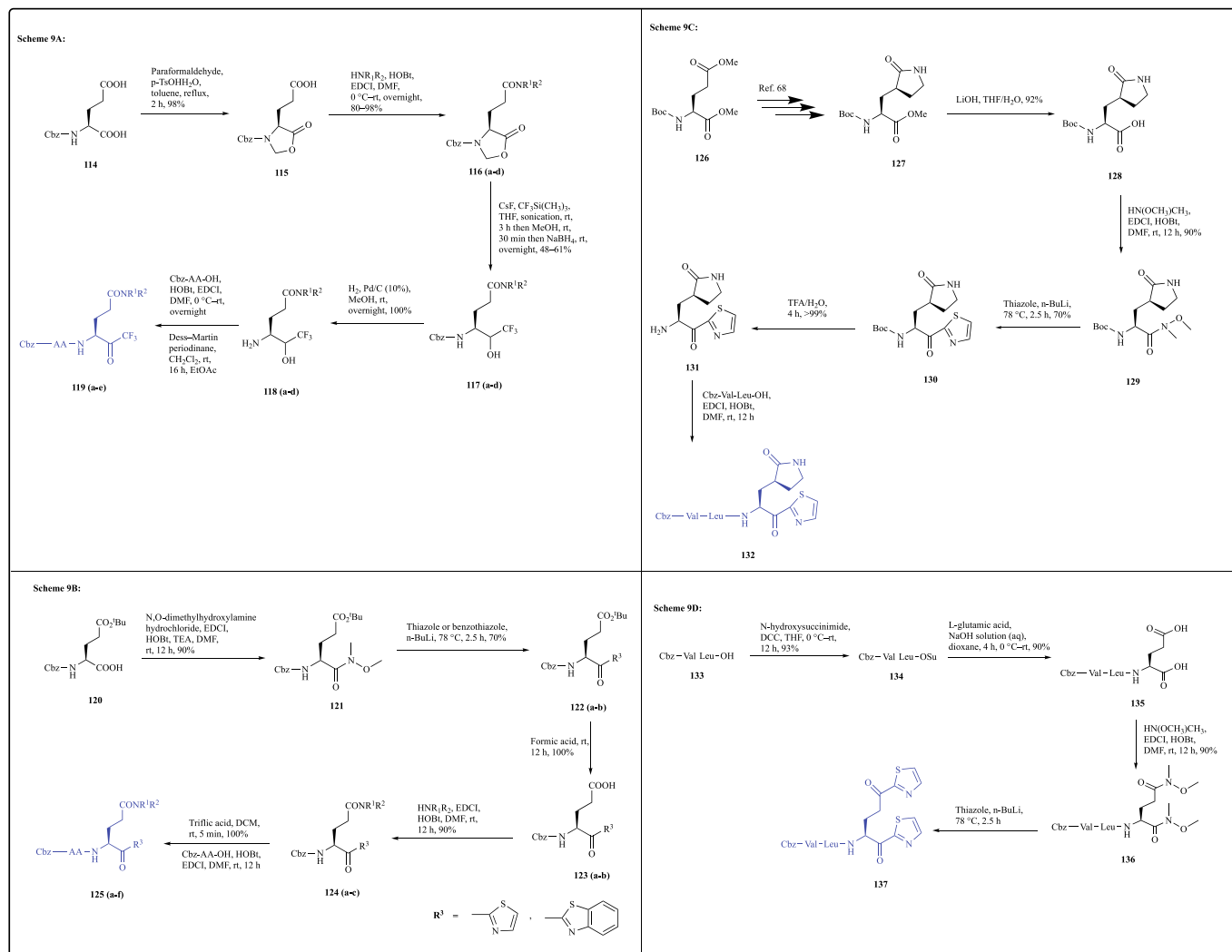
Scheme 7. Synthesis of a cinanserin analogues (Series I, Series II, and Series III).



Scheme 8. Synthesis of trifluoromethyl ketone containing peptides.

was observed that the moderate inhibitory activity of the compounds was due to cyclization of the compounds, which decreases its interaction with the active site of the SARS-CoV 3CLpro⁸¹. To increase the inhibitory activity of trifluoromethyl ketone containing peptides, Regnier T and co-

workers in 2009 designed and synthesized a new trifluoromethyl series benzothiazolyl or thiazolyl ketone-containing peptidic compounds³¹. The two approaches utilized to enhance the inhibitory activity were - Firstly, they modified the side chains of amino acid residues at the P1,



Scheme 9. Synthesis of trifluoromethyl, benzothiazolyl or thiazolyl ketone containing peptidomimetic inhibitors. Scheme 9, 9A: synthesis of CF_3 -ketone containing glutamic acid with Cbz protection, Scheme 9, 9B: Synthesis of peptides with thiazolyl and benzothiazolyl groups, Scheme 9, 9C: synthesis of pyrrolidone containing peptides, and Scheme 9, 9D: synthesis of dithiazolyl containing peptide inhibitor 137.

P2, and P3 sites keeping the trifluoromethyl ketone moiety intact. Secondly, they replaced the trifluoromethyl moiety with electron-withdrawing groups such as thiazolyl and benzothiazolyl group. The synthetic route for target compounds are shown in Scheme 9: 9A, 9B, 9C, and 9D. All the synthesized compounds were subjected to in vitro protease inhibition assay to check their 3CLpro inhibitory activity. Compounds 137 showed good inhibitory activity with K_i values 2.20 ± 0.8 (Figure 8)³¹.

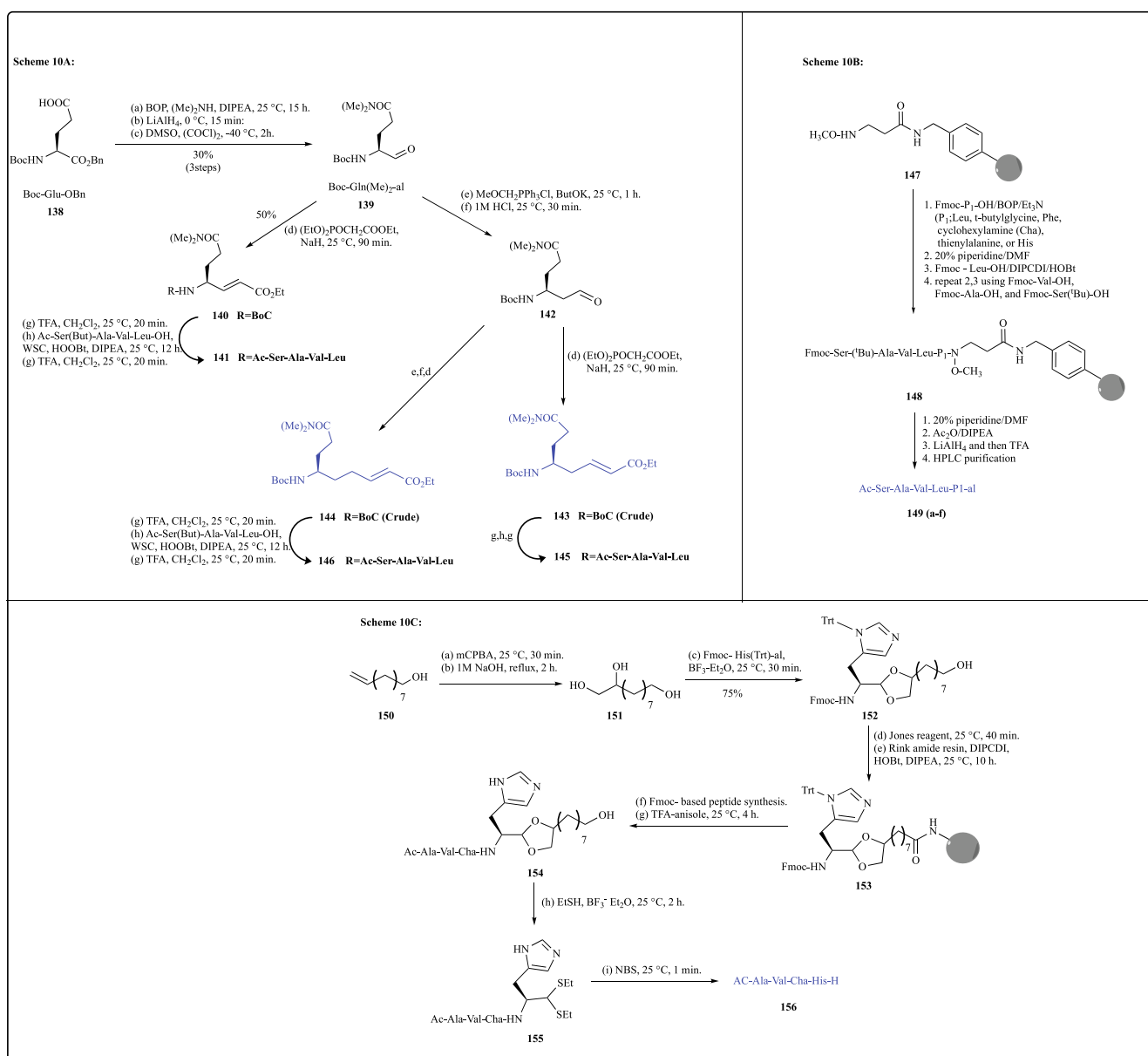
The synthetic strategy of target compounds were divided into four parts, first part: synthesis of CF₃-ketone containing glutamic acid with Cbz protection (Scheme 9, 9A), second part: replacing the trifluoromethyl moiety with electron-withdrawing groups such as thiazolyl and benzothiazolyl groups (Scheme 9, 9B), third part: synthesis of pyrrolidone containing peptides (Scheme 9, 9C), and fourth part: synthesis of dithiazolyl containing peptides (Scheme 9, 9D).

The synthesis of target compounds 119a-e were started from *N*-Cbz-L-glutamine 114 and converted to the compound 115 under specific reaction conditions. Then, compound 115 was reacted with different

amines to form the following compounds 116a-d and further converted to the compound 117a-d by using trifluoromethyltrimethylsilane. The compound 118a-d was prepared by a one-pot reaction from 117a-d under appropriate reaction conditions. In the final step, specific peptide fragments^{26,71} were reacted with previous compound 118a-d and produced the final compounds 119a-e (Scheme 9, 9A)⁷⁵.

The compounds 125a-f were synthesized in four steps. In the first step, the compound 120 was converted to amides 121 and then reacted with thiazole or benzothiazole in the presence of *n*-Butyllithium to get compounds 122a-b. In the next step, treatment with formic acid compounds 122a-b produces the compounds 123a-b and further converted into 124a-e by using substituted amines under appropriate reaction conditions. In the last step, the final compounds 125a-f were formed by reacting the compounds 124a-e with peptide molecule under appropriate reaction conditions (Scheme 9, 9B)⁸².

The compound 132 was synthesized following the previously published literature via multi-step process⁶⁸. In the first step, the compound 127 was prepared from previous literature methods⁶⁸ by using third



Scheme 10. Synthesis of Michael type of peptidomimetic inhibitors. Scheme 10, 10A: synthesis of Michael type inhibitor; Scheme 10, 10B: synthesis of peptide aldehyde 149a-f; Scheme 10, 10C: optimization and synthesis of potent peptide aldehyde inhibitor 156.

starting compound **126**. Then, the compound **127** was converted to the **128** by using lithium hydroxide and further converted to **129** under reaction conditions. After that, the compound was treated with thiazole and *n*-Butyllithium to get compound **130**. The reaction of trifluoroacetic acid and compound **130** converts into compound **131** and further converted to the final product **132** by reacting with Cbz-Val-Leu-OH under reaction conditions (Scheme 9, 9C).

Similarly, dithiazolyl compound **137** was prepared from Cbz-Val-Leu-OH **133** and converted to the compound **134** by reacting with *n*-hydroxy succinimide. Then, compound **134** reacted with glutamic acid to form the compound **135** and converted to the double-weinreb amide **136**. In the final step, the compound **136** reacted with thiazole and *n*-Butyllithium to get the final compound **137** (Scheme 9, 9D).

The binding interaction of compound **137** with the enzyme as observed in the *in silico* study showed that the keto group in the S1 site interacted with Gly143, Ser144, Cys145, the thiazole ring in the S2 site interacted with His41, keto group present in the 2nd position of pyrrolidine ring in the S3 site interacted with His163. Further, the Val-Leu and NH group of pyrrolidine comprise the S4 site found to interact with Gln189, Gln166, and that of amino group in S5 interacts with His164 (Figure 8)³¹.

3.1.10. Michael type of peptidomimetic inhibitors:

Akaji et al reported the design, synthesis and evaluation of peptide aldehyde as an inhibitor of SARS 3CLpro. The compounds were designed based on an initially reported pentapeptide aldehyde inhibitor (IC₅₀ – 37 μM), and the optimum side-chain structure was determined by comparing inhibitory activity with Michael type inhibitors. The synthetic outline and associated reaction conditions are depicted in Scheme 10: **10A**, **10B**, and **10C**, respectively³².

Protease inhibition assay was carried out on R188I mutant protease by simultaneous addition of both inhibitor and substrate to determine IC₅₀ value. The result of the experiment suggested that the peptide aldehyde is a competitive inhibitor of SARS 3CLpro because there was no evidence in the formation of a stable covalent bond between inhibitor and protease.

In literature, structural optimization following X-ray crystallographic analysis of inhibitor-protease complex gives a potent tetrapeptide aldehyde with IC₅₀ value 98 nM. The result demonstrated that peptide aldehyde could be a more effective inhibitor of SARS 3CLpro than Michael-type inhibitors³².

The synthesis of Michael type inhibitor (Scheme 10, **10A**) was started from Boc-L-Glu-OBn (**138**). Coupling of the side chain carboxyl group with dimethylamine in BOP presence as a coupling reagent produces side-chain amide, simultaneous reduction with LiAlH₄ gave alcohol upon Swern oxidation afforded aldehyde **139**⁸³. Horner – Wadsworth – Emmons olefination of aldehyde **139** produced N^α-protected amino acid ester **140**. Cleavage of the protected group by TFA and following coupling with tetrapeptide yield compound **141**. For the preparation of **145**, aldehyde **139** was converted to **142** by Wittig reaction and following an acid treatment. The Horner – Wadsworth – Emmons olefination and coupling with tetrapeptide converted **142** to **145**. To synthesize the analogue **146**, **142** was further subjected to Wittig reaction and an acid treatment as above. The following Horner – Wadsworth – Emmons olefination and coupling with the tetrapeptide yielded **146**³².

Peptide aldehyde **149(a-f)** was synthesized by using conventional Weinreb amide resin (Scheme 10, **10B**)⁸⁴. The conventional Fmoc-based solid-phase synthesis was used to introduce amino acid residues. After peptide chain construction, the resin was reduced with LiAlH₄ to obtain desired compounds.

The synthesis of structurally optimized and potent peptide aldehyde is given in Scheme 10, **10C**. The synthesis was started with commercially available 9,10-decene-1-ol **150**. Which on reaction with mCPBA and following hydrolysis obtained triol linker **151**. Under appropriate reaction conditions, **151** was reacted with Fmoc-His (Trt)al to afford

corresponding acetal **152**. The acetal alcohol on oxidation by Jones reagent yielded carboxylic acid, which in coupling reaction produced amide resin **153**. The amide resin on treatment with TFA converted to peptide acetal amide **154**. After dissolving in AcOH treated with ethane thiol in BF₃-Et₂O, and after quenching with H₂O obtained thioacetal peptide **155**. The thioacetal on treatment with NBS yields final peptide aldehyde **156**³².

The binding interaction of compound **149a** with the 3CLpro was detected from computational modeling. The result showed the interaction of pyrazole in the S1 site of the compound with His163, Phe140, Leu141, Glu166 amino acid residues of the protease. Leucine in the S2 interacted with Met45, Met165, His41. Further, Valine in S3, Alanine in S4, and aldehyde group in S5 site interacted with Glu166, Thr190, Cys145 amino acid residue, respectively (Figure 8)³².

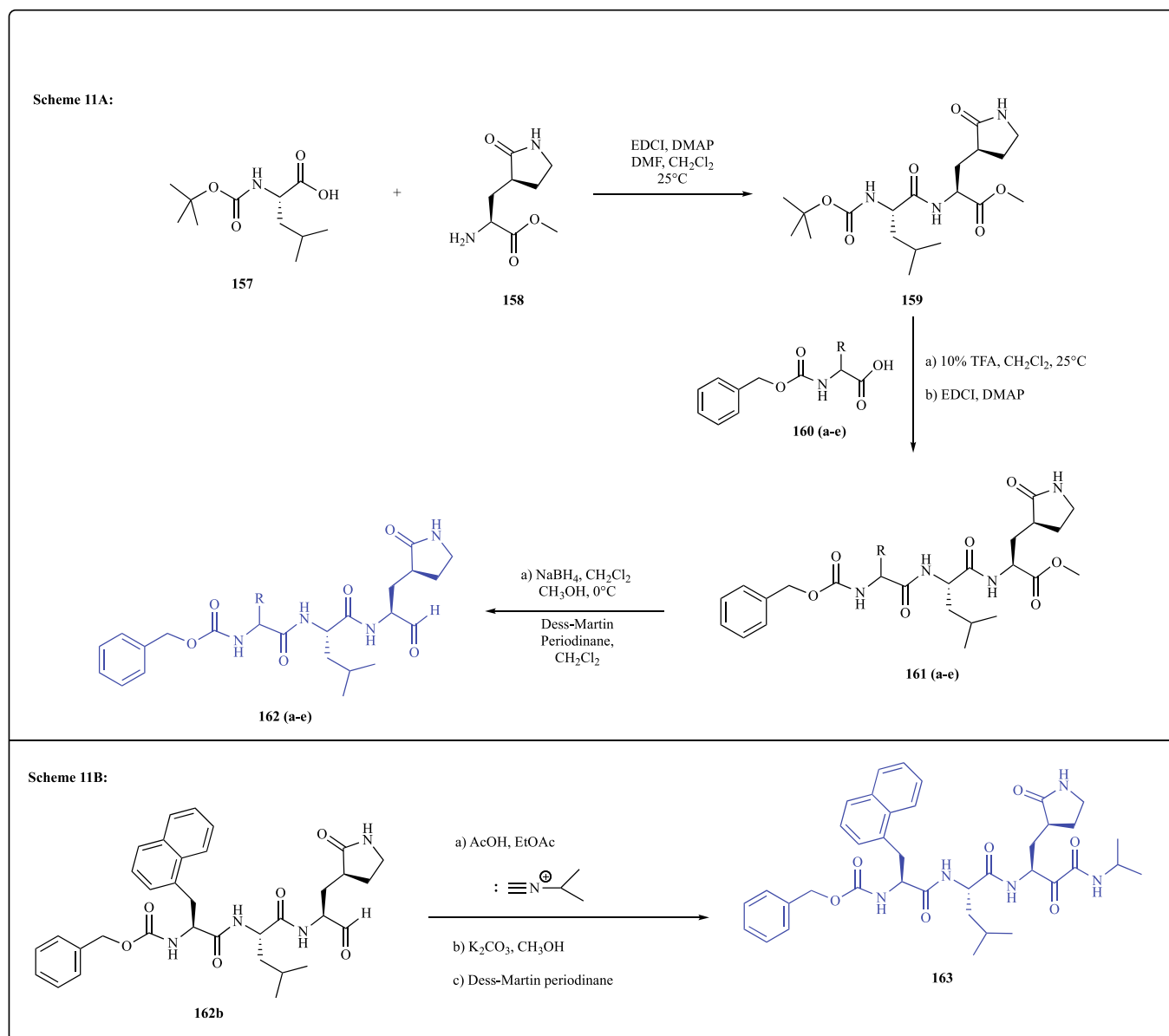
3.1.11. Tripeptide type cysteine protease inhibitors:

Prior et al designed and synthesized few transition state inhibitors in 2013. They designed these inhibitors of 3CLpro such that it contains a tripeptidyl group and warheads that include aldehyde, bisulfite adduct, a-ketoamide, or an alpha-hydroxy phosphonate transition state mimic³³. The glutamine surrogate at the P1 site is essential for recognition because of its compatibility with the substrate specificity for the targeted enzyme. The presence of leucine and arylalanine at the P2 and P3 site enhances the recognition and cell penetrability, respectively. They synthesized the tripeptidyl aldehyde from the starting material glutamine surrogate in five sequential steps, as shown in Scheme 11: **11A** and **11B**³³. The FRET based assay and enzyme-based assay were conducted to evaluate the inhibitory activity of these compounds against SARS-CoV 3CLpro^{85,86}. The IC₅₀ values obtained proved that compounds have moderate to good inhibitory activity. The most potent compound is shown in Figure 8 (**162b**, IC₅₀ value- 0.23 ± 0.1 μM)³³.

Synthesis of tripeptide cysteine protease inhibitors is divided into two parts: synthesis of tripeptide compounds **162a-e** with aldehyde side chain (Scheme 11, **11A**) and second part involve the synthesis of α-Ketoamide tripeptide cysteine protease inhibitors (Scheme 11, **11B**). In the synthesis of tripeptide compounds **162a-e**, the starting material **158** was synthesized based on previously published literature⁶⁸. First, the compound **158** was reacted with *N*-Boc-L-leucine **157** in the presence of EDCl to form compound **159**. After that, reaction with different *N*-Cbz-amino acids **160a-e** and previous compound **159** produces the tripeptide compounds **161a-e** and further treatment with sodium borohydride and methanol converted to the final compounds **162a-e** (Scheme 11, **11A**). In the second part of the synthesis, the starting material was **162b**, which reacts with different conditions and reagents to transform the final compounds **163** (Scheme 11, **11B**)³³.

3.1.12. Potent dipeptide type of peptidomimetic inhibitors:

To develop a low molecular weight compound with 3CLpro inhibitory activity, Thanigaimalai et al designed a series of dipeptide-type compounds based on a previously reported lead compound C-terminal benzothiazolyl ketone containing dipeptide. Initial docking study involving binding interaction between the lead compound and 3CLpro, encouraged the replacement of P3 *N*-(3-methoxyphenyl) glycine with various rigid heterocyclic P3 moieties in the lead compound³⁴. The synthesis of the target compounds (**172a-r**) was achieved by assembling two key moieties: peptidics, **167** and C-terminal benzothiazole derivative, **171**. Synthetic outline along with associated reaction conditions depicted in Scheme 12: **12A** and **12B**. The inhibition constant value (K_i) of the compounds against 3CLpro were determined by accessing kinetic parameters in a fluorometric protease inhibition assay using constant substrate concentration. The IC₅₀ value of only some potent inhibitor determined based on cleavage activity of R188I SARS-CoV 3CLpro on a synthetic peptide (H-TSAVLQSGFRK-NH₂). The K_i/IC₅₀ value was reported as a mean of three independent experiments. The SAR study revealed some potent inhibitors having K_i/IC₅₀ value in the sub-micromolar to nanomolar range. The best potent inhibitor is compound



Scheme 11. Synthesis of tripeptide type cysteine protease inhibitors. **Scheme 11, 11A:** synthesis of tripeptide compounds **162a-e** with aldehyde side chain; **Scheme 11, 11B:** synthesis of α -Ketoamide tripeptide cysteine protease inhibitor **163**.

172a with K_i value, 0.006 μM (6 nM) and IC_{50} value, and 0.74 μM (Figure 8). K_i value of some compounds was also in good agreement with the binding affinity observed in the isothermal titration calorimetry (ITC) study³⁴.

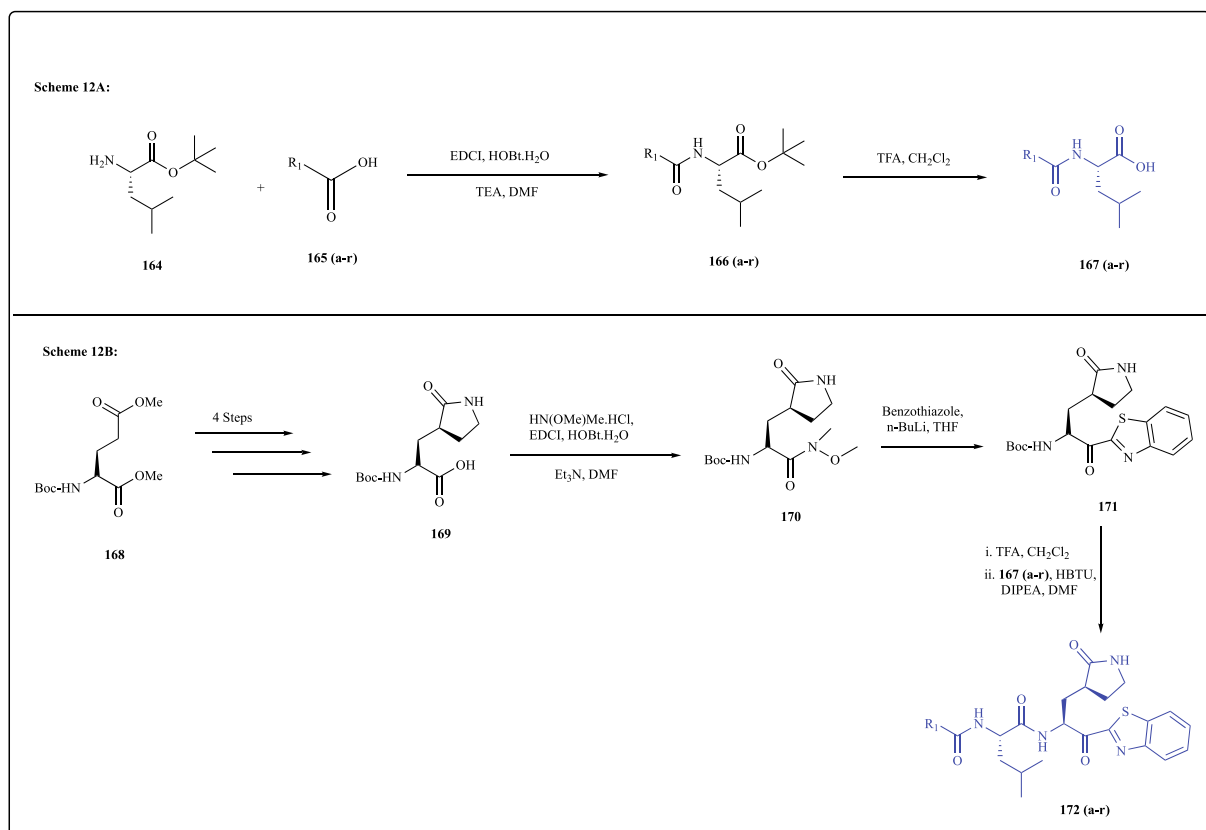
The synthesis of dipeptide cysteine protease inhibitors is divided into two parts: the first part involves the synthesis of peptide fragments **167a-r** with carboxylic acid side chain (Scheme 12, 12A) and the second part involves the synthesis of dipeptide cysteine protease inhibitor **172a-r** (Scheme 12, 12B). The peptide fragments **167a-r** were synthesized via starting with compound **164** which reacted with different substituted carboxylic acid **165a-r** under reaction conditions and formed the compounds **166a-r**. Further, the compounds **166a-r** reacted with trifluoroacetic acid to convert into final compounds **167a-r** (Scheme 12, 12A)³⁴. In the synthesis of dipeptide cysteine protease inhibitor **172a-r**, the main starting compound is **168** and the compound was converted to the **169** by using the method given in published literature^{58,87}. Then, the compound **169** was further reacted with *N,O*-Dimethylhydroxylamine hydrochloride and formed the Weinreb amide **170**. The compound **170** converted to compound **171** by coupling with

benzothiazole in the presence of *n*-Butylamine. Lastly, the reaction of trifluoroacetic acid and previously synthesized compounds **167a-r** produces the final dipeptide compounds **172a-r**³⁴.

The $-\text{NH}$ of the indole group along with the carbonyl moiety and the $-\text{NH}$ group of the pyrrolidin-2-one moiety comprises the S1 site, and this site is found to interact with the Glu166 residue. The $-\text{NH}$ group of S2 and S3 interacted with Gln189 and His164 residues, respectively. The carbonyl moiety of S4 position interacted with Ser144 and the ketone group of the pyrrolidin-2-one moiety was found to have an interaction with His163 residue of the protease (Figure 8)³⁴.

3.1.13. Novel dipeptide type peptidomimetic inhibitors:

In search of novel low molecular weight SARS-CoV 3CLpro inhibitors Thanigaimalai et al designed some dipeptidic compounds based on their previously reported peptide lead compound Z-Val-Leu-Ala(-pyrrolidone-3-yl)-2-benzothiazole ($K_i = 4.1$ nM) by replacing P3 valine unit with varieties of substituents keeping P1 and P1 fixed. Synthesis of the designed dipeptide was achieved through a coupling reaction involving two intermediates, and *N*-protected amino acid esters **175a-f** and a



Scheme 12. Synthesis of dipeptide cysteine protease inhibitors. **Scheme 12, 12A:** synthesis of *N*-protected amino acids **167a-r**; **Scheme 12, 12B:** synthesis of dipeptide cysteine protease inhibitor **172a-r**.

γ -lactam benzothiazole **179**, those were synthesized in separate steps. The steps of synthesis depicted in **Scheme 13: 13A and 13B**. The biological activity of the compounds was determined following a fluorometric protease inhibition assay against 3CLpro. Kinetic parameters were accessed at constant substrate concentration and inhibitor concentration varied to report K_i values. IC_{50} values were determined based on cleavage activity of SARS-CoV 3CL mutant protease (R188I) on a synthetic peptide substrate (H-Thr-Ser-Ala-Val-Leu-Gln-Ser-Gly-Phe-Arg-Lys-NH₂). SAR study revealed two potential inhibitor **180a** ($K_i = 0.39 \mu\text{M}$, $IC_{50} = 10.0 \mu\text{M}$) and **181b** ($K_i = 0.33 \mu\text{M}$, $IC_{50} = 14.0 \mu\text{M}$). Further, a molecular docking study was also performed to understand the binding interaction of **180a** with 3CLpro (**Figure 8**). The minimized energies of **181 m**, obtained from the docking study, were -40.67 and -35.52 kcal/mol ³⁵.

The synthesis of dipeptide cysteine protease inhibitors is divided into two parts, first part involves the synthesis of peptide fragments **175a-f** with carboxylic acid side chain (**Scheme 13, 13A**) and the second part involve the synthesis of dipeptide cysteine protease inhibitor **180a-h**, **181a-n**, and **182a-d** (**Scheme 13, 13B**). The peptide fragments **175a-f** have been synthesized via compound 173a-f which reacted with different substituted carboxylic acid or benzyloxycarbonyl chloride compounds conditions and forms the compounds **174a-f**. Further, the compounds **174a-f** reacted with trifluoroacetic acid or lithium hydroxide under reaction conditions to convert into the final compounds **175a-f** (**Scheme 13, 13A**)³⁵. In the synthesis of dipeptide cysteine protease inhibitor **180a-h**, **181a-n**, and **182a-d**, the main starting compound is **176** and the compound was converted to the **177** by using published literature^{26,31,37,68}. Then, the compound **177** was further reacted with *N,O*-Dimethylhydroxylamine hydrochloride and formed the Weinreb amide **178**. The compound **178** converted to the compound **179** by coupling with benzothiazole or 5-arylated thiazole in the presence of *n*-Butylamine or LDA. Lastly, reaction with trifluoroacetic acid and

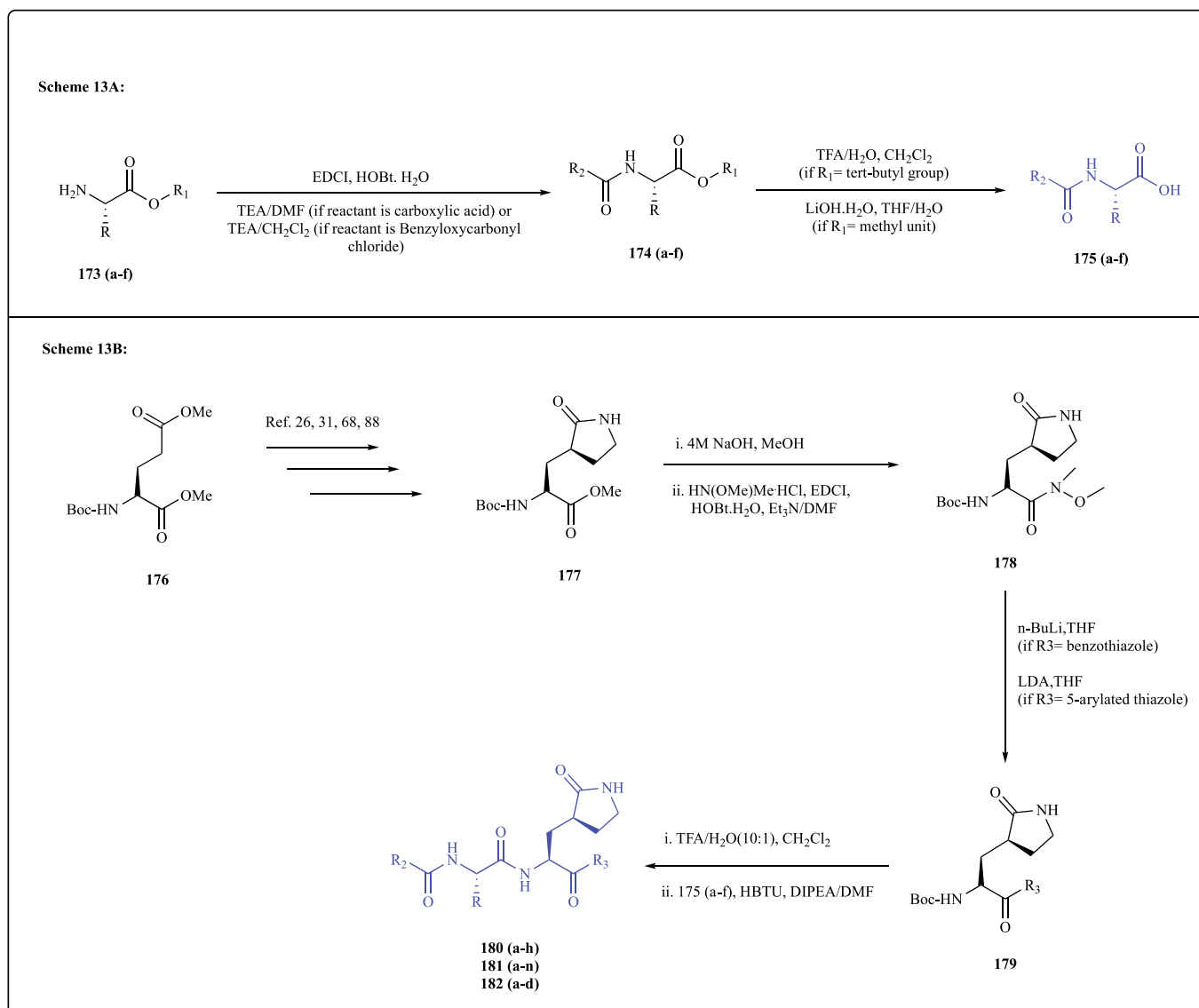
previously synthesized compounds **175a-f** produces the final dipeptide compounds **180a-h**, **181a-n**, and **182a-d** (**Scheme 13, 13B**)^{26,31,37,68}.

In silico studies revealed that the $-\text{NH}$ group of the methoxy aniline, the ketone group and the $-\text{NH}$ of pyrolidin-2-one comprising the S1 is found to interact with the Glu166 residue. The $-\text{NH}$ group of S2 and S3 interacted with Gln189 and His164 residues, respectively. The carbonyl moiety of S4 position interacted with Ser144 and Cys145. In contrast, the pyrolidin-2-one moiety was found to interact with His163 residue of the protease (**Figure 8**)³⁵.

3.1.14. Nitrile based peptidomimetic inhibitors:

In 2013, Wong and co-workers developed a four type of nitrile based broad-spectrum PIs for SARS-CoV 3CLpro. The four molecules were designed and synthesized with different *N*-terminal protective groups, such as, Boc (*tert*-butyloxycarbonyl), Cbz (carboxybenzyl), Mic (5-methylisoxazole-3-carboxyl) and different peptide length (**Scheme 14**). All four PIs **201**, **202**, **203**, and **204** were evaluated by in vitro enzymatic assay against SARS-CoV 3CLpro and the four inhibitors showed potent inhibitory activity against the SARS-CoV 3CLpro with IC_{50} values ranging from 4.6 to 49 μM and among the compounds, **204** showed the best inhibitory activity against the SARS-CoV 3CLpro ($IC_{50} = 4.6 \mu\text{M}$) (**Figure 8**). Due to the best inhibitory effects towards SARS-CoV 3CLpro, the PIs **204** was taken for further study for broad-spectrum inhibition against different human coronavirus strains, such as 229E, NL63, OC43, HKU1 and infectious bronchitis virus. The study revealed that the inhibitor **204** has broad-spectrum activity and effective against SARS-CoV 3CLpro, with IC_{50} values ranging from 1.3 to 3.7 μM ³⁶.

The synthesis of nitrile based PIs was focused on: synthesis of different small peptide compounds containing Boc (*tert*-butyloxycarbonyl), Cbz (carboxybenzyl), and Mic (5-methylisoxazole-3-carboxyl) **195**, **196**, **199**, and **200**; and joined with peptide **187** to get final PIs **201**, **202**, **203** and **204**. First, the synthesis of **187** starts via



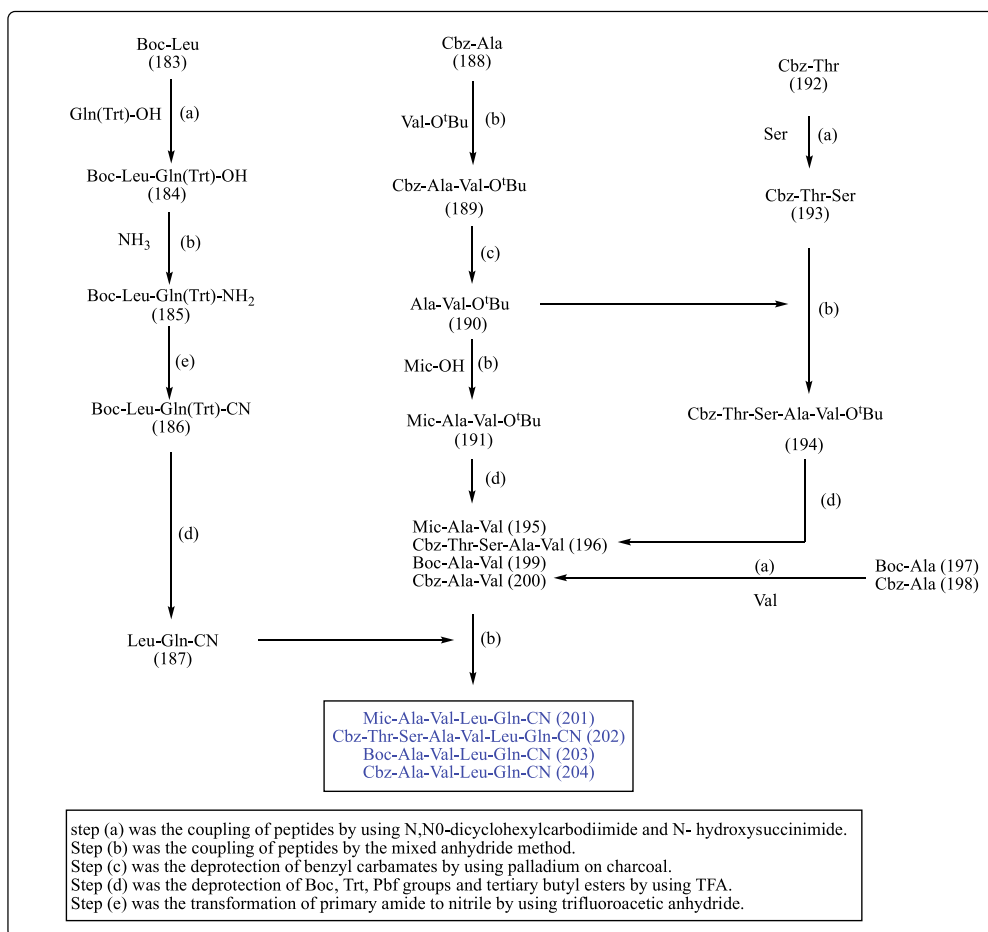
Scheme 13. Synthesis of dipeptide cysteine protease inhibitors. **Scheme 13, 13A:** synthesis of *N*-protected amino acids **175a-f**; **Scheme 13, 13B:** synthesis of dipeptide cysteine protease inhibitor **180a-h**, **181a-n**, and **182a-d**.

coupling of compound **183** and Gln(Trt)-OH in *N,N'*-dicyclohexylcarbodiimide *N*-hydroxysuccinimide; to form the compound **184** and reacts with ammonia, which converts the compound **184** to compound **185**. Next, the primary amine transfer to the nitrile group via treatment with trifluoroacetic anhydride and formed the compound **186** and further deprotection of Boc can convert to the final peptide **187** (Scheme 14). Like previous compound **187** synthesis, the rest 195, 196, 199, and 200 intermediate peptides were formed via different reaction conditions shown in Scheme 14. These intermediate peptides were formed via reacting with different starting material, compound **188** and **192**. In the last step, compound **187** was reacted with different previously synthesized peptides **195**, **196**, **199**, and **200** to form the target compounds **201**, **202**, **203**, and **204**; via coupling the two peptides in mixed anhydride conditions³⁶.

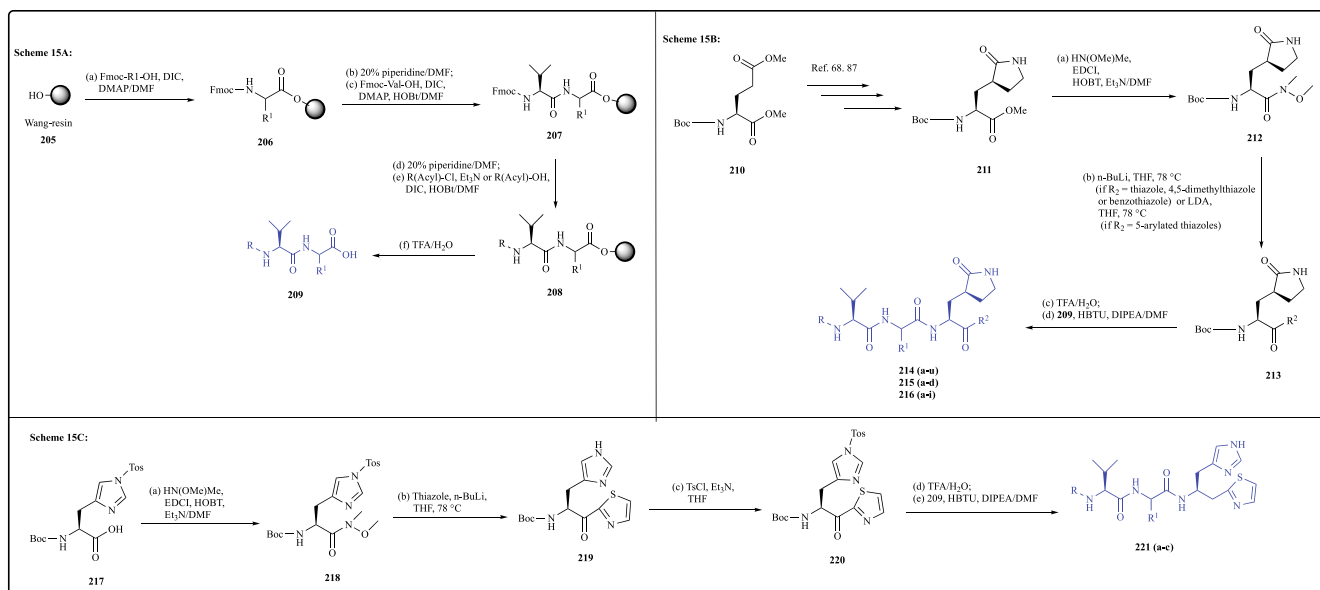
The cyano group of the S1 site was found to interact with the Glu166, Phe140 residues. The amide group of S2 interacted with Cys145. Leu167 was found to interact with the dimethyl group of S3, the amide groups of S4 forms interaction with Thr190, Gln189 and the S5 site comprising the benzyl group interacted with Pro168 of the protease (Figure 8)³⁶.

3.1.15. Tripeptide type of peptidomimetic inhibitors:

With an aim to develop novel peptidomimetics as inhibitors of SARS-CoV 3CLpro, Kanno et al designed a series of tripeptide-type compounds containing 4,5-dimethyl thiazole, 5-methyl thiazole, benzothiazole, and a series of 5-arylated thiazole at P1' position, other substituents at P2 and P4 positions were also rigorously optimized to achieve the best fit for protease inhibition activity. The initial molecular modelling study involving a thiazolyl ketone-containing tripeptidic lead compound (of previous research work on SARS-CoV by the authors) and 3CLpro demonstrated a spacious requirement warhead group rather than a small thiazole in P1' position, encourage to introduce those large groups. Synthetic outline of designed tripeptide-type compounds and associated reaction conditions depicted in Scheme 15. The protease inhibitory activity of synthesized compounds evaluated using R1881 SARS-Cov 3CLpro (SARS-Cov mutant protease) activity on a substrate (H-TSAVLQSGFRK-NH₂). A fluorogenic substrate (Dabcyl-KTSAVLQSGFRKME-Edans) was also used for initial rate measurements. IC₅₀ and/or K_i values were reported as the mean of three independent experiments. The study results revealed some compounds with benzothiazolyl moiety exhibit IC₅₀ or K_i value in submicromolar to nanomolar range with two potential compound **214i** (K_i = 4.1 nM) and **214p** (K_i =



Scheme 14. Synthesis of nitrile-based peptidomimetic inhibitors.



Scheme 15. Synthesis of tripeptide type of peptidomimetic inhibitors. Scheme 15, 15A: synthesis of dipeptidic key fragment 209; Scheme 15, 15B: synthesis of tripeptide inhibitor 214a-u, 215a-d, and 216a-i; and Scheme 15, 15C: synthesis of tripeptide inhibitor-containing imidazole moiety 221a-c.

3.1 nM). The docking study of a potential compound, **214o** of the series, showed strong binding interaction (Minimization energy: -43.65 kcal/mol) with protease enzyme than previously reported lead compound (Minimization energy: -37.56 kcal/mol). Docking structure was

elucidated by X-ray crystallography (PDB ID: 1 WOF, $K_i = 10.7$ μ M) (Figure 8)³⁷.

The synthesis outline of tripeptide type of PIs divided into three parts; the first part involves the synthesis of dipeptide key fragment 209

that has been synthesized with the help of peptide chemistry (Scheme 15, 15A), the second part involves the synthesis of tripeptide inhibitor **214a-u**, **215a-d**, and **216a-i** via synthesizing the key intermediate **213** (Scheme 15, 15B), and third part involve the synthesis of tripeptide inhibitor-containing imidazole moiety **221a-c** via synthesizing the key intermediate **220** (Scheme 15, 15C)³⁷.

The dipeptide key fragment **209** has been synthesized via starting with compound Wang-resin which reacted with different substituted Fmoc-amino acids and coupling reagent diisopropyl-carbodiimide under reaction conditions and formed the compound **206**. To remove the Fmoc group, the compound **206** has been reacted further with 20% piperidine in DMF and treated with Fmoc-valine to produce compound **207**. Next, the compound **207** has been converted to compound **208** by reacting with different acid chlorides or acyl chlorides and 20% piperidine in DMF and further transferred to target fragment **209** by treating with trifluoroacetic acid under specific reaction conditions (Scheme 15, 15A)³⁷.

In the synthesis of tripeptide inhibitors **214a-u**, **215a-d**, and **216a-i**, the main starting compound is **210** and the compound was converted to **211** by following the published literature method^{68,87}. Then, the compound **211** has been further reacted with N,O-Dimethylhydroxylamine hydrochloride under reaction conditions and formed the Weinreb amide **212**. The Weinreb amide **212** has been further converted to the compound **213** by coupling with substituted benzothiazole or 5-arylated thiazole in the presence of *n*-Butylamine or LDA. Lastly, reaction with trifluoroacetic acid and previously synthesized compound **209** produces the final tripeptide compounds **214a-u**, **215a-d**, and **216a-i** (Scheme 15, 15B)^{68,87}.

The synthesis of tripeptide inhibitor-containing imidazole moiety **221a-c** has been started via commercially available compound **217**. First, the compound **217** has been reacted with N,O-Dimethylhydroxylamine hydrochloride under reaction conditions and formed the respective Weinreb amide **218**. Then, the Weinreb amide **218** has been treated with thiazole in the presence of *n*-Butylamine to produce compound **219** and further converted to compound **220** by reacting with tosyl chloride and triethylamine. Lastly, reaction with trifluoroacetic acid and previously synthesized compound **209** produces

the final tripeptide inhibitors **221a-c** (Scheme 15, 15C)³⁷.

The dimethyl aniline group of the S1 site was found to interact with the Ala191 residue. The -NH group and the ketone of S2 interlinked with Glu166. Glu189, His41 residues were found to interact with the amide group of S3, the benzothiazole groups of S4 formed interaction with Cys145, Ser144 and Gly143 and the S5 site comprising the dimethyl group interacted with His163 of the protease (Figure 8)³⁷.

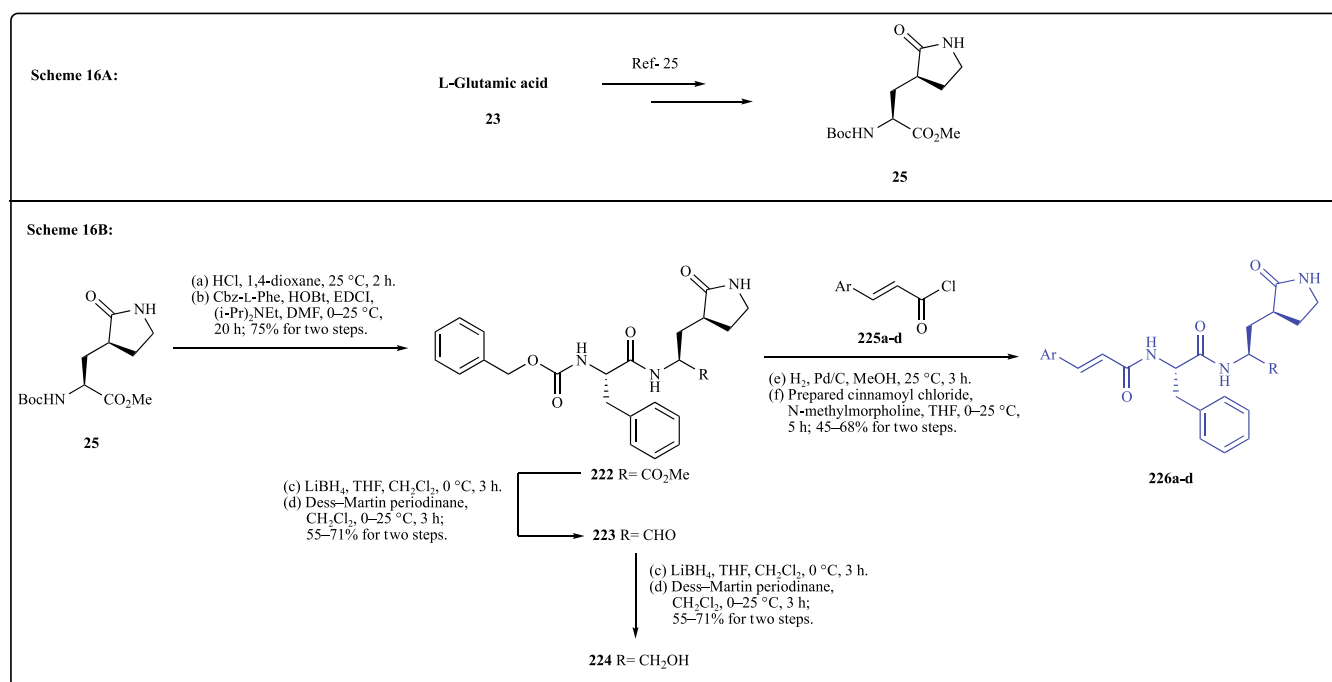
3.1.16. Peptidomimetic containing cinnamoyl warhead:

In 2017, Vathan Kumar and co-workers have identified and evaluated six peptidomimetics as SARS-CoV 3CLpro inhibitors³⁸. They developed peptidomimetics with some modifications based on previous literature. The designed inhibitors were synthesized using previously published literature that was used in the synthesis of 3CLpro inhibitors for enterovirus⁸⁸. All the synthesized compounds were tested in vitro against SARS-CoV 3CLpro as well as MERS-CoV by using previously reported fluorescence assay. The biological evaluation data have reported some potent inhibitors against SARS-CoV 3CLpro, and compound **226d** is one of them with an IC₅₀ value of 0.2 ± 0.07 μM (Figure 8).

The synthesis of PIs containing cinnamoyl warhead and the related compound was synthesized based on previously developed literature⁸⁸. The synthesis strategy was divided into two parts: Scheme 16, 16A, for the synthesis of intermediate **25**; Scheme 16, 16B, for the synthesis of target compounds **226a-d**. At first, in the synthesis of intermediate compound **25**, L-glutamic acid was used as a starting material and similar synthetic protocols were used which describe in Scheme 16, 16A. Further, the intermediate compound **25** was coupled with Cbz-L-Phe under suitable reaction conditions to produce target peptide **222** and under reduction with Dess-martin periodinane and lithium hydride, the compound **222** converted into **223** (Scheme 16). In the final step, the respective compounds **222**, **223**, and **224** were reacted with substituted cinnamoyl derivatives **225a-d** under specific reaction conditions to get desired compounds **226a-d** (Scheme 16).

3.1.17. Peptidomimetic containing decahydroisoquinolin moiety:

With an aim to develop SARS-CoV 3CLpro inhibitor, Ohnishi K et al designed some compounds containing decahydroisoquinolin moiety

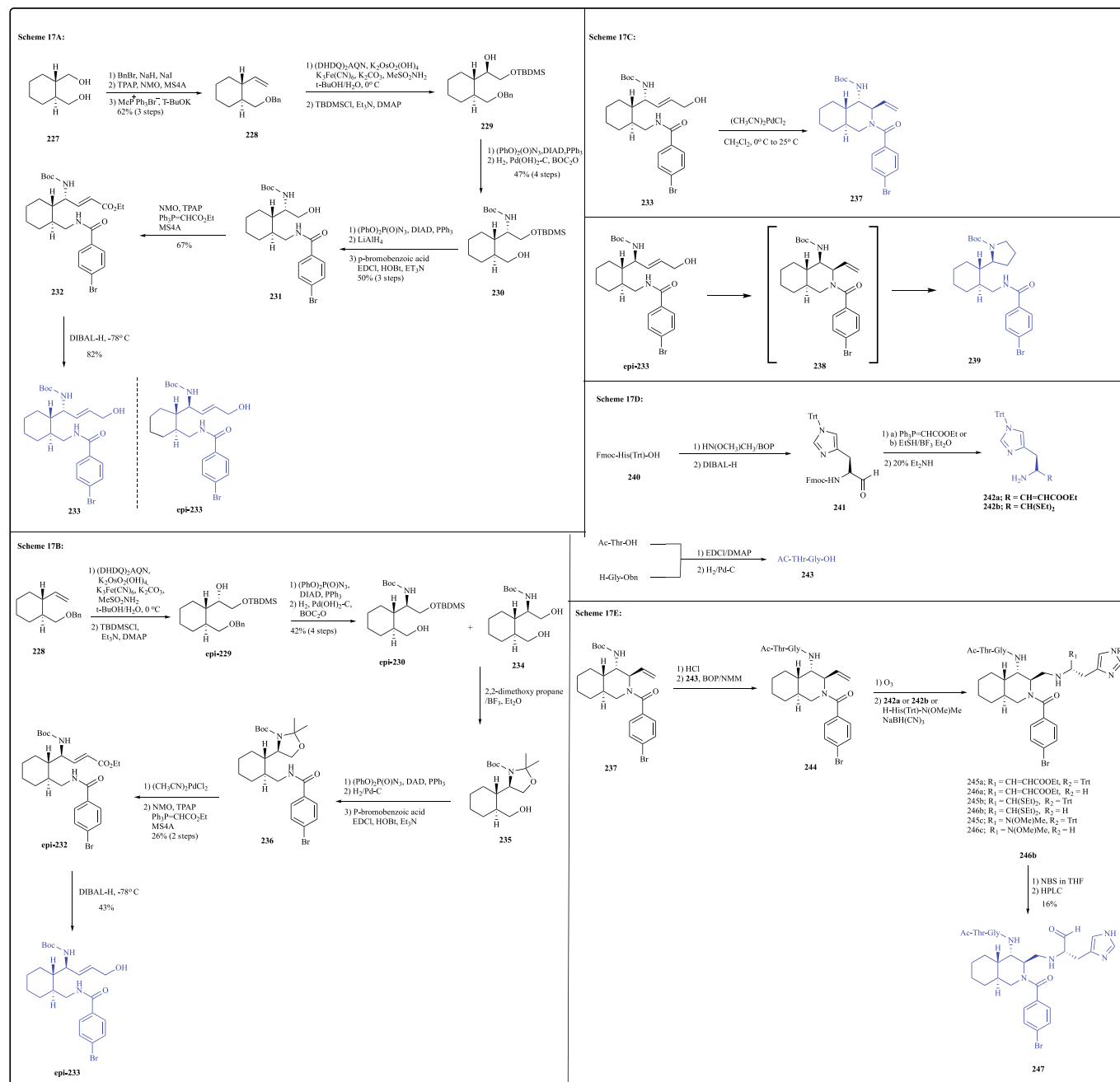


Scheme 16. Synthesis of peptidomimetics containing Cinnamoyl warhead. Scheme 16, 16A: synthesis of intermediate **25**; Scheme 16, 16B: synthesis of target compounds **226a-d**.

with an additional substituent at non-prime site and warheads based on previous C-terminal aldehyde peptide inhibitor. Initially designed compound showed moderate activity, and the analysis of X-ray crystallographic structure of inhibitor in complexation with R188I SARS 3CLpro displayed the absence of interactions covering the P3 to P4 regions of substrate-based inhibitor, which led to the incorporation of a substituent at the non-prime site on the 4-position carbon of decahydroisoquinolin moiety. The synthetic outline and associated reaction condition for the compounds are depicted in Scheme 17. The compound 247 (IC₅₀ = 26 μM) exhibited clear but moderate inhibition potency on R188I SARS-CoV 3CLpro (Figure 8). The result of the study suggested increased interaction between protease and inhibitor 247 after incorporation of the substituent at the non-prime site. In addition, it is revealed from the study that the thioacetal warhead in association with

decahydroisoquinolin moiety could be an efficient strategy for the design of potent SARS 3CLpro inhibitor³⁹.

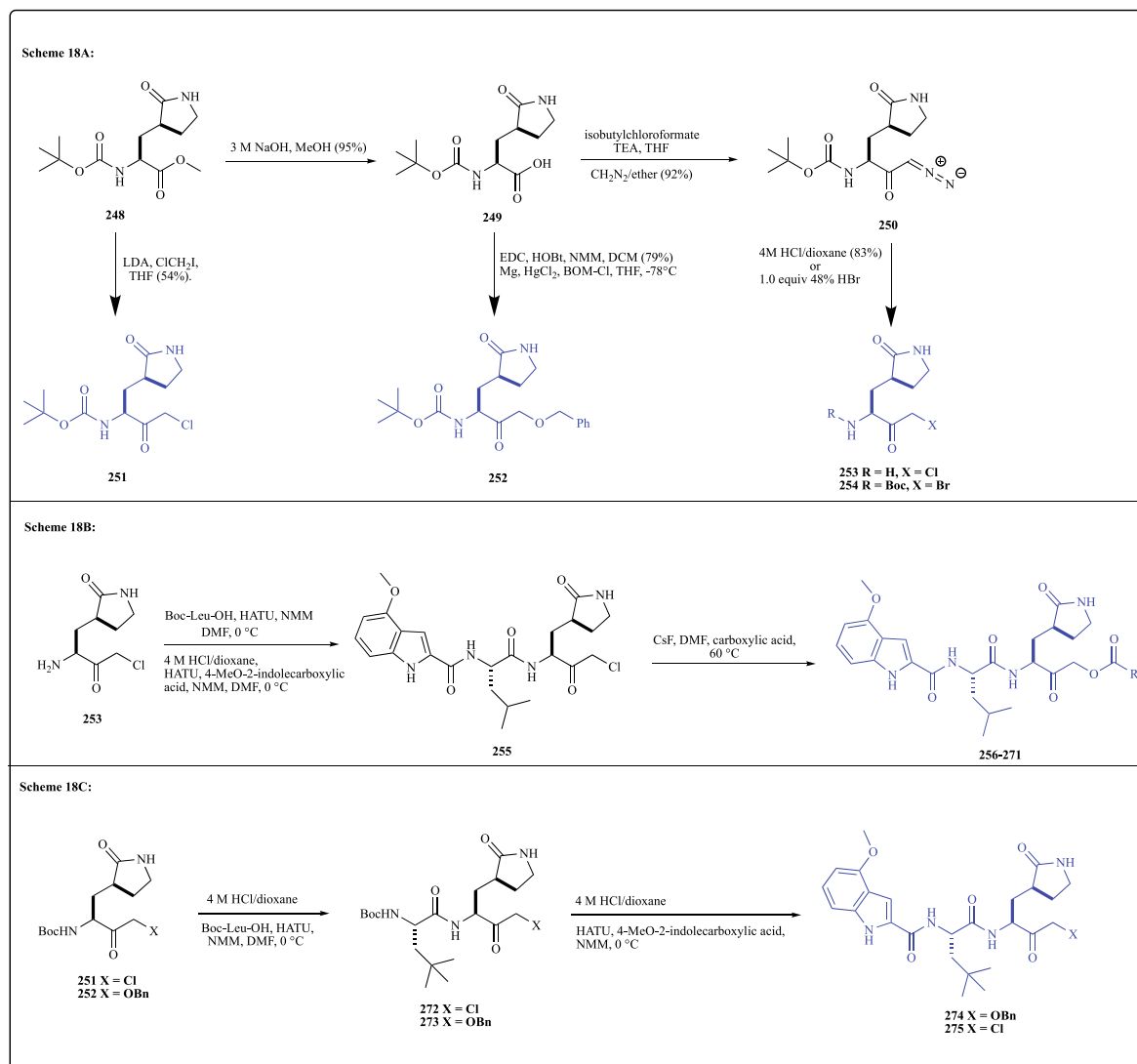
The synthesis of PIs containing decahydroisoquinolin moiety and the related compound was performed based on the retrosynthetic route. From the retrosynthetic analysis, it was revealed that a diol compound 227 is the starting compound for the synthesis of targeted derivatives. Hence, the synthesis of precursor molecule 233 is started from compound 227. The synthesis of decahydroisoquinolin derivatives has been divided into five parts, the first part has focused on the synthesis of precursor molecule 233 (Scheme 17, 17A); the second part has focused on the synthesis of precursor molecule *epi*-233 (Scheme 17, 17B); the third part has focused on the synthesis of intermediate compound 237 (Scheme 17, 17C); the fourth part has focused on the synthesis of intermediate compound 242a, 242b, and 243 (Scheme 17, 17D); and the



Scheme 17. Synthesis of peptidomimetics containing Decahydroisoquinolin moiety. **Scheme 17, 17A:** synthesis of precursor molecule 233; **Scheme 17, 17B:** synthesis of precursor molecule *epi*-233; **Scheme 17, 17C:** synthesis of intermediate compound 237; **Scheme 17, 17D:** synthesis of intermediate compound 242a, 242b, and 243; and **Scheme 17, 17E:** synthesis of target compounds including 247.

fifth part has focused on the synthesis of target compounds including **247** (Scheme 17, 17E). Synthetic route of precursor compound **233** for the Pd(II) catalyzed cyclization given in Scheme 17, 17A. Benzyl protection of one alcohol group and oxidation of other alcohol group to the aldehyde of diol **227**, and then Wittig reaction deliver compound **228**. Protection of a 1,2 diol with TBDMS group, obtained via asymmetric dihydroxylation of compound **228**, yielded an alcohol **229** as a mixture of epimer. Amine **230** with Boc-protection was obtained via Mitsunobu reaction and catalytic hydrogenation of **229** in the presence of (Boc)₂O. Mitsunobu reaction followed by reduction changed the alcohol group of **230** to amine group, which on acylation by p-bromobenzoic acid gave amide **231**. Oxidation of primary alcohol group of **231** to an aldehyde, followed by Wittig reaction gave ether **232**. The precursor compound **233** is obtained by reduction of **232** with DIBALH. After that *epi* **233** with different amine configuration was achieved via synthetic Scheme 17, 17B. The olefin presents at the terminal of **228** is transferred to *epi*-1,2-diol via asymmetric dihydroxylation by the use of different ligand that was used for **229**. Protection of primary alcohol group with TBDMS yield *epi*-**229** as 8:1 diastereo mixture. Then the mixture in appropriate reaction conditions gave **234** as a single diastereomer, in addition to the required *epi*-**230** diastereomixture. To yield a single diastereomeric configuration of *epi*-13, the diol **234** was used. The compound **234** in a sequence of reaction gave compound **236**. Then a single diastereomer

epi **233** was obtained via the desired sequence of reactions. Diastereoselective cyclization catalyzed by Pd(II) was then investigated (Scheme 17, 17C). Bis-acetonitrile palladium chloride catalyzed cyclization of precursor **233** gave decahydroisoquinolin compound **237**. Non-prime site substituents were introduced using compound **237**. The preparation of P1 site fragment (**242a-b**) and nonprime site substituents covering P3 to P4 (**243**), to be incorporated on the decahydroisoquinolin moiety, depicted in Scheme 17, 17D. For the synthesis of P1 site residue, an easily accessible Fmoc-His(Trt)-OH (**240**) was transferred to Weinreb amide, and reduction of the amide with DIBALH produced an aldehyde **241**. The resulting compound **241** was then transformed to α , β -unsaturated ester or thioacetal, and under appropriate reaction conditions yield **242a** or **242b**. EDC/DMAP mediated coupling and additional debenzoylation by catalytic hydrogenation of H-Gly-OBn and Ac-Thr-OH gave P3 to P4 fragment **243**. Ultimately, the synthesized P1 site residue and P3 to P4 site substituent were introduced into the cyclic compound **237** (Scheme 17, 17E). Boc group of **237** was detached using HCl, and then coupling of amine with **243** in presence of BOP yielded **244**. Oxidation of terminal olefin followed by reductive coupling with **242b**, the aldehyde product of **244** gave **245b**. Then **245b** was converted to **246b** via elimination of the Trt group of imidazole in Histidine. To assess the influence of warheads on inhibitory potency, P1 residue **242a** and H-His(Trt)-N(OMe)Me were similarly coupled with



Scheme 18. Synthesis of Ketone-based covalent inhibitors. **Scheme 18, 18A:** synthesis halomethylketone (HMK) intermediates **251**, **252**, **253**, and **254**; **Scheme 18, 18B:** Synthesis of chloromethylketone (CMK) intermediate **255**; and **Scheme 18, 18C:** synthesis of target compounds including **274** and **275**.

244 to yield 246a and 246c. Treatment 246b with NBS changed the thioacetal to an aldehyde group and after purification of the product via preparative HPLC gave compound 247³⁹.

3.1.18. Ketone-based covalent inhibitors:

In continuation of research efforts to develop novel molecule as a SARS-CoV 3CLpro inhibitor, Robert L. Hoffman et al pursued the design of ketone-based reversible and irreversible inhibitors based on previous Michael acceptor by changing warhead moiety and retaining P1 lactam, while P2 and P3 sites were randomly optimized. The synthesis of the designed compound and associated reaction condition depicted in Scheme 18; 18A, 18B, and 18C. The biological experiment was carried out following SARS-CoV-1 protease FRET assay and analysis, based on the proteolytic activity of 3CLpro on fluorogenic peptide substrate following sequence DABCY-LKTSAVLQ-SGFRKME-EDANS. Viral inhibition assay of the compounds was also carried out on SARS-CoV-1 and hCoV 229E. Two classes of potential inhibitors of SARS-CoV-1 have been developed viz. acyloxymethylketones and hydroxyethyl ketones. The biological evaluation data have reported some potent inhibitors against SARS-CoV 3CLpro under acyloxymethylketone derivatives, and compound 256 is one of them with an IC₅₀ value of 0.017 ± 2 μM (Figure 8). Solving crystal structure of the ligand protein complex by X-ray crystallography analysis led to the identification of potent inhibitor PF-00835231 (IC₅₀ = 4 ± 0.3 nM) with additional viral inhibition potential. Further, preclinical investigation of PF-00835231 revealed desirable pharmacokinetic property, which warrants the development of PF-00835231 as a drug candidate against COVID-19 patient¹⁴.

The halomethylketone (HMK) intermediates were obtained via a two-step synthetic procedure as given in Scheme 18, 18A. Aminoester 248 on saponification yielded amino acid 249. The Reaction of acid 249 with isobutylchloroformate and trimethylamine produced mixed anhydride, which after reaction with diazomethane provide 250. Diazo ketone 250 was reacted with HCl for concurrent deprotection of nitrogen and transformation to the intermediate chloromethylketone (CMK) 253. On the other hand, reaction of 250 with stoichiometric amounts of 48% HBr in dichloromethane gave 254. Chloromethylketone (CMK) intermediate can be prepared differently by the treatment of 248 with too much LDA to produce 251. Conversion of 249 to a Weinreb amide, followed by reaction with Grignard of benzylchloromethyl ether produced oxymethylketone intermediate 252.

Substituted methyl ketone derivatives was achieved via generation of the fully elaborated chloromethylketone (CMK) intermediate 255 (Scheme 18, 18B). Compound 253 in a series of reaction produce 255 in moderate yields without epimerization. Reaction of 255 with numerous carboxylic acids in a medium containing CsF gave acyloxymethylketones 256–271. The other derivatives were also obtained by following above synthetic procedure via substitution with appropriate functionalities.

The derivatives containing Hydroxymethylketone (HMK) functionality were obtained via two complementary processes depicted in Scheme 18, 18C. Oxymethylketone intermediate 252 via a series of reactions yielded benzyl ether derivatives 274 in moderate yields. Moreover, by using above synthetic procedures along with the substitution of appropriate functionalities yielded other inhibitors.

The result obtained from the in silico study of compound 256 showed that the pyridine ring in the S1 site of the compound interacted with the Cys145 amino acid residue and that of the carbonyl group of S2 site interacted with the Cys145, Gly143, amino acid residues of the protease (Figure 8)¹⁴.

3.1.19. α-Ketoamides derivatives:

Zhang et al in their research work, developed broad-spectrum antivirals against enterovirus, alpha coronavirus, and beta coronavirus. Because the protease of these virus shares a common active site architecture and an unique specificity for substrate recognition, they pursued a structure-based design of peptidomimetic α-ketoamides near

equipotent against the three virus genera. The proteases targeted in this study specifically cleave peptide following glutamine residue in the P1 position, they have incorporated 5-membered γ-lactam ring (a derivative of glutamine) in P1 position, which causes ten-fold increase in potency of the inhibitors. Synthetic efforts were, therefore, aimed at optimizing the substituents at the P1', P2, and P3 positions of the α-ketoamides. Chemical synthesis of α-ketoamides started with Boc protected L-glutamic acid dimethyl ester, synthetic outline and associated reaction conditions are depicted in Scheme 19; 19A, 19B, and 19C⁴⁰. Synthesized compounds were tested against the recombinant viral proteases, viral replicons, and virus-infected cell cultures; most of them were non-toxic to the cell. The SAR study revealed that optimization at P2 substituent is important for achieving near equipotency against alpha coronavirus, beta coronavirus and enterovirus. Among the compounds, the best near equipotent compounds were 289u (P2 = cyclopentylmethyl) and 289r (P2 = cyclohexylmethyl). These compounds achieved the best fit between the different requirements for P2 substituent. However, in terms of viral protease inhibition activity, compound 289s (IC₅₀ = 0.24 μM) and 289n (IC₅₀ = 0.33 μM) showed the best inhibition activity towards SARS-CoV 3CLpro (Figure 8). This study also demonstrated the fact that as there is a high similarity between the main protease of SARS-CoV and novel betaCoV (SARS-CoV-2/Wuhan/2019). All results reported here for the inhibition of SARS-CoV will most likely also apply to the new virus as well⁴⁰.

The synthesis process of α-Ketoamides derivatives has been divided into three parts, the first part involves the synthesis of key lactam fragment 279 (Scheme 19, 19A), the second part involves the synthesis of amino acids intermediates 283a-u (Scheme 19, 19B), and third part involves the addition of two synthesized intermediate compounds 279 and 283a-u; to produce the target compounds 289a-u (Scheme 19, 19C)⁴⁰.

The key lactam fragment 279 has been synthesized via three steps which started with the N-Boc glutamic acid dimethyl ester 276 and reacted with bromoacetonitrile under specific reaction conditions to form compound 277. In the next step, the intermediate 277 has undergone a hydrogenation reaction and formed a cyclization product 278. In the last step, the cyclization product 278 has been reacted with trifluoroacetic acid to remove the Boc protection and transferred into final lactam fragment 279 (Scheme 19, 19A).

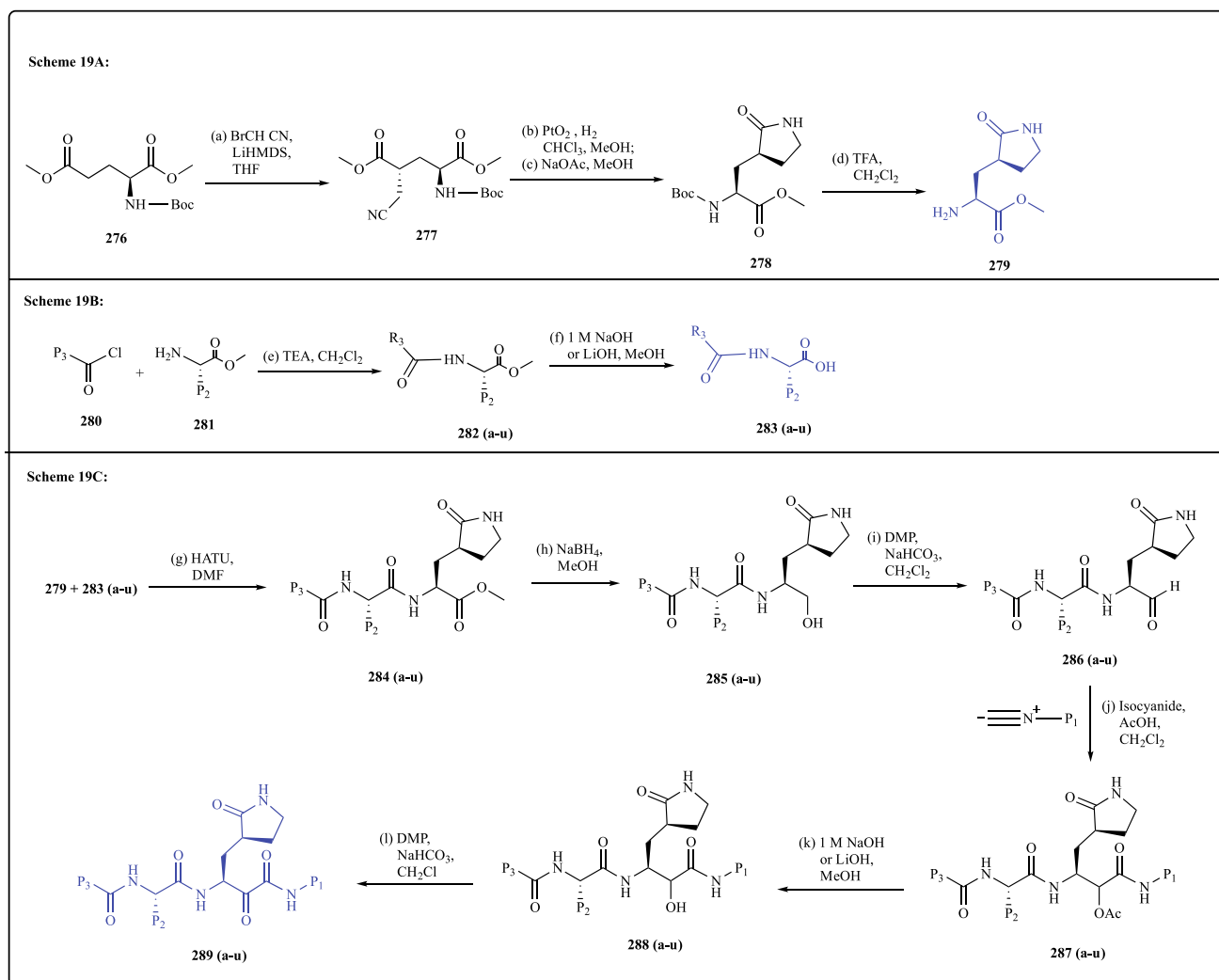
Similarly, the second key amino acid intermediates 283a-u has been synthesized in two steps, which started with the substituted acyl chloride 280 and α-amino acid methyl ester 281. These two starting compounds have reacted with trifluoroacetic acid to produce compounds 282a-u and under alkaline hydrolysis, the compounds 282a-u have transferred into target amino acid intermediates 283a-u (Scheme 19, 19B).

The synthesis of α-Ketoamides derivatives has been started via the addition of two synthesized intermediates 279 and 283a-u. Under specific reaction conditions, these intermediates have transferred into compounds 284a-u. In the next step, the compounds 284a-u have undergone a reduction reaction to form compounds 285a-u by reducing agent sodium borohydride and further reaction with Dess – Martin periodinane 285a-u has converted into 286a-u. In the next step, the compounds 286a-u has transferred into 287a-u by nucleophilic addition of isocyanides in acidic medium. The nucleophilic product 287a-u has converted into 288a-u by removing the acetyl group. In the last step, the alcohol group of 287a-u has converted to keto group by oxidation process with Dess – Martin periodinane and formed the α-Ketoamides 289a-u (Scheme 19, 19C)⁴⁰.

In silico studies between inhibitor 289s and 3CLpro revealed the interaction of cyclopropane of S1 site with amino acid residues such as: Gln189, Arg188, Asp187, Met49, and Met165 (Figure 8)⁴⁰.

3.2. Small-molecule inhibitors (SMIs):

The chemical synthesis of SMIs under isatin derivatives⁴¹,



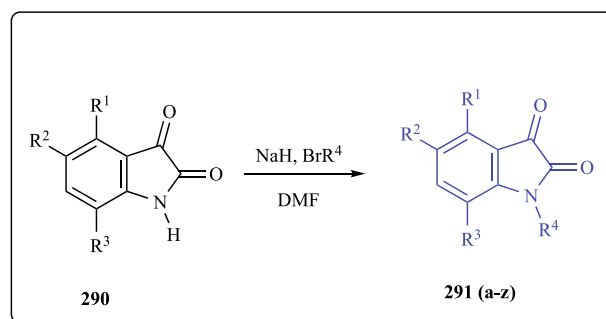
Scheme 19. Synthesis of α -Ketoamides as peptidomimetic inhibitors. **Scheme 19, 19A:** synthesis of key lactam fragment **279**; **Scheme 19, 19B:** synthesis of amino acid intermediates **283a-u**, and **Scheme 19, 19C:** synthesis of α -Ketoamides derivatives **289a-u** by addition of two intermediates **279** and **283a-u**.

Chloropyridyl ester derivatives⁴², pyrazolone derivatives⁴³, pyrimidine derivatives⁴⁴, macrocyclic inhibitors⁴⁵, 5-sulphonyl isatin derivatives⁴⁶, pyrazolone derivatives⁴⁷, serine derivatives⁴⁸, phenylisoserine derivatives⁴⁹, and Octahydroisochromene derivatives⁵⁰; are discussed below:

3.2.1. Isatin derivatives:

N-Substituted isatin derivatives were synthesized and evaluated in vitro against SARS-CoV 3CLpro by Li-Rung Chen and co-researchers. A series of isatin derivatives has been prepared from the reaction of isatin and various bromides (BrR_4) in the presence of a strong base via a single-step process⁴¹. The in vitro SARS-CoV 3CL protease assays have been conducted via FRET analysis for biological evaluation. The assay result showed that some compounds were potent and selective inhibitors with IC_{50} values ranging from 0.95 to 17.50 μM against SARS-CoV 3CLpro⁷¹. The organic synthesis of isatin derivatives **291a-z** is shown in **Scheme 20** and among the synthesized compound, the most potent compound is **291a** ($\text{IC}_{50} = 0.95 \mu\text{M}$), as shown in Figure 9⁴¹.

The *N*-Substituted isatin derivatives **291a-z** have been synthesized via a single-step process, which started with substituted isatin **290**. Compound **290** reacted with different bromides in the presence of a strong base to obtain target compounds **291a-z** (**Scheme 20**). In compound **291a**, the benzothiophene of the S1 site interacted with His164, the carbonyl groups of isatin of S2 site interacted with His41, Cys145,



Scheme 20. Synthesis of *N*-Substituted isatin derivatives.

Gly143, and Iodine group of isatin of S3 site interacted with Phe140 amino acid residues of protease as detected in the in silico study (**Figure 9**)⁴¹.

3.2.2. Chloropyridyl ester derivatives:

Chloropyridyl ester is a class of heteroaromatic organic molecule that was used previously in the development of SARS-CoV 3CLpro inhibitors. The first chloropyridyl ester-containing SARS-CoV 3CLpro inhibitor was reported by the Jianmin Zhang and their co-workers in

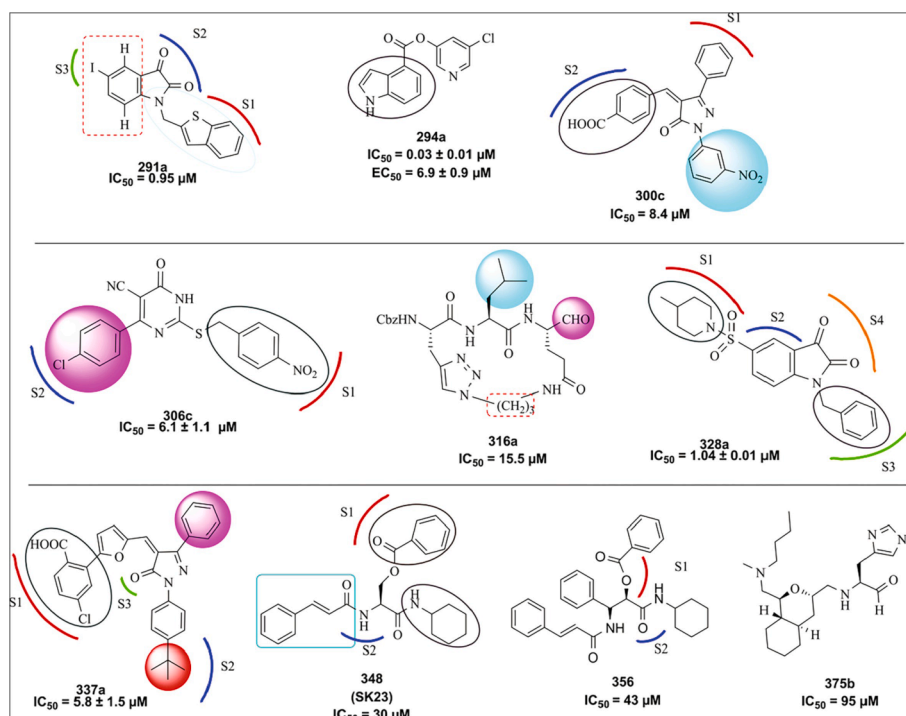


Figure 9. Structure of small-molecule SARS-CoV 3CLpro inhibitors (291a, 294a, 300c, 306c, 316a, 328a, 337a, 348, 356, and 357b).

2007²⁸. Based on the previous history of Chloropyridyl ester as an antiviral potency, in 2008, Ghosh et al developed a series of SMIs containing Chloropyridyl ester and indole moiety, for SARS-CoV 3CLpro⁴². Similarly, they have used another potent SARS-CoV 3CLpro inhibitor (i. e. Benzotriazole ester derivative) for designing the target molecule, which was developed by the Wong research group in 2006⁸⁹. They synthesized the designed SMIs via Scheme 21. All the synthesized compounds were tested against SARS-CoV 3CLpro by using previously reported FRET enzyme assay as well as SARS-CoV cell-based assay. The assay result revealed that some Chloropyridyl esters were a potent inhibitor against SARS-CoV 3CLpro and among them, the most potent inhibitor is 294a ($IC_{50} = 0.03 \pm 0.01 \mu M$, $EC_{50} = 6.9 \pm 0.9 \mu M$) (Figure 9)⁴².

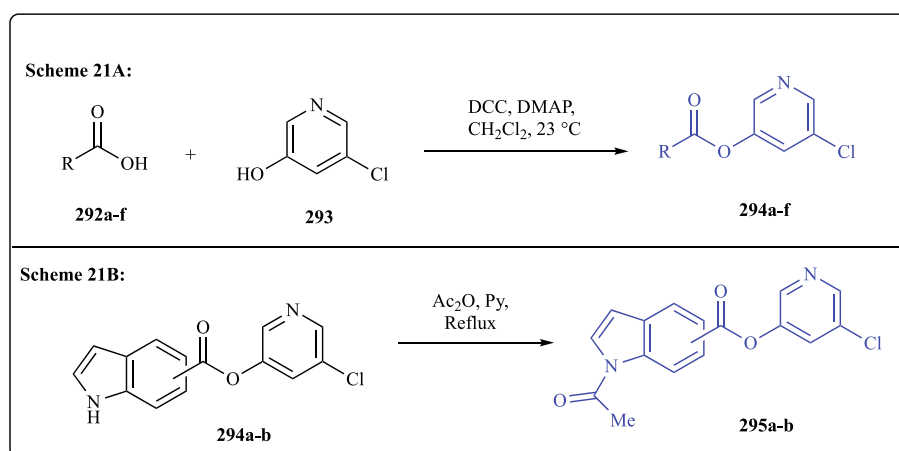
The Chloropyridyl ester derivatives 294a-f have been synthesized via a single step. Various carboxylic acid derivatives 292a-f were coupled with 5-chloro-3-pyridinol 293 in presence of DCC and DMAP under appropriate reaction conditions and produces Chloropyridyl ester

derivatives 294a-f (Scheme 21, 21A). After synthesis of 294a-f, a few of the indole compounds 294a-b were converted to acetyl products 295a-b via acetylation reaction (Scheme 21, 21B). They have also incorporated substituted phenyl sulphonyl group to the indole by direct sulfonation reaction but it has been found that the sulphonyl-indole Chloropyridyl products were not active in the anti-viral activity⁴².

The binding interaction of compound 294a obtained by Gold dock with the enzyme as observed in the in silico study showed that the carbonyl group in the S2 site interacted with Gly143, Ser144, Cys145, the nitrogen of the chloropyridinyl in the S1 site is in close proximity with His163 residue of the macromolecule (Figure 9)⁴².

3.2.3. Pyrazolone Derivatives:

A major class of heterocyclic compounds that exist in many drugs and synthetic products are pyrazolone derivatives⁹⁰. Such molecules has excellent analgesic⁹¹, antituberculosis⁹², antifungal⁹², antimicrobial⁹³, anti-inflammatory⁹⁴, antioxidant⁹⁵ and anti-tumor functions⁹⁶. The



Scheme 21. Synthesis of Chloropyridyl ester derivatives. Scheme 21, 21A: Synthesis of Chloropyridyl ester derivatives 294a-f; Scheme 21, 21B: conversion of indole compounds 294a-b to acetyl products 295a-b.

pyrazolone structure plays an important role because of its easy preparation and rich biological activity and represents a fascinating template for combinatorial and medicinal chemistry. In 2010, Po-Huang Liang et al have reported a series of pyrazolone compounds having inhibitory activity against SARS-CoV 3CLpro. The compounds have been designed based on reported pyrazole containing drugs (like, Edaravone, a medicine that is effective for myocardial ischemia), synthesized and tested for anti SARS-CoV 3CLpro inhibitory activity by in vitro protease inhibition assay using fluorogenic substrate peptide in which several compounds exhibited potent inhibitions towards 3CLpro (Scheme 22). The most potent inhibitor is **300c** with IC₅₀ value 8.4 μM (Figure 9). Incidentally, one of the inhibitors also showed better effectiveness against Coxsackievirus B3 3C protease. They have also determined the cytotoxicity of the synthesized compounds using the MTT (3-(4,5-dimethylthiazol-2-yl)-2,5-diphenyl tetrazolium bromide) assay and found that, none of them were cytotoxic at 200 μM⁴³.

The pyrazolone derivatives **300a-u** have been synthesized via two steps. The reaction started with substituted phenylhydrazine hydrochloride **296** and ethyl benzoylacetate **297**⁹⁷. These two starting materials have reacted in the presence of triethylamine to produce intermediate compounds **298** and further reaction with substituted aldehyde under desired reaction conditions, the compounds **298** has converted to the target compounds **300a-u** (Scheme 22)⁹⁸. The computational studies of compound **300c** showed that the phenyl ring of the S1 site interacted with Met-49, Arg-188, and Gln-189; the 4-carboxy benzyl of the S2 site interacted with Gln-192 residues of protease as detected in Figure 9⁴³.

3.2.4. Pyrimidine Derivatives:

In 2010, Ramajayam and co-workers developed a series of 2-(benzylthio)-6-oxo-4-phenyl-1,6-dihydropyrimidine derivatives as SARS-CoV 3CLpro inhibitors. They have been identified various heterocycles as a novel anti-SARS agent against SARS-CoV 3CLpro from high throughput screening. They have designed the compounds from the data of complete pharmacophore modelling, and synthesized some potential pyrimidine derivatives in two steps (Scheme 23) and tested in vitro against SARS-CoV 3CLpro, by using previously reported fluorescence assay. The biological evaluation data have reported some potent inhibitors against SARS-CoV 3CLpro, and compound **306c** is one of them with IC₅₀ value 6.1 ± 1.1 μM (Figure 9)⁴⁴.

The pyrimidine derivatives **306a-n** has been synthesized via two steps. The reaction started with substituted benzaldehyde **301**, ethyl cyanoacetate **302**, and thiourea **303**; all three compounds have reacted and converted into compounds **306a-n**⁹⁹. In the next step, the compounds **304a-n** were transferred to the target pyrimidine derivatives **306a-n** by reacting with various halides **305** under appropriate reaction conditions (Scheme 23). In compound **306c**, the *para*-nitro benzyl group of S1 site interacted with Gly-143 and Cys-145; the 4-chloro of the phenyl ring of S2 site interacted with Met-49 and Gln-189 amino acid

residues of protease as detected in the in silico study (Figure 9)⁴⁴.

3.2.5. Macrocytic inhibitors:

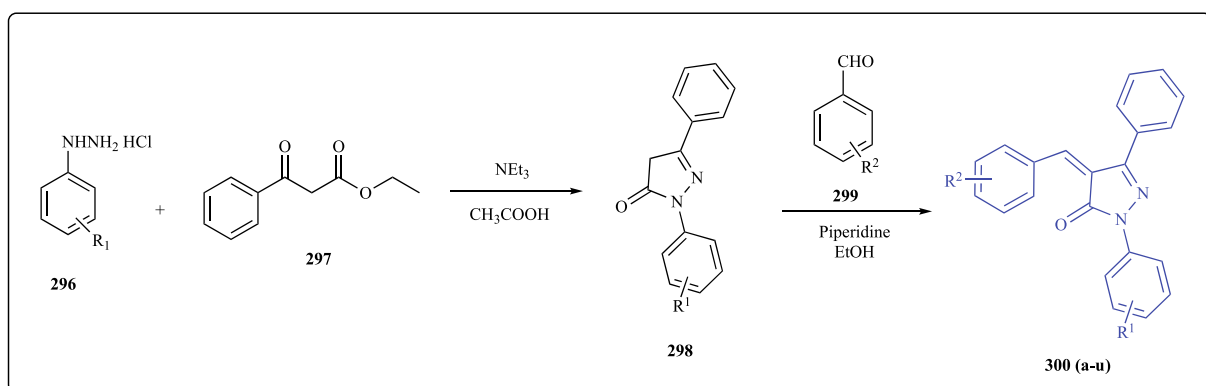
Macrocycle is a large ring-shaped cyclic molecule with exciting features to interact with the intracellular proteins and were used as a potential drug candidate for many pharmacologically important targets through the inhibition of intracellular protein-protein complexes. Several compatible strategies were already developed over the past decade to synthesize and screen the macrocycle libraries for binding to pharmacologically important targets. Due to its important chemical features, such as higher affinity, higher metabolic stability, better membrane permeability, and selectivity towards proteins, macrocyclic inhibitors have attracted considerable attention to researchers in drug discovery. The first macrocyclic inhibitor (**316a**) for SARS-CoV 3CLpro has been designed and synthesized by Sivakoteswara and their research group in 2013. The macrocyclic inhibitor (**316a**) have been evaluated in vitro against different families of virus for anti-viral activity, such as picornaviridae, coronaviridae, and caliciviridae; which showed potent inhibition against 3CLpro of enterovirus (CVB3 Nancy strain), moderate inhibition against 3CLpro of norovirus and weak inhibition against 3CLpro of SARS-CoV with IC₅₀ value 15.5 μM (Figure 9). The macrocyclic inhibitor (**316a**) has been synthesized via the macrocyclization process (Scheme 24, 24C) by joining the previously synthesized intermediate compounds **309** and **312** through multi-step reactions (Scheme 24: **24A** and **24B**)⁴⁵.

The synthesis process of macrocyclic inhibitors **316a-e** has been divided into three parts. The first part involves the synthesis of key acid fragment **309** (Scheme 24, **24A**), the second part involves the synthesis of acyclic intermediates **312** (Scheme 24, **24B**), and the third part the addition of two synthesized intermediate compounds **309** and **312**; to produce the target compounds **316a-e** (Scheme 24, **24C**)⁴⁵.

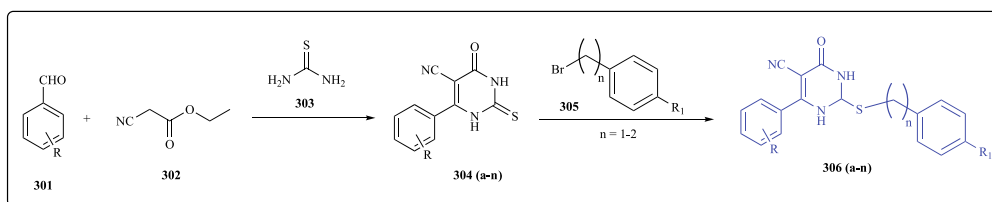
The key acid fragment **309** has been synthesized in two-steps by using previously published literature¹⁰⁰⁻¹⁰³, which started with the Boc-propargyl-Gly-OH **307** and reacted with L-Leucine methyl ester hydrochloride under specific reaction conditions to form dipeptidyl ester **308**. In the final step, the dipeptidyl ester **308** has been reacted with dry HCl under reaction conditions to remove the Boc protection (*N*-terminal) and further reaction with carbobenzoxy chloride transferred to the final cbz-protected acid fragment **309** (Scheme 24, **24A**).

Similarly, the second key azide intermediates **312** has been synthesized via two-step as described in previously published literature, which started with the Boc-Glu-ome **310** and NH₂(CH₂)_nN₃ (*n* = 3). These two compounds have been coupled via EDCl mediated reaction and converted to compound **311**. Further treatment with HCl in dioxane, the compound **311** has converted to final azide intermediate **312** (Scheme 24, **24B**)⁴⁵.

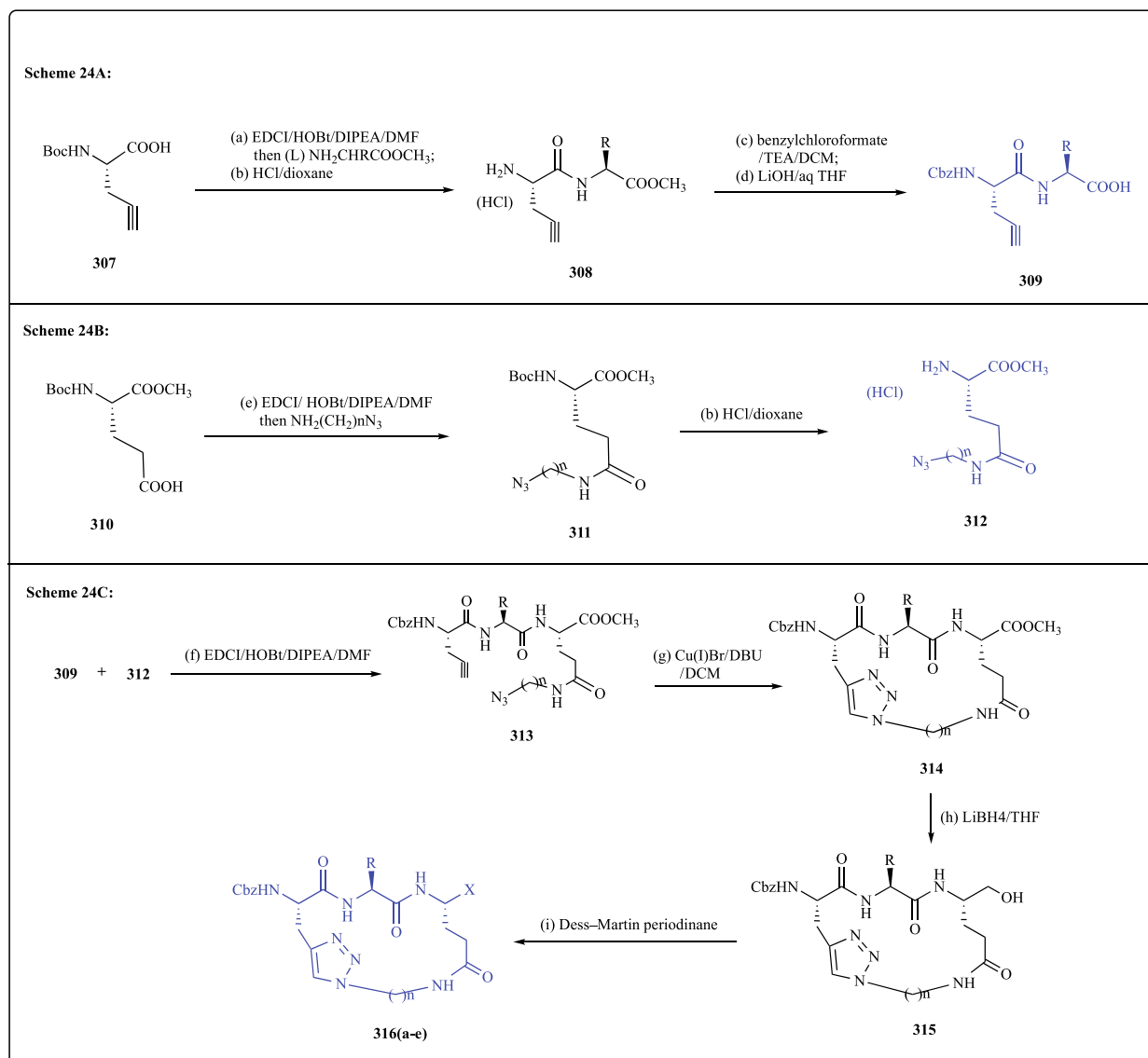
The synthesis of macrocyclic inhibitors **316a-e** has been started via the addition of two synthesized intermediates **309** and **312** and by coupling reaction conditions, the intermediates have transferred into



Scheme 22. Synthesis of pyrazolone derivatives.



Scheme 23. Synthesis of pyrimidine derivatives.



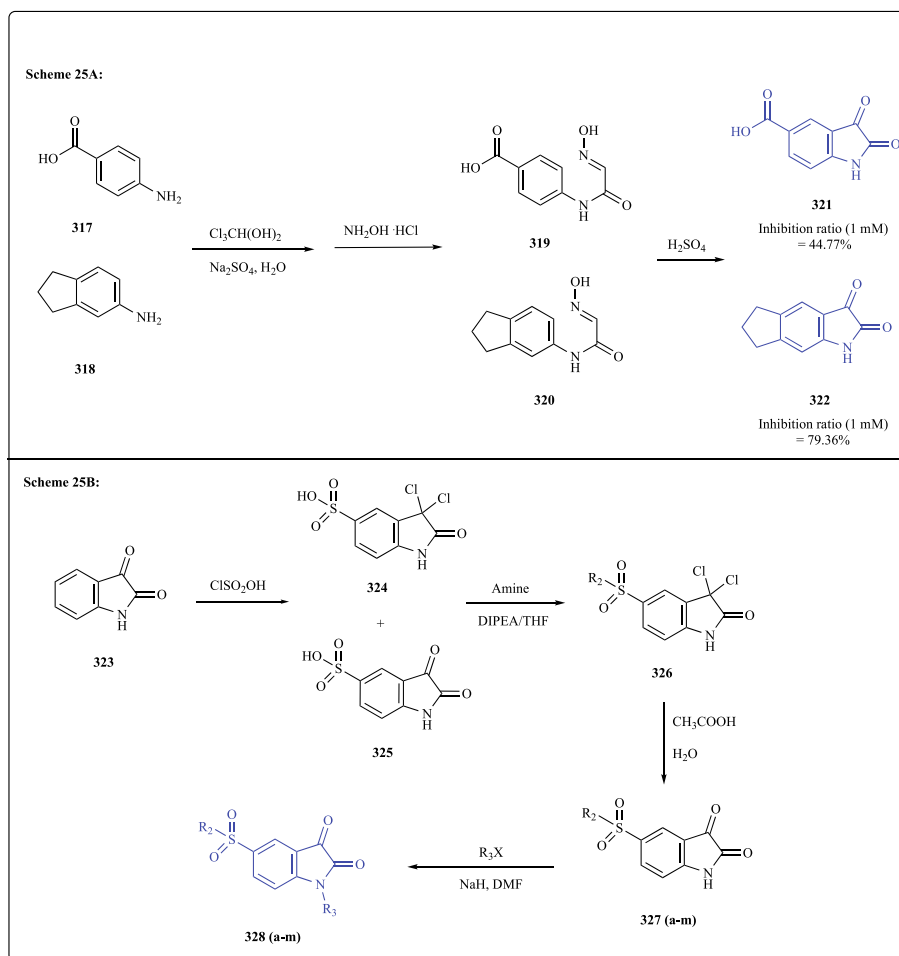
Scheme 24. Synthesis of macrocyclic inhibitors. **Scheme 24, 24A:** synthesis of key acid fragment **309**; **Scheme 24, 24B:** synthesis of azide intermediates **312**, and **Scheme 24, 24C:** synthesis of macrocyclic inhibitors **316a-e** by addition of two key intermediates **309** and **312**.

acyclic compound **313**. In the next step, the compound **313** has undergone a cyclization reaction by applying click chemistry in the presence of Cu(I)Br/DBU and converted to cyclized product **314**. The compound **314** further reacted with lithium borohydride in presence of THF to produce corresponding alcohol **315** and by oxidation of compound **315** with Dess–Martin periodinane produced the final macrocyclic compounds **316a-e** (Scheme 24, 24C)^{45,104}.

3.2.6. 5-sulphonyl isatin derivatives:

The substitution of a carboxamide group with a series of substituted

sulfonamide moieties have been explored by Liu and co-workers in 2014 to enhance the inhibitory effect towards SARS-CoV 3CLpro⁴⁶. They have designed the target compounds based on previously reported non-covalent SARS-CoV 3CLpro inhibitors (*N*-substituted 5-carboxamide-isatin derivatives), which Zhou and co-workers developed in 2006¹⁰⁵. A series of designed compounds have been synthesized via multistep organic reaction (Scheme 25, 25B) and screened by in vitro protease assay using fluorogenic substrate peptide. From the assay result, it has been found that several compounds have potent inhibitory activity against the SARS-CoV 3CLpro and among all the compounds, **328a**



Scheme 25. Synthesis of small-molecule inhibitors containing isatin moiety. **Scheme 25, 25A:** synthesis of isatin compounds **321** and **322**; **Scheme 25, 25B:** synthesis of a series of 5-sulphonyl isatin derivatives **328a-m**.

showed the best inhibitory activity against the SARS-CoV 3CLpro with $IC_{50} = 1.04 \pm 0.01 \mu\text{M}$ (Figure 9)⁴⁶.

The synthesis of isatin derivatives has been divided into two parts, the first part has focused on the synthesis of two compounds **321** and **322** (Scheme 25, 25A); the second part has focused on the synthesis of series of 5-sulphonyl isatin derivatives **328a-m** (Scheme 25, 25B). The target compound **321** and **322** have been synthesized by reacting two corresponding starting material **317** and **318**. Under reaction with hydroxylamine hydrochloride and chloral hydrate, the compounds **317** and **318** have converted to corresponding compounds **319** and **320**. Lastly, reaction with concentrated sulfuric acid converts the compounds **319** and **320** to target isatin compounds **321** and **322** (Scheme 25, 25A)¹⁰⁶.

In the second part of the synthesis, a series of 5-sulphonyl isatin derivatives **328a-m** has been prepared by referring to published literature^{107,108}. First, the isatin molecule **323** has been treated with chlorosulfonic acid that produces two compounds, **324** and **325**. In the next step, both the compounds **324** and **325** have been isolated and reacted with a secondary amine under reaction condition and converted to **326**. The compound **326** has directly converted to **327a-m** by the treatment of secondary amine with high yields. In the last step, the compounds **327a-m** have been alkylated with various bromides or iodides in the presence of sodium hydride to produce 5-sulphonyl isatin derivatives **328a-m** (Scheme 25, 25B)⁴⁶.

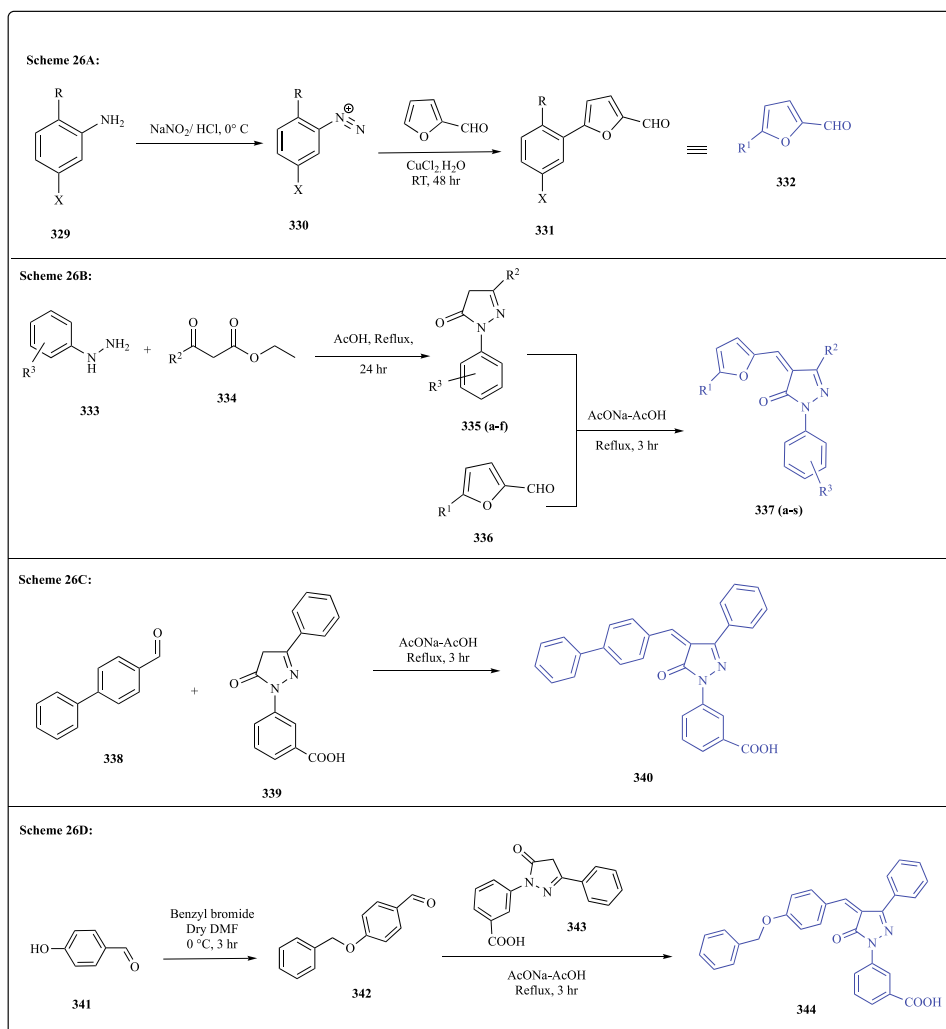
The S1 site composed of the piperidine and the sulfonyl moiety was observed to fit in the hydrophobic pocket formed by Met49, Met165, Gln189, Arg188 residues, and the S2, which is in close proximity with

the Cys145. The benzyl group present in S3 is near Phe140, Glu166, Leu141 residues. The two ketone groups and the nitrogen in S4 were also found to interact with Gly143, Asn142, Ser144 residues of the 3CLpro (Figure 9)⁴⁶.

3.2.7. Pyrazolone derivatives:

Kumar et al have synthesized furfural-based pyrazolone derivatives and screened against SARS-CoV as well as MERS-CoV 3CLpro inhibitors as broad-spectrum antiviral agents. Neuraminidase (NA), is one of the key targets for the release of the viral particle from the cell surface. They have recently reported a new antiviral neuraminidase inhibitor for both N1 and N2 via cell-based antiviral assay¹⁰⁹. These NA inhibitors have some structural similarity with their previously reported SARS-CoV 3CLpro inhibitors⁴³. Due to these background data, they have screened and synthesized these NA analogues for SARS-CoV and MERS-CoV 3CLpro (Scheme 26: **26A**, **26B**, **26C**, and **26D**). The biological activity showed that molecules have low micromolar inhibitory activity and could inhibit NA and 3CLpro enzymes as a dual target antiviral agent. Among all pyrazolone compounds, **337a** has shown the best inhibitory activity against the SARS-CoV 3CLpro with $IC_{50} = 5.8 \pm 1.5 \mu\text{M}$ (Figure 9)⁴⁷.

The substituted furfural aldehyde fragment **332** has been synthesized by using published literature methods¹¹⁰. At first, the diazonium salts **330** were synthesized by starting compound **329** and sodium nitrate under specific reaction conditions. Lastly, the diazonium salts **330** has been converted to final substituted furfural aldehyde fragment **332** by reacting with furfural and Copper (II) chloride (Scheme 26, **26A**)⁴⁷.



Scheme 26. Synthesis of pyrazolone derivatives. **Scheme 26, 26A:** synthesis of substituted furfural aldehyde fragment **332**; **Scheme 26, 26B:** synthesis a series of pyrazolones derivatives **337a-s**; **Scheme 26, 26C:** synthesis of compound **340**; and **Scheme 26, 26D:** synthesis of compound **344**.

In the second part of the synthesis, a series of pyrazolone derivatives **337a-s** was prepared using a multistep organic reaction. To synthesize intermediate compounds **335a-f**, the substituted hydrazines **333** and b-ketoesters **334** has been reacted in the presence of AcOH under reflux condition. Then, the intermediate compounds **335a-f** have been converted to pyrazolone derivatives **337a-s** by reacting with previously synthesized **336** (**Scheme 26, 26B**)⁴⁷.

Similarly, another pyrazolone inhibitor **340** has been synthesized by one-step process via reaction of compounds **338** and **339**; to explore the effect of aldehyde substitution (**Scheme 26, 26C**). In the last part, another pyrazolone inhibitor **344** has been synthesized by a two-step process via the reaction of *para*-hydroxy benzaldehyde **283** and benzyl bromide under appropriate reaction conditions to produce compound **342**. Further, compound **342** has been converted to final compound **344** by reacting with compound **343** under appropriate reaction conditions (**Scheme 26, 26D**)⁴⁷.

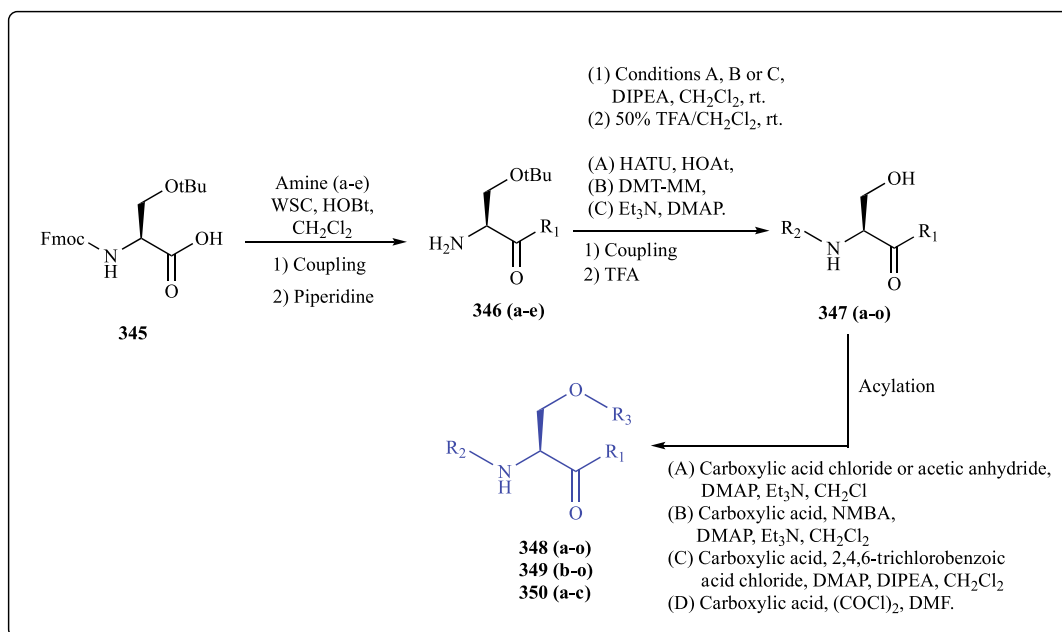
The S1 site composed of the chlorobenzoic acid moiety was observed to interact with Gly143, His163, Ser144, and Cys145 residues and the trimethyl group of S2 fit in the hydrophobic pocket formed by Met49 and Gln189. The carbonyl group of pyrazolone derivative present in the S3 was found to interact with the His41 residue of the 3CLpro (**Figure 9**)⁴⁷.

3.2.8. Serine derivatives:

Konno et al has been aimed to design non-peptidyl SARS-CoV 3CLpro

inhibitors based on previous lead compounds, tetrapeptide aldehyde Ac-Thr-Val-Cha-His-H and Bai's inhibitors of SARS 3CLpro. They have designed a series of functionalized serine derivatives focusing on P1, P2, P4 site interaction of peptide aldehyde inhibitor with 3CLpro. The compounds have been generated through virtual screening on GOLD software with additional docking simulation. The synthetic outline and associated reaction conditions depicted in **Scheme 27**, associated functionalities to prepare serine derivatives are given in **table 1, 2 & 3** of their research article. The biological activity of the compounds has been evaluated using cleavage activity of SARS-3CL mutant protease, R188I, on a synthetic decapeptide with the S01 cleavage sequence as the substrate. In parallel with biological study, a cytotoxicity study of serine derivatives has also been performed on HeLa cells. The SAR study, in combination with docking simulation, revealed two potential inhibitors **ent-290** (SK23) and **ent-291** (SK69), with D-configuration on serine template, have high protease selectivity. The potential compounds of this study practically do not have any cytotoxicity. The most potential inhibitor under serine derivatives is **348** (SK23) with $\text{IC}_{50} = 30 \mu\text{M}$ (**Figure 9**)⁴⁸.

A series of serine derivatives **348a-o**, **349b-o**, and **350a-c** has been prepared using a three-step organic reaction. The synthesis has been started via a coupling reaction of Fmoc-Ser(*t*Bu)-OH **345** and various amines (like cyclohexylamine, piperidine, morpholine, benzylamine, and cyclohexyl methylamine) under reaction conditions and transferred to the intermediate compounds **346a-e**. Using different coupling



Scheme 27. Synthesis of a series of serine derivatives.

reaction conditions (A, B, and C) and deprotection of *t*-butyl group, the compounds 288a-e have been converted to the 347a-o. In the last step, different acylation reaction conditions have been employed to convert the compounds 347a-o to the final serine derivatives 348a-o, 349b-o, and 350a-c (Scheme 27).

Results obtained from in silico study of compound 348 showed that the carbonyl group in the S1 site and amino group in S2 interacted with Cys145 and Gln189 amino acid residues of the enzyme, respectively (Figure 9)⁴⁸.

3.2.9. Phenylisoserine derivatives:

Hiroyuki Konno, has designed and synthesized phenylisoserine derivatives from reported molecule tetrapeptide aldehyde (IC₅₀ = 98 nM) and SK23 (IC₅₀ = 30 μM) for SARS-CoV 3CLpro inhibition by the combination of SAR and docking simulation study. The molecular design of phenylisoserine derivatives has been started using three steps: serine to isoserine backbone, induction of the functionality at the P2 position, and SAR study. The inhibitory activity has been determined using a synthetic decapeptide as a substrate against SARS 3CL R188I mutant protease. The phenylisoserine containing inhibitors 356, 357a-e, 360, and 363 have been synthesized via multistep organic reaction as shown in Scheme 28: 28A, 28B, and 28C. Amongst these synthesized inhibitors, the compound 356 has shown better inhibition against SARS-CoV 3CLpro with IC₅₀ value 43 μM (Figure 9)⁴⁹.

The synthetic preparation of phenylisoserine derivatives 356 and 357a-e have been started via protection of three groups of the starting compound 351 amine, carboxylic acid, and hydroxyl and converted to compound 352. Next, the methyl ester of compound 352 has been saponified under suitable reaction conditions and further coupled with cyclohexylamine to prepare amide compound 353. Treatment with hydrogenation and cinnamic acid under reaction condition, the amide compound 353 has converted to cinnamoyl compound 354. The MOM group in compound 354 has been removed by treatment with trifluoroacetic acid to produce intermediate alcohol compound 355. From the compound 355, the phenylisoserine derivatives 356 and 357a-e have been prepared using appropriate reagents (Scheme 28, 28A)⁴⁹.

Similarly, two other phenylisoserine derivatives 360 and 363 have also been prepared. The synthesis of compound 360 started from compound 358 and converted to compound 359 by treatment with benzyl bromide as protection towards hydroxyl group, saponification, and

introduction of cyclohexylamine under reaction conditions. In the last step, the compound 359 has transferred to the target compound 360 by hydrogenolysis process and coupling with cinnamic acid (Scheme 28, 28B). The phenylisoserine derivatives 363 have also been prepared in two steps from the previous synthesized intermediate 361 (Scheme 28, 28A) as a starting material. The MOM group in compound 361 has been removed by treatment with trifluoroacetic acid and reacted with cinnamic acid to produce compound 362. Further hydrogenolysis process and coupling with cinnamic acid have converted the compound 362 to target compound 363 (Scheme 28, 28C).

The binding interaction of compound 356 with the protease revealed the interaction of the ester group in S1 site of the compound with the amino acid residues Gln189, His41, Cys145 and that of keto in the S2 site interacted with His164 of the protease (Figure 9)⁴⁹.

3.2.10. Octahydroisochromene derivatives:

Shin-ichiro Yoshizawa et al, conducted a study to design and synthesize novel nonpeptidyl inhibitors of SARS-CoV 3CLpro containing octahydrochromene scaffold based on previous peptide aldehyde inhibitor and nonpeptide inhibitor having decahydroisoquinolin moiety. However, in the previous work the effect of substituent on decahydroisoquinolin ring was not fully elaborated. In this study the effect of four substituents on 1-position of the octahydrochromene scaffold was rigorously analyzed. A novel hydrophobic core, octahydroisochromene scaffold has been introduced for interaction with the S2 pocket of the protease enzyme and substituents at 1-position was incorporated to form additional interactions.

Octahydroisochromene scaffold was built via Sharpless-Katsuki asymmetric epoxidation (SKAE) and Sharpless asymmetric dihydroxylation (SAD). The P1 site His-al and the substituent at 1-position was incorporated through subsequent reductive amination reactions. The synthetic outline and associated reaction condition for the construction of compounds are depicted in Scheme 29. The inhibitory potency of the compounds (375a-d) with single diastereomeric configuration clearly indicates that a particular stereo-isomer of the octahydroisochromene moiety, (1S, 3S) 375b (IC₅₀ = 95 μM), guides the P1 site imidazole, substituent at the 1-position and the warhead aldehyde of the fused ring to their proper pockets in the 3CL protease (Figure 9)⁵⁰.

The synthesis of SMIs containing octahydroisochromene moiety and the related compound was performed based on the retrosynthetic route.

Table 1
Summary of protein-inhibitor interaction for SARS-CoV 3CLpro.

Sl. No.	Compound no.	Derivatives	IC ₅₀ / K _i (μM)	Docking Study		Ref.
				PDB ID	Interaction (amino acid residues) Hydrogen = H Hydrophobic = Hb int. Covalent = (C) Van der waals int.	
1	14a	Anilide analogues	0.06	1UK4	H = Ala46Pockets involved = Cys145, Ser144, His163, Phe140 Or Thr25, His41, Cys44, Thr45.	24
2	38c	Peptidomimetic α,β unsaturated esters	1	1c145a	H = Glu166, Gln189, Gln192	25
3	53	Glutamic acid and glutamine peptides	K _i = 116.1	N.A.	N.A.	26
4	69	Peptidomimetic (TG-0205221)	0.6	1Z1I	H = Gln189, His163, His164, Glu166, Cys145, Gly143, Phe140. C = Cys145 Hb int. = Asn142, His41, Met165, Leu167, Pro168, Asp187, Met49, Ala191, Arg188, Thr190	27
5	83a	Phthalhydrazide peptide analogues	0.05	2A5K	H = His163, Ser144, Gly143, Cys145. Van der waals int. = Phe140, Glu166, Leu141, His172, Asn142, Hb int. = Cys145 (with the furan ring)	28
6	108a	Cinanserin analogues	1.06	1UJ1	Hb int. = Thr25, Leu27, Gly143, His41, Met49, Gln189, Met165, Cys145, Glu166, His163, Phe140	29
7	113c	Trifluoromethyl ketone containing peptides	10	1UK4	C = Cys145. H = Gly143, Glu166, Gln189. Hb int. = Met165, Met49, His163, Phe140, Pro168	30
8	137	Trifluoromethyl, benzothiazolyl or thiazolyl ketone containing peptidomimetics	K _i = 2.20 ± 0.8	1WOF	C = Cys145. H = His41, Ser144, Gly143, His163, Gln189, Glu166, His164.	31
9	149a	Michael type of peptidomimetics	5.7	3AW0	H = His163, Glu166, Thr190.	32
10	162b	Cysteine protease inhibitors	0.23 ± 0.1	N.A.	N.A.	33
11	172a	Potent dipeptide type of peptidomimetics	0.74	1WOF	H = Glu166, Gln189, His164, Ser144, His163	34
12	180a	Novel dipeptide type of peptidomimetics	10	1WOF	H = Glu166, Gln189, His164, Ser144, His163	35
13	204	Nitrile based peptidomimetics	4.6	3VB5	C = Cys145. H = Glu166, Phe140, Gln189, Thr190. Hb int. = Pro168	36
14	214o	Tripeptide type of peptidomimetics	0.65	1WOF	H = His41, Glu166, His163, Ser144, Cys145. Hb int. = Ala191	37
15	226d	Peptidomimetic containing Cinnamoyl warhead	0.2 ± 0.07	N.A.	N.A.	38
16	247	Peptidomimetic containing Decahydroisoquinolin moiety	26	4TWW	N.A.	39
17	256	Ketone-based covalent inhibitors	0.017 ± 2	6XHN	H = Gly143, Cys145 C = Cys145	40
18	289s	α-Ketoamides derivatives	0.24 ± 0.08	2BX4	H = Gln189, Phe140, Glu166, Gly143, Ser144, His41. Hb int. = Met49, Met165	41
19	291a	Isatin derivatives	0.95	1UK4	H = Gly143, Cys145, His41. Hb int. = His164, Phe140, Met165	42
20	294a	Chloropyridyl ester derivatives	0.03 ± 0.01	2HOB	H = Cys145, Ser144, Gly143	43
21	300c	Pyrazolone Derivatives	8.4	1UK4	H = Gly143, Gln192, Glu166. Hb int. = Met49, Arg188, Gln189	44
22	306c	Pyrimidines Derivatives	6.1 ± 1.1	1UK4	H = Gly143, Glu166, Cys145. Hb int. = Met49, Gln189	45
23	316a	Macrocyclic inhibitors	15.5	2ZU5	N.A.	46
24	328a	5-sulphonyl isatin derivatives	1.04 ± 0.01	1UK4	H = Gly143, Asn142, Ser144 Hb int. = Met49, Met165, Gln189, Arg188, Cys145, Phe140, Glu166, Leu141	47
25	337a	Pyrazolone derivatives	5.8 ± 1.5	2ALV	H = His41, Ser144, His163, Cys145, Gly143, Hb int. = Met49, Gln189	48
26	348	Serine derivatives	30	3AW1	H = Cys145, Gln189.	49
27	356	Phenylisoserine derivatives	43	3AW1	H = Gln189, His41, Cys145, His164.	50
28	357b	Octahydroisochromene derivatives	95	4TWW	N.A.	

N.A. = Not available.

Table 2
List of amino acid residues for SARS-CoV 3CLpro.

Function in SARS-CoV 3CLpro	Amino acid residues
Catalytic dyad	His41, Cys145
Ligand binding	Cys145, Glu166, Gln189, His163, Gly143, Ser144, Phe140, His41, Met49, His164, Met165, Asn142, Gln192, Pro168, Arg188, Thr190, Ala191, Leu141, Thr25, Ala46, Leu167, Asp187, His172, Leu27.

From the retrosynthetic analysis it was revealed that a diol compound **364** is the starting compound for the synthesis of targeted derivatives. Hence, the synthesis of precursor molecule **369** is started from compound **364**. The key intermediate **369** was synthesized starting with compound **364** following the route shown in Scheme 29, 29A. Protection of one hydroxyl group with TBDPSCl (*tert*-butyl diphenylsilyl chloride) and oxidation of another alcohol group via Ley-Griffith oxidation reaction using TPAP (tetrapropyl ammonium perruthenate) of diol **8**, produced the corresponding aldehyde. The aldehyde without purification after reacting with (methoxymethyl)

Table 3
Summary of cell-based assay for SARS-CoV 3CLpro.

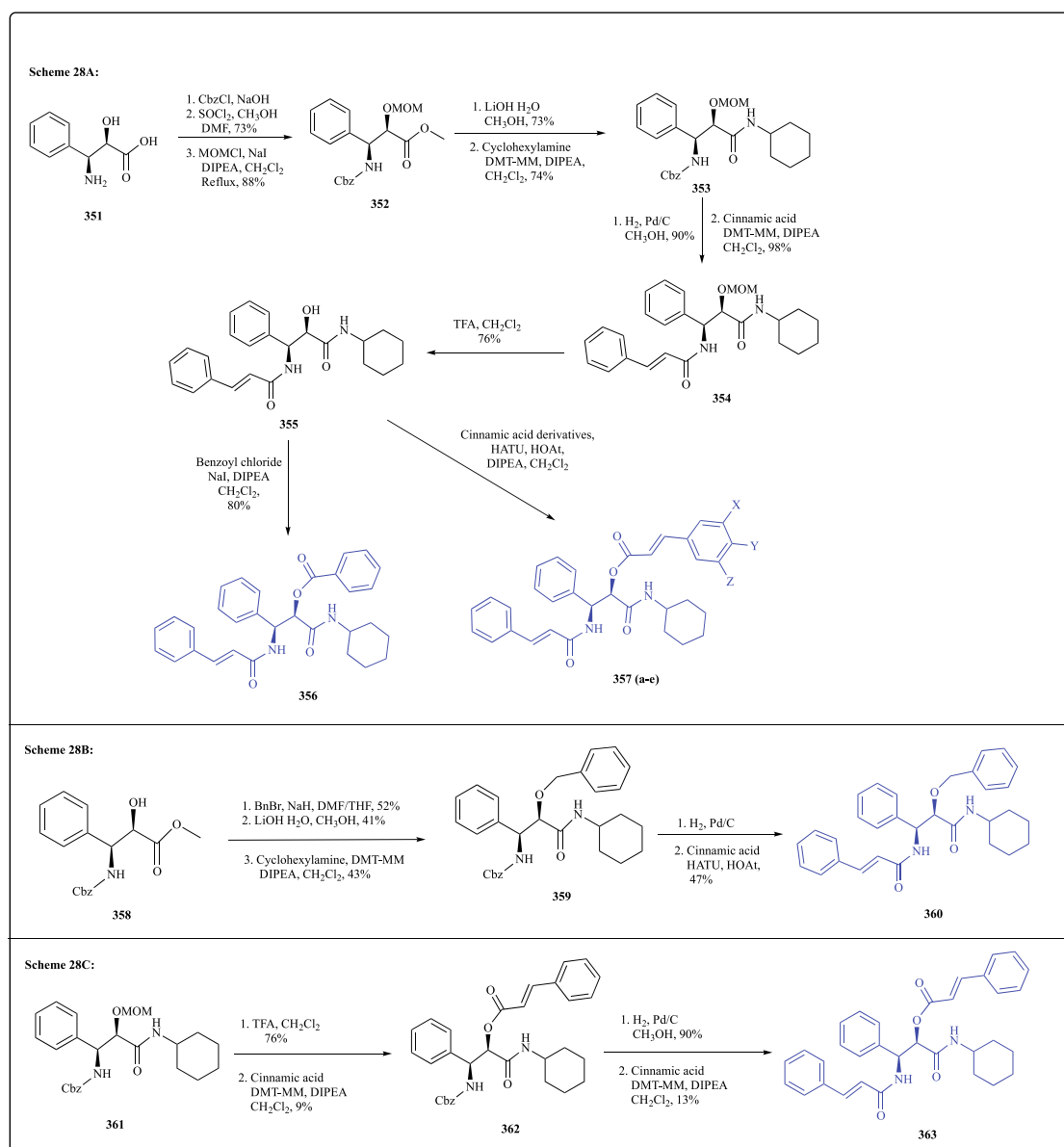
Sl. No.	Compound no.	Derivatives	Cell-based assay		Ref.
			EC ₅₀ (μM)	Cell line	
1	38c	Peptidomimetic α,β unsaturated esters	0.18	Vero E6	25
2	69	Peptidomimetic (TG-0205221)	0.6	Vero E6	27
3	256	Ketone-based covalent inhibitors	5 ± 1.4	Vero 76	14
4	289s	α-Ketoamides derivatives	18.4 ± 6.7	Vero E6	40
5	294a	Chloropyridyl ester derivatives	6.9 ± 0.9	Vero E6	42

triphenylphosphonium chloride yielded **365**. The reaction between **365** and 10-camphorsulfonic acid produced corresponding aldehyde. The isolated aldehyde after reaction with methyl triphenylphosphonium chloride gave terminal olefin. Removal of TBDPS group in the product

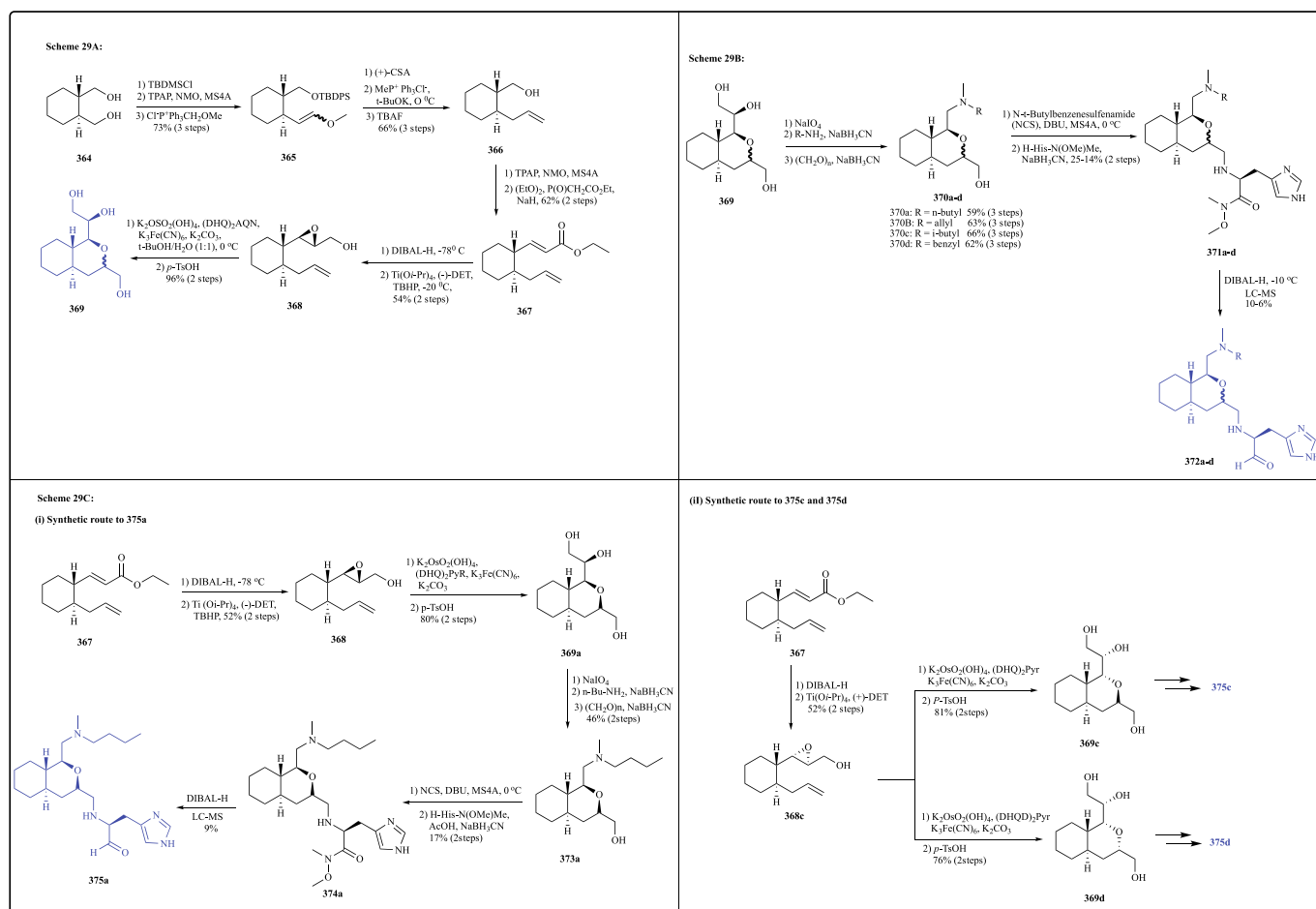
upon treatment with TBAF (tetra-*n*-butylammonium fluoride) produced the intermediate **366**. Oxidation of the primary alcohol in **366** via a Ley–Griffith oxidation reaction and homologation of the corresponding aldehyde through Horner–Wadsworth–Emmons (HWE) reaction using ethyl 2-(diethoxyphosphoryl) acetate produced **367**.

Reduction of ethyl ester in **367** with DIBAL-H and stereo-specific oxidation of corresponding allylic alcohol via a SKAE reaction utilizing TBHP (*tert*-butyl hydroperoxide) mediated by (*S,S*)-diethyltartrate ((-)-DET) and titanium tetrakisopropoxide (TTIP) gave **368** as a single diastereomer. The terminal olefin in **368** was oxidized via a Sharpless asymmetric dihydroxylation reaction under desired conditions. The production of the anticipated diol was confirmed by ¹H NMR spectroscopy with the concurrent formation of a small proportion of the cyclic product **369** produced via the nucleophilic addition of the resultant alcohol. Then, desired cyclized product **369** was obtained via treatment of the mixture with *p*-toluenesulfonic acid without further purification.

The key intermediate **369** was transferred into the final product following the synthetic route displayed in [Scheme 29](#), [29B](#). Oxidative cleavage using sodium periodate followed by reductive amination of the



Scheme 28. Synthesis of phenylisoserine derivatives. [Scheme 28, 28A](#): synthesis a series of phenylisoserine derivatives **356** and **357a-e**; [Scheme 28, 28B](#): synthesis of phenylisoserine containing inhibitor **360**; [Scheme 28, 28C](#): synthesis of phenylisoserine containing inhibitor **363**.



Scheme 29. Synthesis of Octahydroisochromene derivatives. **Scheme 29, 29A:** synthesis of key intermediate **369**; **Scheme 29, 29B:** conversion of key intermediate **369** into the final product **372a-d**; **Scheme 29, 29C:** synthetic route for the preparation of **375a**, **375c** and **375d**.

corresponding aldehyde with four distinct amines by using NaBH_3CN leads to aminated products. Methylation of aminated products by paraformaldehyde gave **370a-d**. Oxidation of primary alcohol in the products and followed by reductive condensation of associated aldehyde with H-His-N(OMe)Me leads to Weinreb amides (**371a-d**). Reduction of each amide to aldehyde by treatment of DIBAL-H and followed by purification via LC/MS gave the required aldehyde products (**372a-d**). The synthetic route for the preparation (1-*S*, 3-*R*) **375a** is depicted in **Scheme 29, 29C (i)**. The allylic alcohol produced after reducing the ester **367** was oxidized via Sharpless-Katsuki asymmetric epoxidation reaction in presence of (-)-DET as the chiral ligand to yield a single diastereoisomer **368**. Oxidation of terminal olefin in **368** by Sharpless asymmetric dihydroxylation using a chiral ligand, $(\text{DHQD})_2\text{Pyr}$ gave a primary product **369a**⁵⁰.

Oxidative breakdown of the 1,2-diol in **369a** and followed by reductive amination reaction using *n*-butyl amine in presence of paraformaldehyde were performed as illustrated for compound **370a**. Finally coupling reaction with H-His-N(OMe)Me and following reduction by DIBAL-H was conducted as mentioned for compound **372a** (**Scheme 29, 29C-i**) yield **375a** as the primary product. The diastereoisomer Compound **375b** with the (1-*S*, 3-*S*) configuration was synthesized by using a combination of $(\text{DHQD})_2\text{Pyr}$ and (-)-DET, those were employed in the SKAE reaction and the Sharpless asymmetric dihydroxylation reaction, respectively. Diastereoisomers, **375c** and **375d**, were synthesized with the (1-*R*, 3-*R*) and (1-*R*, 3-*S*) configurations, respectively; this was accomplished by using synthetic outline displayed in **Scheme 29, 29C-ii**. To create the (1-*R*, 3-*R*) configuration in **13c**, a combination of (+)-DET and $(\text{DHQD})_2\text{Pyr}$ was utilized, those were used in the SKAE reaction

(producing a single diastereoisomer) and the SAD reaction, respectively. In a similar way the (1-*R*, 3-*S*) configuration in **369d** build using (+)-DET and $(\text{DHQD})_2\text{Pyr}$ as ligand. Both the product then transferred to **375c** and **375d** following the given procedure⁵⁰.

4. Computational chemistry aspects:

Computational chemistry and pharmaceutical chemistry plays a tremendous role in drug discovery and development from the last decade¹¹¹. Nowadays, discovering lead molecules or identifying potential drug candidates for various diseases is one of the challenging scenarios for researchers. To overcome this challenge, the research groups are focusing on using pharmacoinformatic tools to minimize the time, cost, manpower, and errors for developing the potential drugs. By using the above tools, searching thousands of molecules from various databases and simultaneous identification of the best fit molecules for target protein becomes less tedious¹¹². The interactive information derived between proteins (macromolecule) and ligands can help the chemist to design and synthesize the most potent inhibitors against SARS-CoV by analyzing the SAR^{113,114}. Here, we have summarized the computational chemistry aspects of SARS-CoV 3CLpro inhibitors, including the various SARS-CoV 3CL proteases (PDB IDs), types of bond between the ligands and various amino acids of the protease, frequency of amino acid residues involved in the interaction (**Table 1**).

For virus replication and infection cycles, Mpro enzyme is critical, allowing it a perfect tool for the development of antiviral drugs. The binding site of 3CLpro comprises a catalytic dyad where a cysteine residue (Cys145) behaves as a nucleophile and a histidine residue

(His41) serves either as general acid or base^{4,115}. The list of residues of amino acids that serve a vital part in ligand binding with the SARS-CoV 3CLpro are shown in Table 2. As found from various literature surveys amino acid residues and their percentage frequency are Cys145 (13.2%), Glu166 (11.1%), Gln189 (10.4%), His163 (8.3%), Gly143 (9%), Ser144 (6.3%), Phe140 (5.6%), His41 (5.6%), Met49 (4.9%), His164 (4.2%), Met165 (4.2%), Asn142 (2.8%), Gln192 (2.1%), Pro168 (2.1%), Thr190 (2.1%), Arg188 (1.4%), Ala191 (1.4%), Leu141 (1.4%), Thr25 (0.7%), Ala46 (0.7%), Leu167 (0.7%), Asp187 (0.7%), His172 (0.7%), Leu27

(0.7%) plays a vital role for the various interactions which includes hydrogen-bonding (55.9%), covalent (3.4%), hydrophobic (37.2%) and van der waals interactions (3.4%) in Figure 10, 10A. It was observed that the 11 frequent amino acid residues are mainly responsible for the interactions, which include Cys145, Glu166, Gln189, His163, Gly143, Ser144, Phe140, His41, Met49, His164, Met165 (Figure 10, 10B).

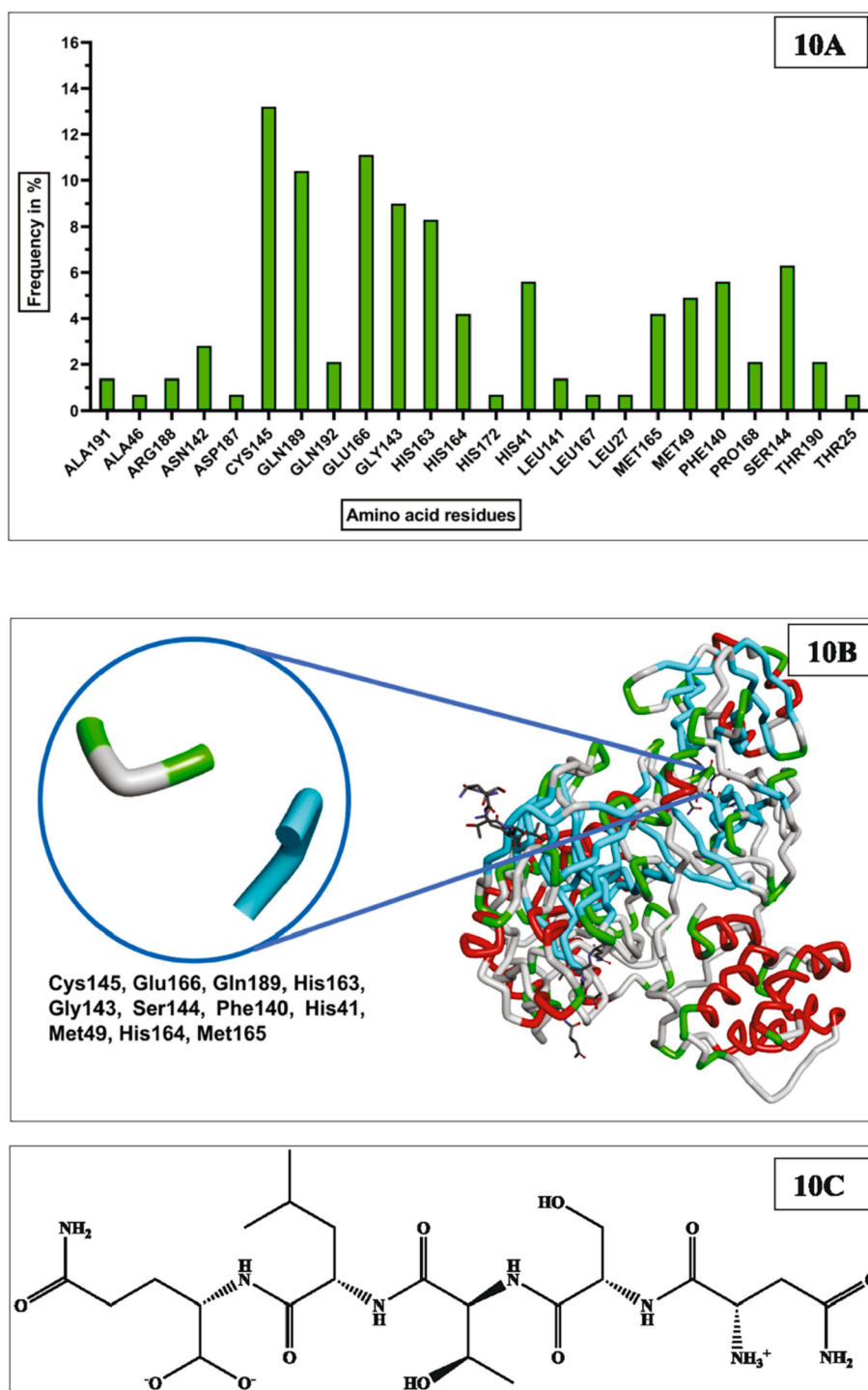


Figure 10. Amino acid residues predominantly involved in protein-ligand interactions. **10A.** Amino acid residues occurrence in percentage. **10B.** This figure represents the 11 most crucial amino acids responsible for interaction with the ligands present in the SARS-CoV 3CLpro (PDB ID: 1UK4)⁵⁸ with 5-mer peptide of inhibitor (**10C**).

5. Cell-based assay:

Cell-based therapies can revolutionize contribution to currently unfulfilled healthcare problems, hence making effective manufacturing critical. Before any of this could become a possibility, numerous barriers must be solved, as well as a deeper understanding of the specific requirements for cell-based technologies. Vero E6, Vero 76, and other commonly known cell lines may be utilized for virus replication in vitro with evident cytopathic effects. The cytopathic effect of several viruses is known to be mediated by virus-induced apoptosis or cell necrosis. The 'Vero' cells that are used, are extracted from kidney epithelial cells of African green monkey. Vero E6 cells have been widely employed in SARS-CoV research in cell culture-based infection models since 2003, owing to their ability to sustain viral replication to high titers, due to their higher expression of the ACE-2 receptor¹¹⁶. Translation cell-based assays for SARS-CoV had given proper insight into the mechanism of action of the potential inhibitors that are may be helpful for the drug discovery process in the near future^{117,118}. Table 3 shows the activities of cell-based assays of various inhibitors that are used in this review.

6. Conclusion & future perspective:

3CLpro is an important drug target for SARS-CoV, as virus-encoded protease involves the processing of the two viral polyproteins and responsible for the viral replication and infection process⁵. This review deals with the chemical synthesis and medicinal chemistry perspectives of PIs and SMIs targeting SARS-CoV 3CLpro, which has been chemically synthesized and biologically screened as newer derivatives from 2004 to 2020 for therapeutic inventions of SARS-CoV. In this overview, we have also identified the most potent compounds from each derivative and highlighted their structural features and binding modes.

In the current scenario, the warhead-based strategy plays a high impact in the medicinal chemistry for the development of SMIs and PIs. Most of the PIs and SMIs for SARS-CoV 3CLpro have been designed by applying a warhead-based strategy, but few inhibitors have shown better inhibition and potency. Most of the inhibitor has been evaluated via in vitro SARS-CoV 3CL protease assays using FRET analysis. The majority of PIs have not been studied further for in-vivo evaluation due to their less optimal physicochemical characteristics and undesirable frameworks.

In the development of potential compounds against SARS-CoV 3CLpro, it has been observed that the first synthetic peptidomimetic compounds are under keto-glutamine analogue. It has been designed and synthesized in 2004 from previously reported anti-viral compounds like hepatitis virus 3C and human rhinovirus 3C inhibitors (Figure 6). Compound **9b** is an example of a peptidomimetic inhibitor-containing cyclic keto-glutamine moiety that showed better inhibition against SARS-CoV 3CLpro with IC₅₀ value 0.60 μM. Comparing the molecular docking study, inhibitor **9b** is the only compound under SARS-CoV 3CLpro inhibitors studied with human rhinovirus-14 (PDB ID: 1CQQ).

From the keto-glutamine analogues other peptidomimetic inhibitors have been explored during this timeframe for the development of potential drug candidates, such as peptidomimetic containing α,β-unsaturated esters, anilide analogues, glutamic acid–glutamine peptides, and phthalhydrazide peptide; to improve the biological efficacy and potency against SARS-CoV 3CLpro. The chemical synthesis of many SMIs is also discussed in this review. The majority of inhibitors showed micromolar potency against SARS-CoV 3CLpro. The most promising inhibitors under SMIs are **291a**, **294a**, **300c**, **306c**, **316a**, **328a**, **337a**, **348**, **356**, and **357b**.

From the computational chemistry and protein interaction information's data of SARS-CoV 3CLpro inhibitors, it may be suggested that peptidomimetics (covalent and non-covalent inhibitors) and SMIs exhibited specific and effective active-site inhibition. The protein-drug interaction of inhibitors **14a**, **38c**, **69**, **83a**, **108a**, **113c**, **137**, **149a**, **172a**, **180a**, **204**, **214o**, **256**, **289s**, **291a**, **294a**, **300c**, **306c**, **328a**,

337a, **348**, and **356** has been also analyzed with different PDB IDs, except inhibitors **53**, **162b**, **226d**, **247**, **316a**, and **357b** (Table 1).

3CLpro inhibitors have been extensively studied, enabling the production of a percentage frequency graph that displays the most critical amino acid residues detected for interaction with the ligands. From this, it was verified that these compounds interact via hydrogen-bonding (55.9%), covalent (3.4%), hydrophobic (37.2%), and van der Waals interactions (3.4%), where the Cys145 residue is the most frequent to exhibit hydrogen bond formation. His41-Cys145 is a part of a catalytic dyad. Met165 residue exhibits the most frequent hydrophobic interacting sites. Cys145 is the amino acid residue for which the covalent interaction is responsible. The 11 frequent amino acid residues responsible for the interactions includes Cys145, Glu166, Gln189, His163, Gly143, Ser144, Phe140, His41, Met49, His164, and Met165 that are discussed earlier in the medicinal chemistry perspective section and will be crucial for drug development process in future.

However, some of the peptidomimetics showed less inhibition activity against the SARS-CoV 3CLpro and poor absorption, distribution, metabolism, and excretion parameters to be a drug-like molecule. Peptidomimetic has few drawbacks over the SMIs, like high molecular weight, poor pharmacokinetic properties and pharmacodynamic property. To develop potential 3CLpro inhibitors against coronavirus, the strategy should be focused on developing low-molecular weight peptidomimetic inhibitors and its lead optimization for improvement of pharmacokinetic and pharmacodynamic properties. This project may soon emerge as a pioneer in the discovery of SARS-CoV 3CLpro inhibitors to succeed in the fight against coronavirus.

Declaration of Competing Interest

The authors declare that they have no known competing financial interests or personal relationships that could have appeared to influence the work reported in this paper.

Acknowledgements

Abhik Paul is thankful to the All-India Council for Technical Education (AICTE), New Delhi, India for awarding a fellowship (AICTE-NDF). Arnab Sarkar, Sanjukta Saha and Pritha Janah are thankful to the All-India Council for Technical Education (AICTE), New Delhi, India for awarding the fellowship. Avik Maji is thankful to RUSA 2.0 of University Grants Commission (UGC), New Delhi for awarding a fellowship. The authors heartily thank Mind the GRAPH (Senior plan) for providing graphical illustrations, and <https://www.rcsb.org/> for providing 3D structures of macromolecules. The authors also thank the support from the Department of Pharmaceutical Technology, Jadavpur University, Kolkata for providing research amenities.

References

- Kuiken T, Fouchier RAM, Schutten M, et al. Newly discovered coronavirus as the primary cause of severe acute respiratory syndrome. *Lancet*. 2003;362(9380): 263–270. [https://doi.org/10.1016/S0140-6736\(03\)13967-0](https://doi.org/10.1016/S0140-6736(03)13967-0).
- Kahn JS, McIntosh K. History and Recent Advances in Coronavirus Discovery. *Pediatr Infect Dis J*. 2005;24(11):S223–S227. <https://doi.org/10.1097/01.inf.0000188166.17324.60>.
- Rota PA, Oberste MS, Monroe SS, et al. Characterization of a novel coronavirus associated with severe acute respiratory syndrome. *Science*. 2003;300(5624): 1394–1399. <https://doi.org/10.1126/science.1085952>.
- Snijder EJ, Bredenbeek PJ, Dobbe JC, et al. Unique and conserved features of genome and proteome of SARS-coronavirus, an early split-off from the coronavirus group 2 lineage. *J Mol Biol*. 2003;331(5):991–1004. [https://doi.org/10.1016/S0022-2836\(03\)00865-9](https://doi.org/10.1016/S0022-2836(03)00865-9).
- Ghosh AK, Brindisi M, Shahabi D, Chapman ME, Mesecar AD. Drug Development and Medicinal Chemistry Efforts toward SARS-Coronavirus and Covid-19 Therapeutics. *ChemMedChem*. 2020;15(11):907–932. <https://doi.org/10.1002/cmdc.202000223>.
- Pillaiyar T, Manickam M, Namasivayam V, Hayashi Y, Jung SH. An overview of severe acute respiratory syndrome-coronavirus (SARS-CoV) 3CL protease inhibitors: Peptidomimetics and small molecule chemotherapy. *J Med Chem*. 2016; 59(14):6595–6628. <https://doi.org/10.1021/acs.jmedchem.5b01461>.

- 7 Shi Z, Hu Z. A review of studies on animal reservoirs of the SARS coronavirus. *Virus Res.* 2008;133(1):74–87. <https://doi.org/10.1016/j.virusres.2007.03.012>.
- 8 Dömling A, Gao L. Chemistry and Biology of SARS-CoV-2. *Chem.* 2020;6(6): 1283–1295. <https://doi.org/10.1016/j.chempr.2020.04.023>.
- 9 European Centre for Disease Prevention and Control. Rapid Risk Assessment: Severe Respiratory Disease Associated with Middle East Respiratory Syndrome Coronavirus (MERS-CoV), 20th Update, 27 August 2015.; 2015.
- 10 Wu F, Zhao S, Yu B, et al. A new coronavirus associated with human respiratory disease in China. *Nature.* 2020;579(7798):265–269. <https://doi.org/10.1038/s41586-020-2008-3>.
- 11 World Health Organizations, Emergencies, Diseases. Coronavirus disease (COVID-19). <https://www.who.int/emergencies/diseases/novel-coronavirus-2019>.
- 12 Vandyck K, Deval J. Considerations for the discovery and development of 3-chymotrypsin-like cysteine protease inhibitors targeting SARS-CoV-2 infection. *Curr Opin Virol.* 2021;49:36–40. <https://doi.org/10.1016/j.coviro.2021.04.006>.
- 13 Cannalire R, Cerchia C, Beccari AR, Di Leva FS, Summa V. Targeting SARS-CoV-2 Proteases and Polymerase for COVID-19 Treatment: State of the Art and Future Opportunities. *J Med Chem.* Published online November 2020. doi:10.1021/acs.jmedchem.0c01140.
- 14 Hoffman RL, Kania RS, Brothers MA, et al. Discovery of Ketone-Based Covalent Inhibitors of Coronavirus 3CL Proteases for the Potential Therapeutic Treatment of COVID-19. *J Med Chem.* 2020;63(21):12725–12747. <https://doi.org/10.1021/acs.jmedchem.0c01063>.
- 15 Vandyck K, Abdelnabi R, Gupta K, et al. ALG-097111, a potent and selective SARS-CoV-2 3-chymotrypsin-like cysteine protease inhibitor exhibits in vivo efficacy in a Syrian Hamster model. *Biochem Biophys Res Commun.* 2021;555:134–139. <https://doi.org/10.1016/j.bbrc.2021.03.096>.
- 16 Amin SA, Jha T. Fight against novel coronavirus: A perspective of medicinal chemists. *Eur J Med Chem.* 2020;201, 112559. <https://doi.org/10.1016/j.ejmech.2020.112559>.
- 17 Silva LR, da Silva Santos-Júnior PF, de Andrade Brandão J, et al. Druggable targets from coronaviruses for designing new antiviral drugs. *Bioorganic Med Chem.* 2020; 28(22), 115745. <https://doi.org/10.1016/j.bmc.2020.115745>.
- 18 Mohapatra S, Nath P, Chatterjee M, et al. Repurposing therapeutics for COVID-19: Rapid prediction of commercially available drugs through machine learning and docking. *PLoS ONE.* 2020;15(11), e0241543. <https://doi.org/10.1371/journal.pone.0241543>.
- 19 Alamri MA, Tahir ul Qamar M, Mirza MU, et al. Pharmacoinformatics and molecular dynamics simulation studies reveal potential covalent and FDA-approved inhibitors of SARS-CoV-2 main protease 3CLpro. *J Biomol Struct Dyn.* Published online June 2020;1–13. doi:10.1080/07391102.2020.1782768.
- 20 Bhowmik D, Sharma RD, Prakash A, Kumar D. "Identification of Nafamostat and VR23 as COVID-19 drug candidates by targeting 3CLpro and PLpro.". *J Mol Struct.* 2021;1233:130094. doi:10.1016/j.molstruc.2021.130094.
- 21 Blakemore DC, Castro L, Churcher I, et al. Organic synthesis provides opportunities to transform drug discovery. *Nat Chem.* 2018;10(4):383–394. <https://doi.org/10.1038/s41557-018-0021-z>.
- 22 Campos KR, Coleman PJ, Alvarez JC, et al. The importance of synthetic chemistry in the pharmaceutical industry. *Science.* 2019;363(6424):eaat0805. <https://doi.org/10.1126/science.aat0805>.
- 23 Jain RP, Petterson HI, Zhang J, et al. Synthesis and evaluation of keto-glutamine analogues as potent inhibitors of severe acute respiratory syndrome 3CLpro. *J Med Chem.* 2004;47(25):6113–6116. <https://doi.org/10.1021/jm0494873>.
- 24 Shie JJ, Fang JM, Kuo CJ, et al. Discovery of potent anilide inhibitors against the severe acute respiratory syndrome 3CL protease. *J Med Chem.* 2005;48(13): 4469–4473. <https://doi.org/10.1021/jm050184y>.
- 25 Shie JJ, Fang JM, Kuo TH, et al. Inhibition of the severe acute respiratory syndrome 3CL protease by peptidomimetic α , β -unsaturated esters. *Bioorganic Med Chem.* 2005;13(17):5240–5252. <https://doi.org/10.1016/j.bmc.2005.05.065>.
- 26 Sydnes MO, Hayashi Y, Sharma VK, et al. Synthesis of glutamic acid and glutamine peptides possessing a trifluoromethyl ketone group as SARS-CoV 3CL protease inhibitors. *Tetrahedron.* 2006;62(36):8601–8609. <https://doi.org/10.1016/j.tet.2006.06.052>.
- 27 Yang S, Chen SJ, Hsu MF, et al. Synthesis, crystal structure, structure-activity relationships, and antiviral activity of a potent SARS coronavirus 3CL protease inhibitor. *J Med Chem.* 2006;49(16):4971–4980. <https://doi.org/10.1021/jm0603926>.
- 28 Zhang J, Petterson HI, Huitema C, et al. Design, synthesis, and evaluation of inhibitors for severe acute respiratory syndrome 3C-like protease based on phthalhydrazide ketones or heteroaromatic esters. *J Med Chem.* 2007;50(8): 1850–1864. <https://doi.org/10.1021/jm061425k>.
- 29 Yang Q, Chen L, He X, Gao Z, Shen X, Bai D. Design and synthesis of cinaserin analogs as severe acute respiratory syndrome coronavirus 3CL protease inhibitors. *Chem Pharm Bull.* 2008;56(10):1400–1405. <https://doi.org/10.1248/cpb.56.1400>.
- 30 Shao YM, Bin Yang W, Kuo TH, et al. Design, synthesis, and evaluation of trifluoromethyl ketones as inhibitors of SARS-CoV 3CL protease. *Bioorganic Med Chem.* 2008;16(8):4652–4660. <https://doi.org/10.1016/j.bmc.2008.02.040>.
- 31 Regnier T, Sarma D, Hidaka K, et al. New developments for the design, synthesis and biological evaluation of potent SARS-CoV 3CLpro inhibitors. *Bioorganic Med Chem Lett.* 2009;19(10):2722–2727. <https://doi.org/10.1016/j.bmcl.2009.03.118>.
- 32 Akaji K, Konno H, Mitsui H, et al. Structure-based design, synthesis, and evaluation of peptide-mimetic SARS 3CL protease inhibitors. *J Med Chem.* 2011;54(23): 7962–7973. <https://doi.org/10.1021/jm200870n>.
- 33 Prior AM, Kim Y, Weerasekara S, et al. Design, synthesis, and bioevaluation of viral 3C and 3C-like protease inhibitors. *Bioorganic Med Chem Lett.* 2013;23(23): 6317–6320. <https://doi.org/10.1016/j.bmcl.2013.09.070>.
- 34 Thanigaimalai P, Konno S, Yamamoto T, et al. Development of potent dipeptide-type SARS-CoV 3CL protease inhibitors with novel P3 scaffolds: Design, synthesis, biological evaluation, and docking studies. *Eur J Med Chem.* 2013;68:372–384. <https://doi.org/10.1016/j.ejmech.2013.07.037>.
- 35 Thanigaimalai P, Konno S, Yamamoto T, et al. Design, synthesis, and biological evaluation of novel dipeptide-type SARS-CoV 3CL protease inhibitors: Structure-activity relationship study. *Eur J Med Chem.* 2013;65:436–447. <https://doi.org/10.1016/j.ejmech.2013.05.005>.
- 36 Chuck CP, Chen C, Ke Z, Chi-Cheong Wan D, Chow HF, Wong KB. Design, synthesis and crystallographic analysis of nitrile-based broad-spectrum peptidomimetic inhibitors for coronavirus 3C-like proteases. *Eur J Med Chem.* 2013;59:1–6. <https://doi.org/10.1016/j.ejmech.2012.10.053>.
- 37 Konno S, Thanigaimalai P, Yamamoto T, et al. Design and synthesis of new tripeptide-type SARS-CoV 3CL protease inhibitors containing an electrophilic arylketone moiety. *Bioorganic Med Chem.* 2013;21(2):412–424. <https://doi.org/10.1016/j.bmc.2012.11.017>.
- 38 Kumar V, Shin JS, Shie JJ, et al. Identification and evaluation of potent Middle East respiratory syndrome coronavirus (MERS-CoV) 3CLPro inhibitors. *Antiviral Res.* 2017;141:101–106. <https://doi.org/10.1016/j.antiviral.2017.02.007>.
- 39 Ohnishi K, Hattori Y, Kobayashi K, Akaji K. Evaluation of a non-prime site substituent and warheads combined with a decahydroisoquinolin scaffold as a SARS 3CL protease inhibitor. *Bioorganic Med Chem.* 2019;27(2):425–435. <https://doi.org/10.1016/j.bmc.2018.12.019>.
- 40 Zhang L, Lin D, Kusov Y, et al. α -Ketoamides as Broad-Spectrum Inhibitors of Coronavirus and Enterovirus Replication: Structure-Based Design, Synthesis, and Activity Assessment. *J Med Chem.* 2020;63(9):4562–4578. <https://doi.org/10.1021/acs.jmedchem.9b01828>.
- 41 Chen LR, Wang YC, Yi WL, et al. Synthesis and evaluation of isatin derivatives as effective SARS coronavirus 3CL protease inhibitors. *Bioorganic Med Chem Lett.* 2005; 15(12):3058–3062. <https://doi.org/10.1016/j.bmcl.2005.04.027>.
- 42 Ghosh AK, Gong G, Grum-Tokars V, et al. Design, synthesis and antiviral efficacy of a series of potent chloropyridyl ester-derived SARS-CoV 3CLpro inhibitors. *Bioorganic Med Chem Lett.* 2008;18(20):5684–5688. <https://doi.org/10.1016/j.bmcl.2008.08.082>.
- 43 Ramajayam R, Tan KP, Liu HG, Liang PH. Synthesis and evaluation of pyrazolone compounds as SARS-coronavirus 3C-like protease inhibitors. *Bioorganic Med Chem.* 2010;18(22):7849–7854. <https://doi.org/10.1016/j.bmc.2010.09.050>.
- 44 Ramajayam R, Tan KP, Liu HG, Liang PH. Synthesis, docking studies, and evaluation of pyrimidines as inhibitors of SARS-CoV 3CL protease. *Bioorganic Med Chem Lett.* 2010;20(12):3569–3572. <https://doi.org/10.1016/j.bmcl.2010.04.118>.
- 45 Mandadapu SR, Weerawarna PM, Prior AM, et al. Macrocyclic inhibitors of 3C and 3C-like proteases of picornavirus, norovirus, and coronavirus. *Bioorganic Med Chem Lett.* 2013;23(13):3709–3712. <https://doi.org/10.1016/j.bmcl.2013.05.021>.
- 46 Liu W, Zhu HM, Niu GJ, et al. Synthesis, modification and docking studies of 5-sulfonyl isatin derivatives as SARS-CoV 3C-like protease inhibitors. *Bioorganic Med Chem Lett.* 2014;22(1):292–302. <https://doi.org/10.1016/j.bmc.2013.11.028>.
- 47 Kumar V, Tan KP, Wang YM, Lin SW, Liang PH. Identification, synthesis and evaluation of SARS-CoV and MERS-CoV 3C-like protease inhibitors. *Bioorganic Med Chem.* 2016;24(13):3035–3042. <https://doi.org/10.1016/j.bmc.2016.05.013>.
- 48 Konno H, Wakabayashi M, Takanuma D, Saito Y, Akaji K. Design and synthesis of a series of serine derivatives as small molecule inhibitors of the SARS coronavirus 3CL protease. *Bioorganic Med Chem.* 2016;24(6):1241–1254. <https://doi.org/10.1016/j.bmc.2016.01.052>.
- 49 Konno H, Onuma T, Nitanai I, et al. Synthesis and evaluation of phenylisoserine derivatives for the SARS-CoV 3CL protease inhibitor. *Bioorganic Med Chem Lett.* 2017;27(12):2746–2751. <https://doi.org/10.1016/j.bmcl.2017.04.056>.
- 50 Yoshizawa S, Ichiro, Hattori Y, Kobayashi K, Akaji K. Evaluation of an octahydroisochromene scaffold used as a novel SARS 3CL protease inhibitor. *Bioorganic Med Chem.* 2020;28(4):115273. doi:10.1016/j.bmc.2019.115273.
- 51 Marra MA, Jones SJM, Astell CR, et al. The genome sequence of the SARS-associated coronavirus. *Science.* 2003;300(5624):1399–1404. <https://doi.org/10.1126/science.1085953>.
- 52 Brian DA, Baric RS. Coronavirus genome structure and replication. *Curr Top Microbiol Immunol.* 2005;287:1–30. https://doi.org/10.1007/3-540-26765-4_1.
- 53 Masters PS. The Molecular Biology of Coronaviruses. *Adv Virus Res.* 2006;65: 193–292. [https://doi.org/10.1016/S0065-3527\(06\)66005-3](https://doi.org/10.1016/S0065-3527(06)66005-3).
- 54 Dimitrov DS. Virus entry: Molecular mechanisms and biomedical applications. *Nat Rev Microbiol.* 2004;2(2):109–122. <https://doi.org/10.1038/nrmicro817>.
- 55 Gallagher TM, Buchmeier MJ. Coronavirus spike proteins in viral entry and pathogenesis. *Virology.* 2001;279(2):371–374. <https://doi.org/10.1006/viro.2000.0757>.
- 56 Ziebuhr J. The coronavirus replicase. *Curr Top Microbiol Immunol.* 2005;287:57–94. https://doi.org/10.1007/3-540-26765-4_3.
- 57 Stoermer M. Homology Models of Coronavirus 2019-NCoV 3CLpro Protease.; 2020. doi:10.26434/chemrxiv.11637294.
- 58 Yang H, Yang M, Ding Y, et al. The crystal structures of severe acute respiratory syndrome virus main protease and its complex with an inhibitor. *Proc Natl Acad Sci U S A.* 2003;100(23):13190–13195. <https://doi.org/10.1073/pnas.1835675100>.
- 59 Ratia K, Saikatendu KS, Santarsiero BD, et al. Severe acute respiratory syndrome coronavirus papain-like-protease: Structure of a viral deubiquitinating enzyme. *Proc Natl Acad Sci U S A.* 2006;103(15):5717–5722. <https://doi.org/10.1073/pnas.0510851103>.
- 60 Ivanov AA, Khuri FR, Fu H. Targeting protein-protein interactions as an anticancer strategy. *Trends Pharmacol Sci.* 2013;34(7):393–400. <https://doi.org/10.1016/j.tips.2013.04.007>.

- 61 Hruby VJ, Qiu W, Okayama T, Soloshonok VA. Design of nonpeptides from peptide ligands for peptide receptors. In: *Methods in Enzymology*. Vol 343. Academic Press; 2002:91-123. doi:10.1016/S0076-6879(02)43129-1.
- 62 Cowell S, Lee Y, Cain J, Hruby V. Exploring Ramachandran and Chi Space: Conformationally Constrained Amino Acids and Peptides in the Design of Bioactive Polypeptide Ligands. *Curr Med Chem*. 2012;11(21):2785-2798. <https://doi.org/10.2174/0929867043364270>.
- 63 Burgess A, Chia KM, Haupt S, Thomas D, Haupt Y, Lim E. Clinical overview of MDM2/X-targeted therapies. *Front Oncol*. 2016;6:7. <https://doi.org/10.3389/fonc.2016.00007>.
- 64 Bates E, Bode C, Costa M, et al. Intracoronary KAI-9803 as an adjunct to primary percutaneous coronary intervention for acute ST-segment elevation myocardial infarction. *Circulation*. 2008;117(7):886-896. <https://doi.org/10.1161/CIRCULATIONAHA.107.759167>.
- 65 Ramtohl YK, James MNG, Vederas JC. Synthesis and evaluation of keto-glutamine analogues as inhibitors of hepatitis A virus 3C proteinase. *J Org Chem*. 2002;67(10):3169-3178. <https://doi.org/10.1021/jo0157831>.
- 66 Bosch BJ, Martina BEE, Van Der Zee R, et al. Severe acute respiratory syndrome coronavirus (SARS-CoV) infection inhibition using spike protein heptad repeat-derived peptides. *Proc Natl Acad Sci U S A*. 2004;101(22):8455-8460. <https://doi.org/10.1073/pnas.0400576101>.
- 67 Jain RP, Vederas JC. Structural variations in keto-glutamines for improved inhibition against hepatitis A virus 3C proteinase. *Bioorganic Med Chem Lett*. 2004;14(14):3655-3658. <https://doi.org/10.1016/j.bmcl.2004.05.021>.
- 68 Tian Q, Nayyar NK, Babu S, et al. An efficient synthesis of a key intermediate for the preparation of the rhinovirus protease inhibitor AG7088 via asymmetric dianionic cyanomethylation of N-Boc-L-(+)-glutamic acid dimethyl ester. *Tetrahedron Lett*. 2001;42(39):6807-6809. [https://doi.org/10.1016/S0040-4039\(01\)01416-2](https://doi.org/10.1016/S0040-4039(01)01416-2).
- 69 Hsu JTA, Kuo CJ, Hsieh HP, et al. Evaluation of metal-conjugated compounds as inhibitors of 3CL protease of SARS-CoV. *FEBS Lett*. 2004;574(1-3):116-120. <https://doi.org/10.1016/j.febslet.2004.08.015>.
- 70 Wu CY, Chang CF, Chen JSY, Wong CH, Lin CH. Rapid diversity-oriented synthesis in microtiter plates for in situ screening: Discovery of potent and selective α -fucosidase inhibitors. *Angew Chem - Int Ed*. 2003;42(38):4661-4664. <https://doi.org/10.1002/anie.200351823>.
- 71 Kuo CJ, Chi YH, Hsu JTA, Liang PH. Characterization of SARS main protease and inhibitor assay using a fluorogenic substrate. *Biochem Biophys Res Commun*. 2004;318(4):862-867. <https://doi.org/10.1016/j.bbrc.2004.04.098>.
- 72 Krausslich HG, Wimmer E. Viral proteinases. *Annu Rev Biochem*. 1988;57:701-754. <https://doi.org/10.1146/annurev.bi.57.07188.003413>.
- 73 Dragovich PS, Prins TJ, Zhou R, et al. Structure-based design, synthesis, and biological evaluation of irreversible human rhinovirus 3C protease inhibitors. 4. Incorporation of P1 lactam moieties as L-glutamine replacements. *J Med Chem*. 1999;42(7):1213-1224. <https://doi.org/10.1021/jm9805384>.
- 74 Ohba T, Ikeda E, Takei H. Inactivation of serine protease, α -chymotrypsin by fluorinated phenylalanine analogues. *Bioorganic Med Chem Lett*. 1996;6(16):1875-1880. [https://doi.org/10.1016/0960-894X\(96\)00342-3](https://doi.org/10.1016/0960-894X(96)00342-3).
- 75 Luesch H, Hoffmann D, Hevel JM, Becker JE, Golakoti T, Moore RE. Biosynthesis of 4-methylproline in cyanobacteria: Cloning of nosE and nosF genes and biochemical characterization of the encoded dehydrogenase and reductase activities. *J Org Chem*. 2003;68(1):83-91. <https://doi.org/10.1021/jo026479q>.
- 76 Schmidt U, Utz R, Lieberknecht A, et al. Amino acids and peptides; 60.1 synthesis of biologically active cyclopeptides; 10. Synthesis of 16 structural isomers of dolastatin 3; II:2 synthesis of the linear educts and the cyclopeptides. *Synth*. 1987;1987(3):236-241. <https://doi.org/10.1055/s-1987-27900>.
- 77 Katritzky AR, Suzuki K, Singh SK. Highly diastereoselective peptide chain extensions of unprotected amino acids with N-(Z- α -aminoacyl)benzotriazoles. *Synthesis (Stuttg)*. 2004;2004(16):2645-2652. <https://doi.org/10.1055/s-2004-831255>.
- 78 Patick AK, Binford SL, Brothers MA, et al. In vitro antiviral activity of AG7088, a potent inhibitor of human rhinovirus 3C protease. *Antimicrob Agents Chemother*. 1999;43(10):2444-2450. <https://doi.org/10.1128/aac.43.10.2444>.
- 79 Blanchard JE, Elowe NH, Huitema C, et al. High-throughput screening identifies inhibitors of the SARS coronavirus main proteinase. *Chem Biol*. 2004;11(10):1445-1453. <https://doi.org/10.1016/j.chembiol.2004.08.011>.
- 80 Chen L, Gui C, Luo X, et al. Cinanserin Is an Inhibitor of the 3C-Like Proteinase of Severe Acute Respiratory Syndrome Coronavirus and Strongly Reduces Virus Replication In Vitro. *J Virol*. 2005;79(11):7095-7103. <https://doi.org/10.1128/jvi.79.11.7095-7103.2005>.
- 81 Zhang HZ, Zhang H, Kemnitzer W, et al. Design and synthesis of dipeptidyl glutaminy fluoromethyl ketones as potent severe acute respiratory syndrome coronavirus (SARS-CoV) inhibitors. *J Med Chem*. 2006;49(3):1198-1201. <https://doi.org/10.1021/jm0507678>.
- 82 Maynard GD, Cheng HC, Kane JM, Staeger MA. A convergent synthesis of 4-(2-benzothiazoyl)piperidines with antimicrobial activity. *Bioorganic Med Chem Lett*. 1993;3(4):753-756. [https://doi.org/10.1016/S0960-894X\(01\)81268-3](https://doi.org/10.1016/S0960-894X(01)81268-3).
- 83 Castro B, Dormoy JR, Evin G, Selve C. Reactifs de couplage peptidique I (1) - l'hexafluorophosphate de benzotriazolyl N-oxyltrisdimethylamino phosphonium (B. O.P.). *Tetrahedron Lett*. 1975;16(14):1219-1222. [https://doi.org/10.1016/S0040-4039\(00\)72100-9](https://doi.org/10.1016/S0040-4039(00)72100-9).
- 84 Fehrentz JA, Paris M, Heitz A, et al. Improved solid phase synthesis of C-terminal peptide aldehydes. *Tetrahedron Lett*. 1995;36(43):7871-7874. [https://doi.org/10.1016/0040-4039\(95\)01646-Y](https://doi.org/10.1016/0040-4039(95)01646-Y).
- 85 Chang KO, Takahashi D, Prakash O, Kim Y. Characterization and inhibition of norovirus proteases of genogroups I and II using a fluorescence resonance energy transfer assay. *Virology*. 2012;423(2):125-133. <https://doi.org/10.1016/j.virol.2011.12.002>.
- 86 Chang KO, Sosnovtsev SV, Belliot G, King AD, Green KY. Stable expression of a Norwalk virus RNA replicon in a human hepatoma cell line. *Virology*. 2006;353(2):463-473. <https://doi.org/10.1016/j.virol.2006.06.006>.
- 87 Webber SE, Okano K, Little TL, et al. Tripeptide aldehyde inhibitors of human rhinovirus 3C protease: Design, synthesis, biological evaluation, and cocystal structure solution of P1 glutamine isosteric replacements. *J Med Chem*. 1998;41(15):2786-2805. <https://doi.org/10.1021/jm980071x>.
- 88 Kuo CJ, Shie JJ, Fang JM, et al. Design, synthesis, and evaluation of 3C protease inhibitors as anti-enterovirus 71 agents. *Bioorganic Med Chem*. 2008;16(15):7388-7398. <https://doi.org/10.1016/j.bmc.2008.06.015>.
- 89 Wu CY, King KY, Kuo CJ, et al. Stable Benzotriazole Esters as Mechanism-Based Inactivators of the Severe Acute Respiratory Syndrome 3CL Protease. *Chem Biol*. 2006;13(3):261-268. <https://doi.org/10.1016/j.chembiol.2005.12.008>.
- 90 Zhao Z, Dai X, Li C, et al. Pyrazolone structural motif in medicinal chemistry: Retrospect and prospect. *Eur J Med Chem*. 2020;186, 111893. <https://doi.org/10.1016/j.ejmech.2019.111893>.
- 91 Ragab FAF, Abdel-Gawad NM, Georger HH, Said MF. Pyrazolone derivatives: Synthesis, anti-inflammatory, analgesic quantitative structure-activity relationship and in vitro studies. *Chem Pharm Bull*. 2013;61(8):834-845. <https://doi.org/10.1248/cpb.c13-00314>.
- 92 Krishnasamy SK, Namasivayam V, Mathew S, et al. Design, Synthesis, and Characterization of Some Hybridized Pyrazolone Pharmacophore Analogs against Mycobacterium tuberculosis. *Arch Pharm (Weinheim)*. 2016;349(5):383-397. <https://doi.org/10.1002/ardp.201600019>.
- 93 Al-Saheb R, Makharza S, Al-Battah F, Abu-El-Halawa R, Kaimari T, Abu Abed OS. Synthesis of new pyrazolone and pyrazole-based adamantly chalcones and antimicrobial activity. *Biosci Rep*. 2020;40(9). <https://doi.org/10.1042/BSR20201950>.
- 94 Shabaan MA, Kamal AM, Faggal SI, Elsahar AE, Mohamed KO. Synthesis and biological evaluation of pyrazolone analogues as potential anti-inflammatory agents targeting cyclooxygenases and 5-lipoxygenase. *Arch Pharm (Weinheim)*. 2020;353(4), e1900308. <https://doi.org/10.1002/ardp.201900308>.
- 95 Anwar T, Nadeem H, Sarwar S, et al. Investigation of antioxidant and anti-nociceptive potential of isoxazolone, pyrazolone derivatives, and their molecular docking studies. *Drug Dev Res*. 2020;81(7):893-903. <https://doi.org/10.1002/ddr.21711>.
- 96 Wang L, Yang Z, Ni T, et al. Discovery of pyrazolone spirocyclohexadienone derivatives with potent antitumor activity. *Bioorganic Med Chem Lett*. 2020;30(1), 126662. <https://doi.org/10.1016/j.bmcl.2019.126662>.
- 97 Wang XJ, Tan J, Grozinger K. Cross-coupling of 1-aryl-5-bromopyrazoles: Regioselective synthesis of 3,5-disubstituted 1-arylpurazoles. *Tetrahedron Lett*. 2000;41(24):4713-4716. [https://doi.org/10.1016/S0040-4039\(00\)00704-8](https://doi.org/10.1016/S0040-4039(00)00704-8).
- 98 Dhal PM, Achary TE, Nayak A. Studies on 1,3-diaryl pyrazolones and their derivatives. *Chem Informationsd*. 1975;7(12):1196-1199. <https://doi.org/10.1002/chin.197629200>.
- 99 Ram VJ, Berghe DAV, Vlietinck AJ. 5-Cyano-6-arylyluracil and 2-thiouracil derivatives as potential chemotherapeutic agents. *J Heterocycl Chem*. 1984;21(5):1307-1312. <https://doi.org/10.1002/jhet.5570210513>.
- 100 Röper S, Kolb HC. Click Chemistry for Drug Discovery. *Fragm Approaches Drug Discov*. 2006;34:311-339. <https://doi.org/10.1002/3527608761.ch15>.
- 101 Kelly AR, Wei J, Kesavan S, et al. Accessing skeletal diversity using catalyst control: Formation of n and n + 1 macrocyclic triazole rings. *Org Lett*. 2009;11(11):2257-2260. <https://doi.org/10.1021/ol900562u>.
- 102 Peherer AD, Abell AD. New β -strand templates constrained by Huisgen cycloaddition. *Org Lett*. 2012;14(5):1330-1333. <https://doi.org/10.1021/ol3002199>.
- 103 Zhang J, Kemmink J, Rijkers DTS, Liskamp RMJ. Cu(I)- and Ru(II)-mediated "click" cyclization of tripeptides toward vancomycin-inspired mimics. *Org Lett*. 2011;13(13):3438-3441. <https://doi.org/10.1021/ol201184b>.
- 104 Mandadapu SR, Weerawarna PM, Gunnam MR, et al. Potent inhibition of norovirus 3CL protease by peptidyl α -ketoamides and α -keto heterocycles. *Bioorganic Med Chem Lett*. 2012;22(14):4820-4826. <https://doi.org/10.1016/j.bmcl.2012.05.055>.
- 105 Zhou L, Liu Y, Zhang W, et al. Isatin compounds as noncovalent SARS coronavirus 3C-like protease inhibitors. *J Med Chem*. 2006;49(12):3440-3443. <https://doi.org/10.1021/jm0602357>.
- 106 Kaila N, Janz K, DeBernardo S, et al. Synthesis and biological evaluation of quinoline salicylic acids as P-selectin antagonists. *J Med Chem*. 2007;50(1):21-39. <https://doi.org/10.1021/jm0602256>.
- 107 Jiang Y, Hansen TV. Isatin 1,2,3-triazoles as potent inhibitors against caspase-3. *Bioorganic Med Chem Lett*. 2011;21(6):1626-1629. <https://doi.org/10.1016/j.bmcl.2011.01.110>.
- 108 Lee D, Long SA, Murray JH, et al. Potent and selective nonpeptide inhibitors of caspases 3 and 7. *J Med Chem*. 2001;44(12):2015-2026. <https://doi.org/10.1021/jm0100537>.
- 109 Kumar V, Chang CK, Tan KP, et al. Identification, synthesis, and evaluation of new neuraminidase inhibitors. *Org Lett*. 2014;16(19):5060-5063. <https://doi.org/10.1021/ol502410x>.
- 110 Racañè L, Tralić-Kulenović V, Boykin DW, Karminski-Zamola G. Synthesis of new cyano-substituted bis-benzothiazolyl arylfurans and arylthiophenes. *Molecules*. 2003;8(3):342-349. <https://doi.org/10.3390/80300342>.
- 111 Hillisch A, Heinrich N, Wild H. Computational Chemistry in the Pharmaceutical Industry: From Childhood to Adolescence. *ChemMedChem*. 2015;10(12):1958-1962. <https://doi.org/10.1002/cmdc.201500346>.

- 112 Rognan D. The impact of in silico screening in the discovery of novel and safer drug candidates. *Pharmacol Ther.* 2017;175:47–66. <https://doi.org/10.1016/j.pharmthera.2017.02.034>.
- 113 Lo YC, Rensi SE, Torng W, Altman RB. Machine learning in chemoinformatics and drug discovery. *Drug Discov Today.* 2018;23(8):1538–1546. <https://doi.org/10.1016/j.drudis.2018.05.010>.
- 114 Xu J, Hagler A. Chemoinformatics and drug discovery. *Molecules.* 2002;7(8):566–600. <https://doi.org/10.3390/70800566>.
- 115 Anand K, Ziebuhr J, Wadhvani P, Mesters JR, Hilgenfeld R. Coronavirus main proteinase (3CLpro) Structure: Basis for design of anti-SARS drugs. *Science.* 2003;300(5626):1763–1767. <https://doi.org/10.1126/science.1085658>.
- 116 Ogando NS, Dalebout TJ, Zevenhoven-Dobbe JC, et al. SARS-coronavirus-2 replication in Vero E6 cells: Replication kinetics, rapid adaptation and cytopathology. *J Gen Virol.* 2020;101(9):925–940. <https://doi.org/10.1099/jgv.0.001453>.
- 117 Yan H, Xiao G, Zhang J, et al. SARS coronavirus induces apoptosis in Vero E6 cells. *J Med Virol.* 2004;73(3):323–331. <https://doi.org/10.1002/jmv.20094>.
- 118 Qinfen Z, Jinming C, Xiaojun H, et al. The life cycle of SARS coronavirus in Vero E6 cells. *J Med Virol.* 2004;73(3):332–337. <https://doi.org/10.1002/jmv.20095>.